WDL-TR10941
January 1987

APPLICATION OF ADAPTIVE ANTENNA TECHNIQUES TO FUTURE COMMERCIAL SATELLITE COMMUNICATIONS

CONTRACT NAS3-24892

Prepared for:
National Aeronautics and Space Administration
Lewis Research Center
Cleveland, Ohio 44135

Prepared by:
Ford Aerospace & Communications Corporation
Western Development Laboratories Division
3939 Fabian Way
Palo Alto, California 94303-4697

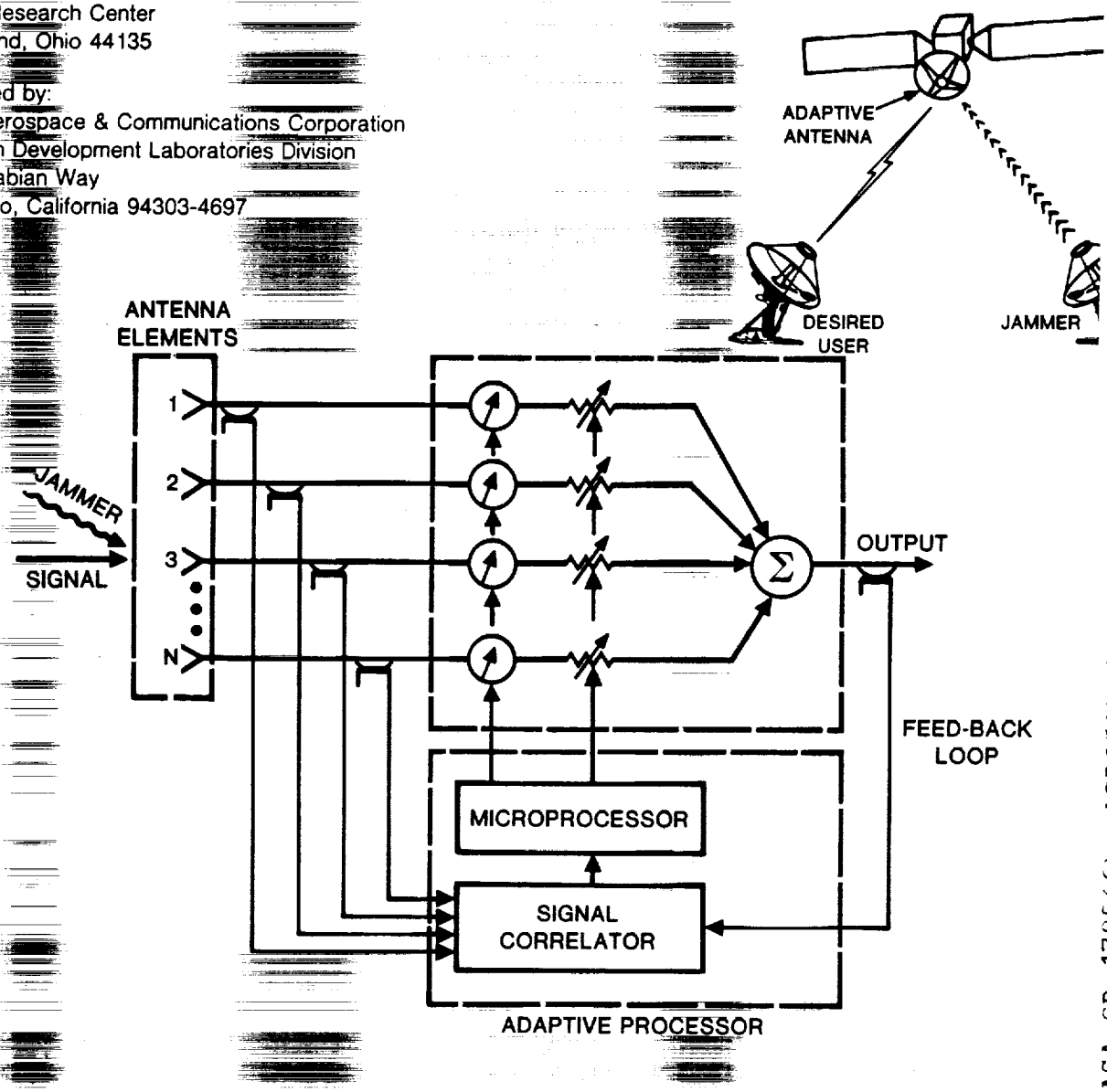

1. Report No.	2. Government Accession No.	3. Recipient's Catalog No.
		WDL TR 10941

4. Title and Subtitle

Application of Adaptive Antenna Techniques to Future Commercial Satellite Communication

5. Report Date

January 1987

6. Performing Organization Code

650-60-26

7. Author(s) (In alphabetical order)

L. Ersoy, E. A. Lee, and E. W. Matthews

8. Performing Organization Report No.

10. Work Unit No.

9. Performing Organization Name and Address

Ford Aerospace & Communications Corporation
3939 Fabian Way
Palo Alto, CA 94303

11. Contract or Grant No.

NAS3-24892

12. Sponsoring Agency Name and Address

NASA Lewis Research Center
Cleveland, Ohio 44135

13. Type of Report and Period Covered

Final
April 1986 - January 1987

14. Sponsoring Agency Code

15. Supplementary Notes

NASA Contract Manager: Richard Lee

16. Abstract

The purpose of this contract was to identify the application of adaptive antenna technique in future operational commercial satellite communication systems and to quantify potential benefits. The contract consisted of two major subtasks. Task I, "Assessment of Future Commercial Satellite System Requirements", was generally referred to as the "Adaptive" section. Task II dealt with "Pointing Error Compensation Study for a Multiple Scanning/Fixed Spot Beam Reflector Antenna System" and was referred to as the "reconfigurable" system. Each of these tasks was further subdivided into smaller subtasks. It should also be noted that the reconfigurable system is usually defined as an open-loop system while the adaptive system is a closed-loop system. The differences between the open- and close-loop systems were defined. Both the "adaptive" and "reconfigurable" systems were explained and the potential applications of such systems were presented in the context of commercial communication satellite systems.

17. Key Words (Suggested by Author(s))	18. Distribution Statement
Adaptive Reconfigurable Close-loop Antenna Open-loop Antenna Multiple Beam Antenna Land Mobile Antenna Advanced Communications Technology Satellite	General Release

19. Security Classif. (of this report)	20. Security Classif. (of this page)	21. No. of pages	22. Price*

*For sale by the National Technical Information Service, Springfield, Virginia 22161

TABLE OF CONTENTS

1.0 INTRODUCTION

The purpose of the AAATFCSC contract was to identify the application of adaptive antenna techniques in future commercial satellite communication systems and to quantify potential benefits. The contract consisted of two major subtasks. Task I, "Assessment of Future Commercial Satellite System Requirements", was generally referred to as the "Adaptive" section. Task II dealt with the "Pointing Error Compensation Study for a Multiple Scanning/Fixed Spot Beam Reflector Antenna System" and was referred to as the "Reconfigurable" system. Each of these tasks was further subdivided into smaller subtasks. It should also be noted that the reconfigurable system is usually defined as an open-loop system while the adaptive system is a closed-loop system. However, it is possible to define a closed-loop reconfigurable system as well. Needless to say, the latter system is actually a form of an adaptive one also.

In this report, the differences between the adaptive and reconfigurable systems are presented first. This is followed by a section describing the three different commercial communications systems considered in this contract. The subtasks I and II are subsequently presented. Evaluation of results and recommendations are presented in sections 6 and 7.

2.0 ADAPTIVE_AND_RECONFIGURABLE_SYSTEMS

There appear to be two fundamental aspects associated with a communications system. The first is related to the transmission of the signal over a channel connecting the transmitter to the receiver. The second aspect is the signal processing at either end of the communications channel, that is needed to prepare the signal for transmission or to extract desired information at the receiver. In general, neither the transmission channel nor the signal itself is ideal, well defined, or well known; this factor may cause

system performance degradation in the absence of proper safeguards. One alternative to improve system performance is to propose an over-designed system, which would perform properly in the worst adverse conditions. Such "overkill", however, would be very expensive. Another alternative is to design an average system for a typical operating environment with the understanding that the system performance may not be acceptable some of the time. A third alternative is to design a "smart system" which can "adapt" itself to changes in the environment. While such an adaptive system could be quite expensive as well, in most cases a reasonable compromise can be found between the system smartness (and the resulting system performance) and the cost factor.

For the purpose of this contract, the adaptive system is assumed to consist of input port(s) and sampling coupler(s), output port(s) and sampling coupler(s), a variable beamforming network (VBFN) for signal processing, and an adaptive processor containing the algorithm that determines the parameters of the VBFN. Such an adaptive system is depicted in Figure 2-1 for the receive antenna application. This system is referred to as a closed-loop system since there exists a feedback loop between the output port of the antenna and the adaptive processor. While higher level closed-loop systems such as a system between the spacecraft and the earth station with a feedback loop were also considered in this project, Figure 2-1 remains the basic adaptive system of interest.

In contrast, a reconfigurable system is assumed to consist of input port(s), output port(s), a VBFN, and a controller unit as shown in Figure 2-2a. The controller unit could be a simple device receiving commands from a ground station or a preprogrammed "clock" with a look-up table containing the desired setting parameters for the VBFN. An open-loop reconfigurable system may utilize a set of sampling couplers at the antenna elements to help in determining the VBFN settings. Such a system is illustrated

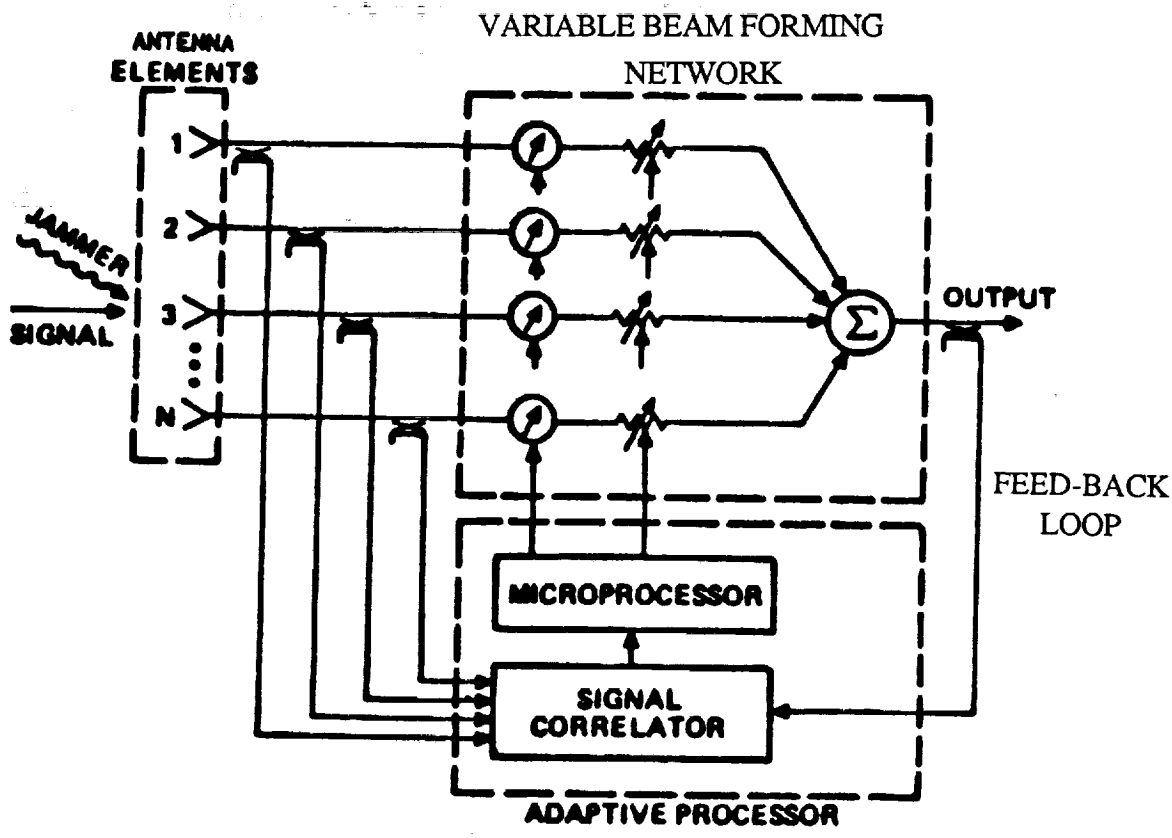

FIG. 2-1. ADAPTIVE SYSTEM FOR A RECEIVE ANTENNA

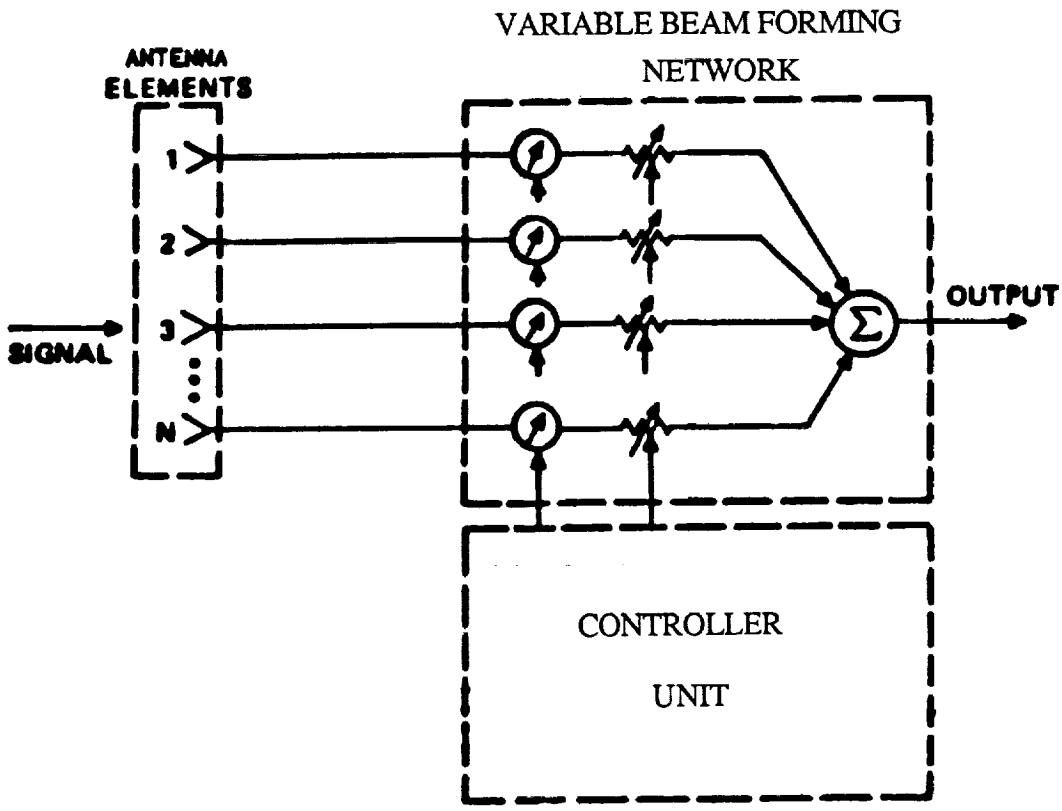

FIG. 2-2a. BASIC RECONFIGURABLE SYSTEM FOR A RECEIVE ANTENNA

in Figure 2-2b. On the other hand, a closed-loop reconfigurable system consists of a basic reconfigurable system with a feedback loop between the VBFN output and the controller unit as depicted in Figure 2-2c. The absence of the sampling couplers at the antenna elements is compensated for by systematically perturbing the parameters of the VBFN and observing the change at the output port of the system. The ways to determine the VBFN's parameters for open and closed-loop reconfigurable systems are discussed in Section 5.3. As can be seen from Figures 2-1 and 2-2, the reconfigurable system is less complicated and therefore a more cost effective version of an adaptive system.

3.0 COMMERCIAL COMMUNICATIONS SYSTEMS

Three commercial communication systems have been considered in the AAATFCSC contract. These are the scanning/fixed spot beams, multiple shaped beams and land-mobile system concepts.

The scanning/fixed spot beam antenna concept forms the basis of the Advanced Communications Technology Satellite (ACTS) system, and was developed on Contracts NAS3-22498 and 22499. The concept consists of a multi-horn feed array illuminating a dual reflector antenna configuration. Individual horns produce spot beams at different positions, depending upon horn location. Low sidelobe spot beams are produced by exciting a seven-horn cluster with the proper amplitude and phases. The coverage area is subdivided into 6 regions with one scanning spot beam per region, as depicted in Figure 3-1. In addition to the scanning spot beams, there are 18 fixed spot beams distributed throughout the coverage area. The fixed beams and the scanning beams in a given region are isolated from each other by frequency diversity. The scanning beams in adjacent regions are isolated from each other by polarization reversal. The beams are assumed to be linearly polarized. It should be clear from the above explanation that each scanning beam utilizes all the

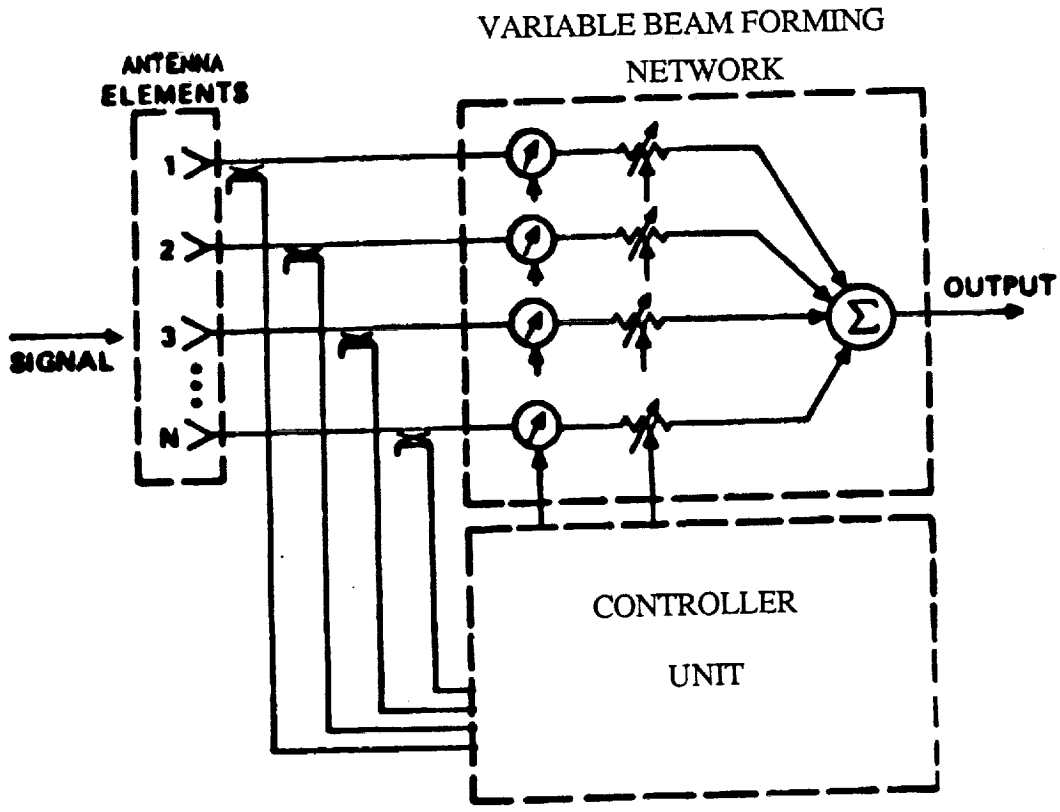

FIG. 2-2b. OPEN-LOOP RECONFIGURABLE SYSTEM FOR RECEIVE ANTENNA

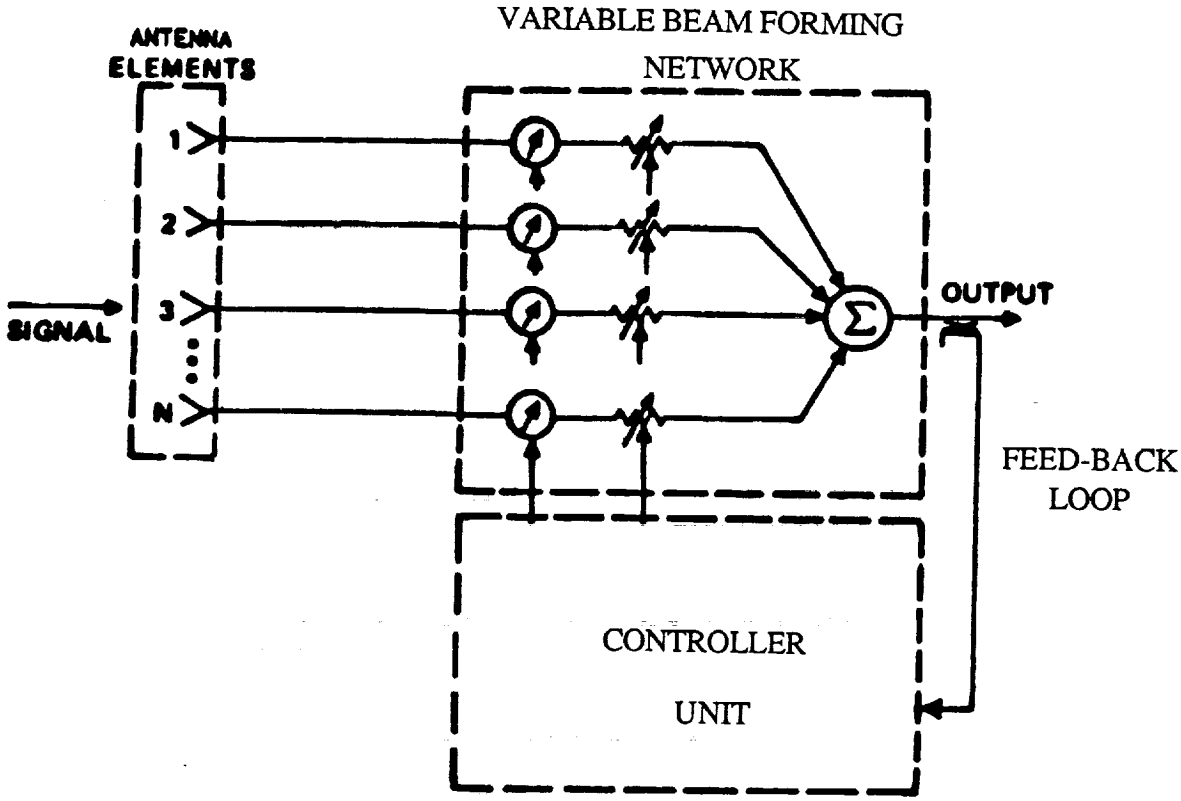

FIG. 2-2c. CLOSED-LOOP RECONFIGURABLE SYSTEM FOR RECEIVE ANTENNA

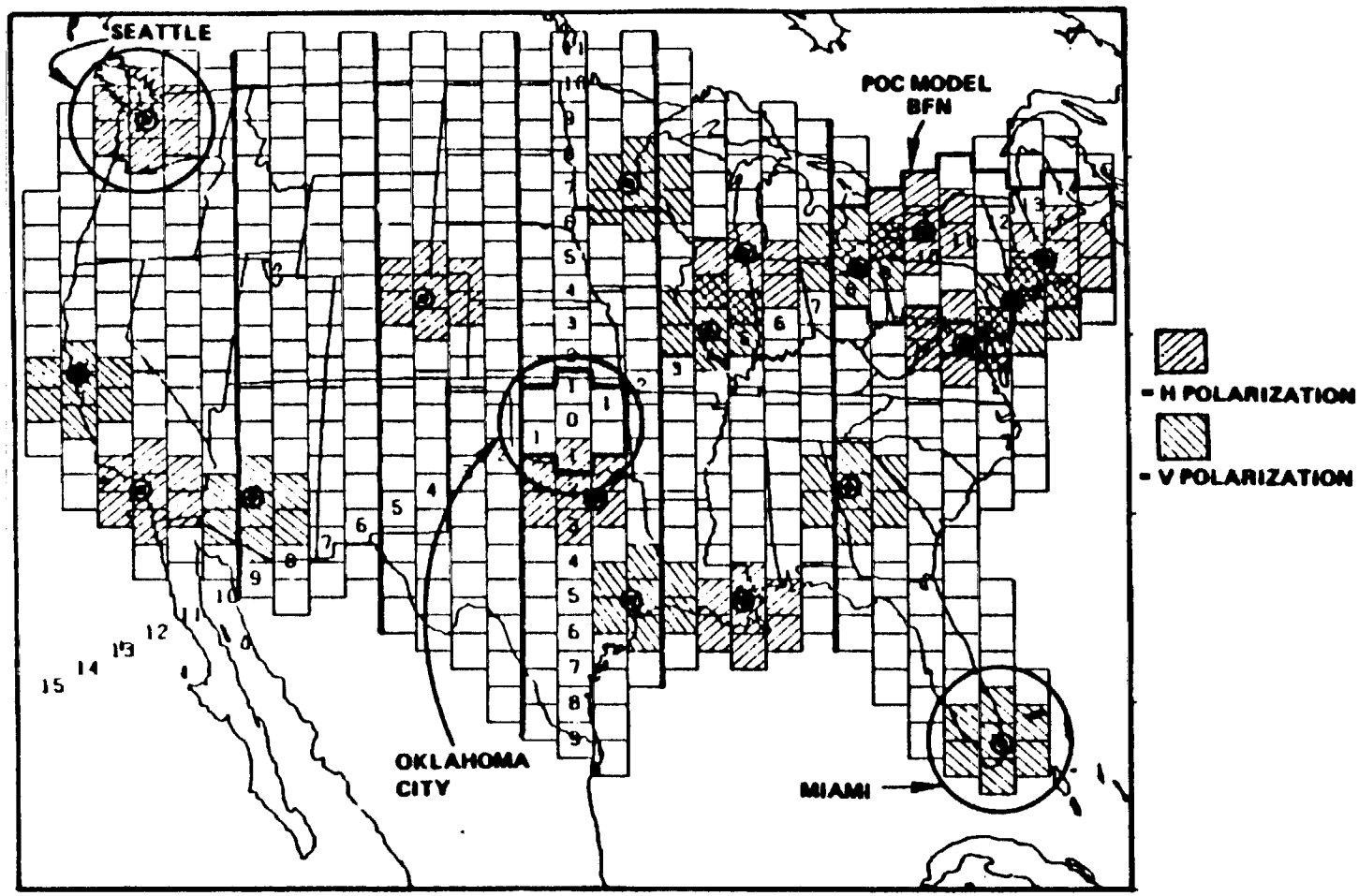

FIG. 3-1. TYPICAL ACTS MULTIBEAM COVERAGE SCENARIO

frequency channels available to the scanning beams, but provides a TDMA type of service within its designated region.

In contrast, the beams in a land-mobile system provide simultaneous service to the entire coverage area. There are enough pencil beams to blanket the area under consideration. While this system provides a very high gain, one cannot utilize all the available frequency channels for all the beams as frequency diversity is needed for isolation purposes among the adjacent pencil beams. In this type of system there are sacrifices in the number of available channels in favor of continuous coverage with high gain over the entire coverage region. A typical land-mobile system is depicted in Figure 3-2.

The multiple shaped beam antenna system also provides continuous coverage over a given region, but all channels are available for use. This is accomplished at the expense of antenna gain. The feed horns in a cluster are combined in a beamforming network (BFN) to generate a single shaped beam. Each beam utilizes the entire frequency band. A typical multiple shaped beam antenna system is depicted in Figure 3-3.

It is determined that adaptive concepts can be used with all three communications systems. The reasoning behind this determination is that an adaptive system requires that a given beam should be generated by a number of feed elements. In all three systems above, this requirement is met. While it is true that in the case of the scanning/fixed spot beam antenna concept and the land-mobile system only few horn elements (about 7) are used to generate each beam, there are adjacent elements available to be used if needed. Furthermore, in many cases, even a seven-feed cluster is sufficient for an adaptive antenna application, so long as the number of "jammers" is less than the horn elements and the user(s) and jammer(s) are sufficiently separated from each other. In commercial application, it was assumed that there would be a few unintentional "jammers".

BEAM POSITIONS

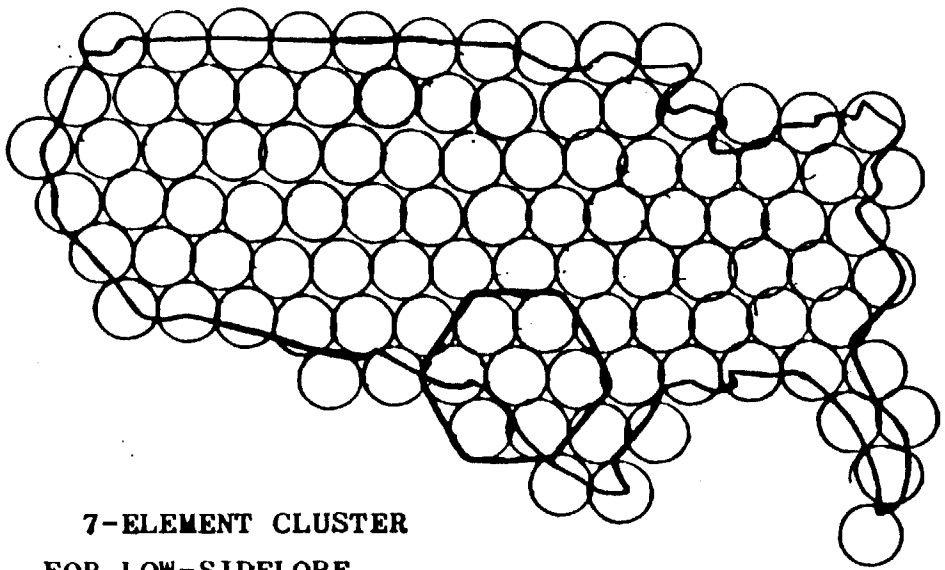

7-ELEMENT CLUSTER
FOR LOW-SIDELOBE
INDIVIDUAL BEAM

FREQUENCY ASSIGNMENTS
FOR ISOLATION ENHANCEMENT

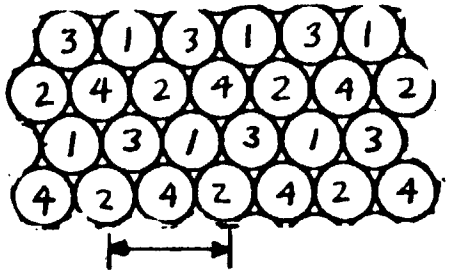

1-Beamwidth Separation

A. FOUR FREQUENCY SETS

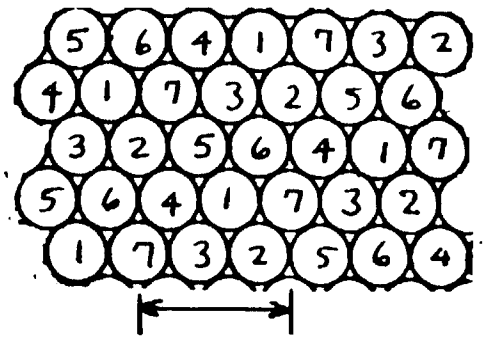

2-Beamwidth Separation

B. SEVEN FREQUENCY SETS

FIG. 3-2. TYPICAL LAND-MOBILE BEAM COVERAGE SCENARIO

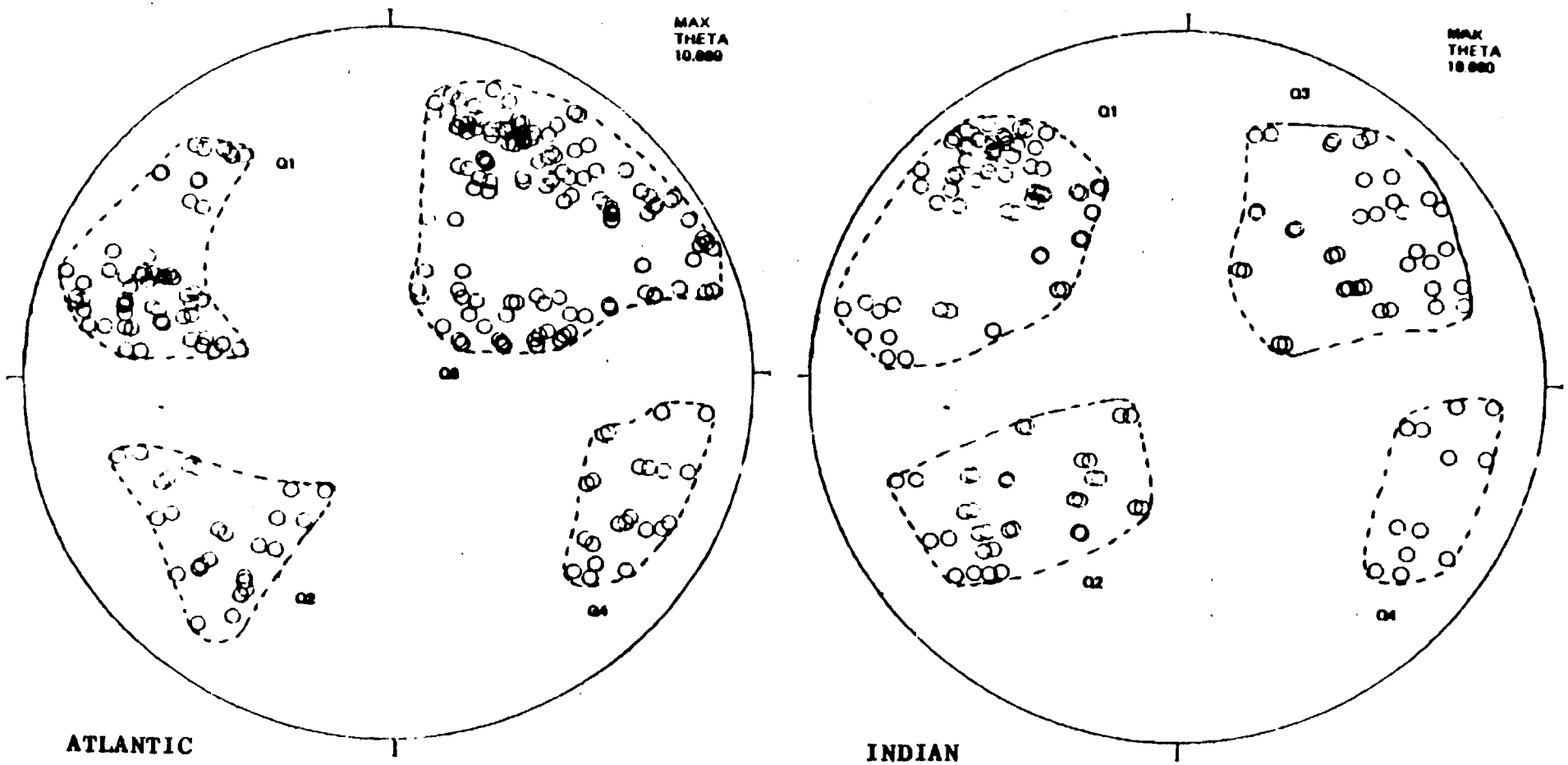

FIG. 3-3. TYPICAL MULTIPLE SHAPED BEAM ANTENNA SCENARIO

One common characteristic of all three systems is that they are all reflector antennas. In a reflector antenna, the pattern shape is controlled by varying both the amplitude and the relative phase between the feed elements. Hence, even if there are only a few elements in a cluster, there should still be enough parameters available per feed to control the pattern shaping, leading again to the conclusion that the adaptive concepts could be used in all three communications systems.

Furthermore, multiple beam antennas with switches to change cluster configurations and an ACTS system with scanning beams are presently available systems, with, if not adaptive, at least reconfigurable antennas. Hence, these systems could be converted into fully adaptive antennas with relative ease.

Finally, there are enough applications (as presented below) suitable for an adaptive system operating in a commerical environment. This should provide sufficient motivation for the market place to come up with the necessary technological advancements to make adaptive systems practical for commercial applications.

4.0 TASK I - ASSESSMENT OF FUTURE COMMERCIAL SATELLITE SYSTEM REQUIREMENTS

The purpose of this task is to identify and assess the feasibility of using adaptive techniques in future commercial satellite communication systems and to quantify the potential benefits.

There are three commercial communication systems which have been considered: the scanning/fixed spot beams, multiple shaped beams, and land-mobile system concepts. These systems are described in Section 3.0.

The purpose of adaptive antenna systems is to enhance existing antenna capabilities. This capability enhancement may be realized at the expense of increased complexity and cost of the system; however, it should not jeopardize the existing antenna coverage requirements. For example, in order to

cancel a jamming signal from an arbitrary direction, the radiation pattern could form a null in that jamming direction adaptively. Due to the finite null width, the EIRP of the area close to the jamming direction will be reduced. If this reduction of EIRP is not acceptable, the employment of such an adaptive mechanism may not be desirable. On the other hand, if the adaptive process reduces interference to the point where signals over part of the coverage area are useful, it may be worthwhile. Based on these important criteria, evaluations of the applicability of adaptive antenna functions to three communication systems have been carried out.

Five adaptive antenna functions have been investigated. These functions are interference control, sidelobe control, accurate beamforming, in-orbit testing and adjustments, and compensation of propagation effects. A separate section is used to address the applicability of each adaptive function to the three communication systems. For each adaptive function, potential applications for the communication systems are described; potential benefits for the space and ground stations are quantified; and the hardware requirements for implementation are assessed. A summary section concludes the efforts on Task I. In the summary section, the applicability of the adaptive functions to the communication systems, the potential benefits for the systems, and the hardware requirements for implementation are compared and summarized.

4.1 Interference Control

4.1.1 Applicability

The use of interference control is widespread in the military sector, where the interference sources are mostly intentional and the jamming scenarios are rapidly varying with time. In commercial communications systems, the sources of interference are assumed to be unintentional and slowly varying. These sources could include ground-based transmissions, cross-link transmissions from other satellites, solar noise, multipath

reflections, and scattering from other antenna systems on the same satellite or platform. The adaptive antenna systems can treat all interference sources alike; the antenna pattern is adjusted to place nulls on interference sources, while disturbing the desired antenna pattern (the quiescent pattern) as little as possible. A pattern null in the jamming direction is formed by adjusting primarily the excitation coefficients of a small number of horns which receive the most jamming signal power. For a multibeam antenna system, a shaped beam is typically formed by a large number of feed elements. Adjusting the excitation coefficients of only a small number of feed elements therefore would not seriously perturb the quiescent pattern. In other words, the adaptive antenna system could cancel the jamming signal without significantly altering the fundamental coverage gain and isolation performance. On the other hand, for the land-mobile systems and the fixed/scanning spot beam systems, a typical spot beam is formed by a 7-horn cluster. Formation of a null could significantly change the quiescent pattern for these two systems. Fortunately, only one or two isolated users need to be served from each spot beam. As far as we can maintain sufficient gain towards the user, we can still implement the adaptive nulling function in the system. This implies that accurate tracking of the users is necessary. Being able to track the users accurately allows us to implement some user-direction constrained adaptive algorithms into the antenna system. Next, we could dynamically steer the 7-horn cluster beam so that the jamming signal is always located in the sidelobe region. Finally, we could dynamically vary the number of horns in the feed cluster so that more degrees of freedom could be available for interference cancellation. Note that the adaptive nulling system would not work if the interfering sources were too close to the users. In that case, certain waveform coding may be required in order to suppress the jamming signals.

4.1.2 Algorithms and Design Parameters

The functional diagram of a typical N-element adaptive nulling system is shown in Figure 2-1. The adaptive nulling system consists of three components. The first component is the antenna. There are two basic approaches to the antenna design: the multiple beam antenna, where each antenna element looks at a different part of the field of view, and the phased array where each element looks at the full field of view. The second component is the adaptive nulling processor, which requires high speed, high reliability, light weight, and low cost. The third component is the adaptive algorithm. There are two major algorithms: Widrow's LMS algorithm and Applebaum's maximum signal-noise-ratio algorithm (see references). Although they differ in their implementations, they are mathematically equivalent. There are many other specific algorithms available in the literature (see references). However, they are all derivatives of these two major kinds.

There are many system parameters affecting the performance of an adaptive nulling system. The primary parameters are the jammer power, gain factor, and the system bandwidth. In order to illustrate the effects of these parameters on the nulling performance, an M-element power inversion array is used as an example.

Problem Formulation

Figure 4.1-1 shows a one-dimensional array with M elements and a single jammer with complex voltage $A_J e^{j\phi_J}$ arriving from a direction θ_J relative to the coordinate system. It is assumed that the power level of any desired signal is below the control loop threshold; consequently, the desired signals are minimized only when they are close to a jamming source. Based on this assumption, the desired signal is not included in the scenario.

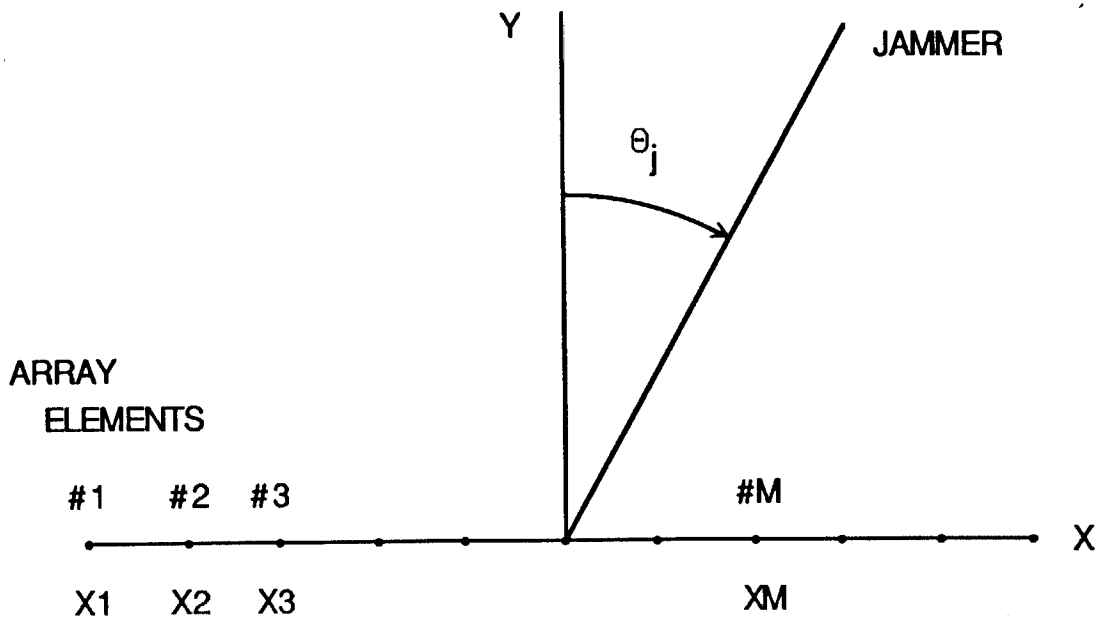

FIG 4.1-1. LINEAR ARRAY CONFIGURATION

The complex voltage received at each antenna is

$$V_i(\theta_J)=[g_i(\theta_J)e^{jkX_i\mathrm{Sin}(\theta_J)}]\bullet(A_J e^{j\phi_J})\ ;\quad i=1,2,.....,M \tag{1}$$

where $g_i(\theta_J)$ is the radiation pattern of ith element,

x_i is the coordinate of ith element, and

k is the wave number.

Define an element signal vector X in which the ith component is V_i in Eq. (1):

$$X=[V_1,V_2,.....V_M]^T \tag{2}$$

The expected value of X^*X^T yields the input correlation matrix associated with the jammer:

$$R_J \triangleq E\{X^* X^T\} \tag{3}$$

The symbol "*" denotes the complex conjugate and the symbol "T" denotes the matrix transpose.

For a broadband system with bandwidth Δf around center frequency f_o, the broadband correlation matrix is

$$R_{\Delta f} = (1/\Delta f)\int_{f_0-\Delta f/2}^{f_0+\Delta f/2} R_J\,\delta f \tag{4}$$

Each component of the matrix $R_{\Delta f}$ is

$$r_{il}' = (1/\Delta f)\int_{f_0-\Delta f/2}^{f_0+\Delta f/2} r_{il}\,\delta f \tag{5}$$

where r_{i1} is the corresponding component of the matrix R_J.

We use Equations (1), (3), and (5) to derive

$$r_{il}' = (1/\Delta f) \int_{f_0-\Delta f/2}^{f_0+\Delta f/2} A_J^2 \cdot g_i^*(\theta_J) \cdot g_l(\theta_J) \cdot e^{j(2\pi f/c)(X_l \mathrm{Sin}\theta_J - X_i \mathrm{Sin}\theta_J)} \cdot \delta f \qquad (6)$$

We assume the antenna element radiation pattern is frequency-independent and define

$$\phi_{il} = \frac{2\pi f_0}{c}(X_l \cdot \mathrm{Sin}\theta_J - X_i \cdot \mathrm{Sin}\theta_J)$$

$$FBW = \Delta f / f_0$$

We obtain

$$r_{il}' = A_J^2 \cdot g_i^*(\theta_J) \cdot g_l(\theta_J) e^{j\phi_{il}} \cdot \mathrm{Sinc}(FBW \cdot \phi_{il}/2) \qquad (7)$$

where $\mathrm{sinc}(1/2 \cdot FBW \cdot \phi_{i\ell}) = \sin(1/2 \cdot FBW \cdot \phi_{i\ell})/(1/2 \cdot FBW \cdot \phi_{i\ell})$

The control equation for the power inversion algorithm is

$$W = (I + \mu R)^{-1} V \qquad (8)$$

where W is the optimum weight vector

I is the identity matrix

μ is the control loop gain factor

R is the correlation matrix

V is the steering vector

For the scenario considered in this communication, we have

$$R \triangleq R_{\Delta f} + R_N$$

where R_N is the receiver noise correlation matrix. It is practical to assume $R_N = \sigma_o^2 I$, where σ_o^2 is the thermal noise power at each element.

The interference-to-receiver noise ratio (INR) before adaptation is

$$INR_b = (V^{*T} R_{\Delta f} V) / (V^{*T} R_N V) \tag{9}$$

The interference-to-receiver noise ratio after adaptation is

$$INR_a = (W^{*T} R_{\Delta f} W) / (W^{*T} R_N W) \tag{10}$$

The ratio between INR_b and INR_a gives a measure of the nulling performance and is defined as the cancellation ratio C,

$$C = INR_a / INR_b \tag{11}$$

An explicit expression for C will be derived for a two-element power inversion array in the following section.

A_Two-Element_Array

For a two-element broadband array with isotropic element pattern and a single jammer, the correlation matrix is

$$R = \begin{bmatrix} A_J^2 + \sigma_0^2 & A_J^2 e^{j\phi_{12}} \cdot \mathrm{Sinc}(FBW\phi_{12} / 2) \\ A_J^2 e^{-j\phi_{12}} \cdot \mathrm{Sinc}(FBW\phi_{12} / 2) & A_J^2 + \sigma_0^2 \end{bmatrix} \tag{12}$$

where

A_J^2 is the jammer power

σ_o^2 is the receiver noise power at each antenna element

FBW is the fractional bandwidth ($= \Delta f / f_o$)

$\phi_{12} = \frac{2\pi f_o}{c} (x_1 \sin\theta_J - x_2 \sin\theta_J)$

x_1 and x_2 are the two antenna element coordinates, and

θ_J is the jammer arrival angle relative to the coordinate system.

Assume the steering vector $V = [1, \ 0]^T$. We substitute Eq. (12) and the steering vector V into Eq. (8) to obtain

$$W = \{[1 + \mu(A_J^2 + \sigma_0^2)]^2 - \mu^2 A_J^4 \mathrm{Sinc}^2(\mathrm{FBW}\phi_{12} / 2)\}^{-1} \cdot [1 + \mu(A_J^2 + \sigma_0^2) \ , \ -\mu A_J^2 e^{-j\phi_{12}} \cdot \mathrm{Sinc}(\mathrm{FBW}\phi_{12} / 2)]^T \quad (13)$$

It is straightforware to derive

$$INR_b = A_J^2 / \sigma_0^2 \quad (14)$$

We use Equations (13), (10), (14), and (11) to derive

$$C = \frac{\{1+\mu(A_J^2+\sigma_0^2)\}^2 - \{2+\mu(A_J^2+2\sigma_0^2)\}\mu A_J^2 \mathrm{Sinc}^2(\mathrm{FBW}\phi_{12} / 2)}{\{1+\mu(A_J^2+\sigma_0)^2\}^2 + \mu^2 A_J^4 \mathrm{Sinc}^2(\mathrm{FBW}\phi_{12} / 2)} \quad (15)$$

Equation (15) indicates that the cancellation ratio depends on the jammer power A_J^2, the gain factor μ, the fractional bandwidth FBW and the interelement phase delay ϕ_{12}. Since the receiver noise power σ_o^2 is generally small compared to the jammer power, it does not affect the cancellation ratio.

Several interesting conclusions can be drawn by analyzing Eq. (15). Note that the first term of the numerator and the first term of the denominator in Equation (15) are positive and identical. The second term of both numerator and denominator has a common factor $\mathrm{sinc}^2(1/2 \cdot FBW \cdot \phi_{12})$. Since $1 \geq \mathrm{sinc}^2(1/2 \cdot FBW \cdot \phi_{12}) \geq 0$, the denominator is always positive. The numerator is

$$\{1+\mu(A_J^2+\sigma_0^2)\}^2 - \{2+\mu(A_J^2+2\sigma_0^2)\}\mu A_J^2 \mathrm{Sinc}^2(FBW\phi_{12}/2)$$
$$\geq \{1+\mu(A_J^2+\sigma_0^2)\}^2 - \{2+\mu(A_J^2+2\sigma_0^2)\}\mu A_J^2$$
$$= (1+\mu\sigma_0^2)^2$$

The numerator is therefore also positive. In sum, we conclude that $1 \geq C > 0$. (The ratio C could approach zero for certain theoretical extremes as discussed later).

We next explore the relationship between the cancellation ratio and the gain factor and jammer power. Let bandwidth be equal to zero, i.e. $\mathrm{sinc}(1/2 \cdot FBW \cdot \phi_{12}) = 1$. We obtain

$$C = \frac{(1+\mu\sigma_0^2)^2}{(1+\mu\sigma_0^2+\mu A_J^2)^2 + \mu^2 A_J^4} \tag{16}$$

For either $\mu = 0$ or $A_J^2 = 0$, we obtain C = 1; and the array will not cancel any jamming power. It is straightforward to derive

$$\frac{\delta C}{\delta \mu} = -\frac{(1+\mu\sigma_0^2)(2A_J^2+2\mu\sigma_0^2A_J^2+4\mu A_J^4)}{\{(1+\mu\sigma_0^2+\mu A_J^2)^2+\mu^2A_J^4\}^2} \tag{17}$$

$$\frac{\delta C}{\delta A_J^2} = -\frac{(1+\mu\sigma_0^2)^2\{2\mu(1+\mu\sigma_0^2+\mu A_J^2)+2\mu^2A_J^4\}}{\{(1+\mu\sigma_0^2+\mu A_J^2)^2+\mu^2A_J^4\}^2} \tag{18}$$

Equations (17) and (18) indicate that the cancellation ratio C is a decreasing monotonic function for both gain factor μ and jammer power A_J^2. Theoretically, if either μ or A_J^2 grows extremely large, the ratio C could approach zero. That is, the system is completely blanked (no signals received).

We finally investigate the effect of bandwidth on cancellation ratio. Equation (15) indicates that the bandwidth affects the cancellation ratio throught term $\text{sinc}^2(1/2 \cdot FBW \cdot \phi_{12})$. If the argument in the sinc function grows large, the numerator in Equation (15) will get larger and the denominator will get smaller. Consequently, the cancellation ratio will get larger. For any extremely large argument in the sinc function, the cancellation ratio could approach unity. That is, the nulling capability of the system is totally destroyed.

The argument in the sinc function is

$$FBW\ \phi_{12} / 2 = FBW \cdot 2\pi \cdot (f_0 / C) \cdot (X_1 - X_2) \cdot \text{Sin}\theta_J / 2$$
$$= \pi \cdot FBW \cdot (D / \lambda) \cdot \text{Sin}\theta_J$$

The parameters associated with bandwidth affecting the cancellation ratio are FBW, (D/λ), and $\sin\theta_J$. If any of these parameters grows large, the nulling capability of the array will be reduced.

As a summary, we have shown that the cancellation ratio is a decreasing monotonic function for both gain factor and jammer power. The system bandwidth affects the cancellation ratio through the term $\text{sinc}^2\left(FBW \cdot \frac{D}{\lambda} \sin\theta_J\right)$.

If the argument in the sinc function grows extremely large, the array cancellation performance will severely deteriorate.

The above conclusions apply, in general, to a more complicated system such as a multiple-jammers scenario with a multiple beam antenna, except that the interaction between the various parameters would become more complex.

Iterative Algorithm

In the hardware implementation the control equation (8) is converted into an iterative algorithm.

$$W(n+1) = \alpha\, W(n) - \beta\, R\, W(n) + (1-\alpha)\, V \qquad (19)$$

where

W(n+1) is the new weight vector,

W(n) is the previous weight vector,

RW(n) is the correlation vector,

V is the steering vector,

α and β are constants

The two control factors "alpha" and "beta" are related to the gain factor by

$$\mu = \beta / (1-\alpha) \qquad (20)$$

In order for the iterative process to converge to the optimal solution, "alpha" and "beta" must be chosen to satisfy

$$1 > \alpha > 0, \text{ and } 2/\lambda_{max} > \beta > 0 \qquad (21)$$

where λ_{max} is the largest eigenvalue of the correlation matrix.

The total output power of all elements is given by

$$\sum_{k=1}^{L} \lambda_k = \sum_{k=1}^{L} \langle |X_k|^2 \rangle \qquad (22)$$

where

L is the number elements in the MBA, and

X is the total signal measured at element k.

Since $\langle X^{*T} X \rangle = \sum_{k=1}^{L} \langle |X_k|^2 \rangle = \sum_{k=1}^{L} \lambda_k > \lambda_{max}$ we can derive

$$(2 / \langle X^{*T} X \rangle) > \beta > 0 \qquad (23)$$

Since the total output power $\langle X^{*T} X \rangle$ is known or can be measured, equation (23) is normally used. Note that

(a) Small beta results in slow convergence.

(b) Large beta results in fast convergence.

(c) If beta exceeds the upper bound in equation (23), the iterative process becomes unstable.

(d) Small alpha results in small interference cancellation.

(e) Large alpha results in large interference cancellation.

These theoretical expectations are verified by the simulation data presented below.

Typical simulation data are shown in Figures 4.1-2 and 4.1-3. Figure 4.1-2 shows the results for different "beta" factors, keeping "alpha" constant (=0.99), and verifies theoretical expectations (a), (b), and (c). Figure 4.1-3 compares results for different "alpha" factors, while keeping "beta" = 0.20, and confirms theoretical expectations (d) and (e).

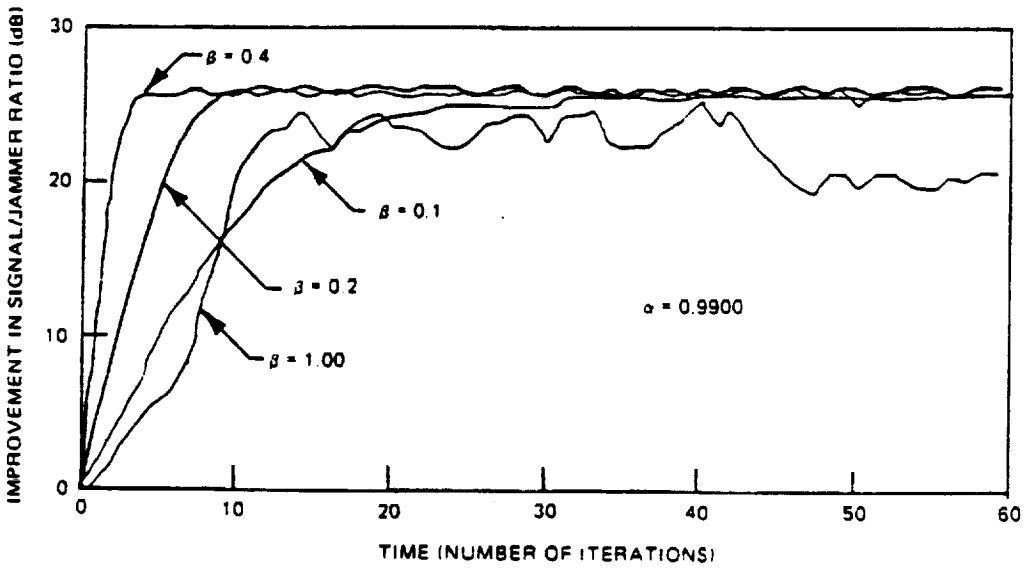

FIG. 4.1-2. EFFECT OF "BETA" ON CONVERGENCE SPEED

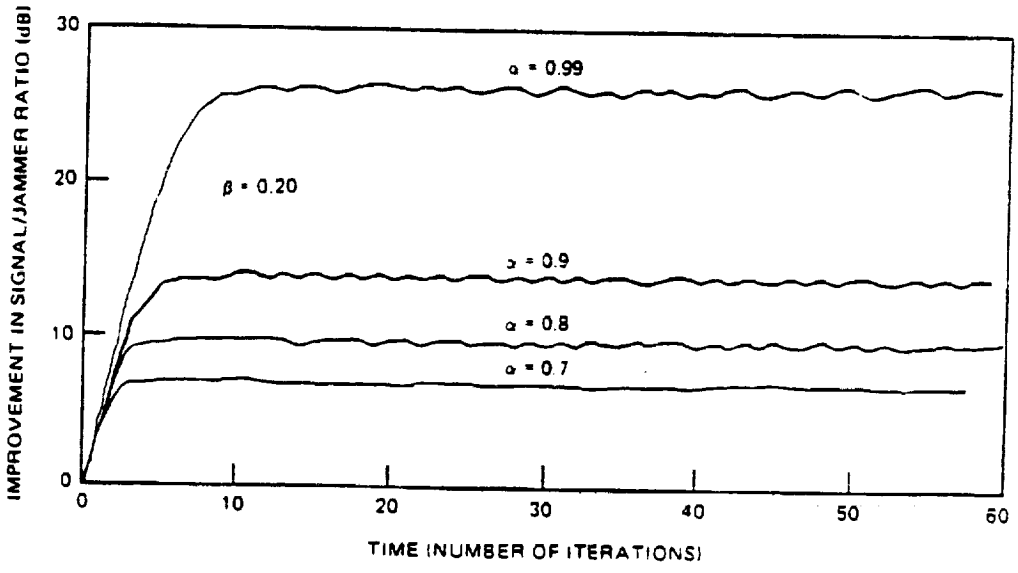

FIG. 4.1-3. EFFECT OF "ALPHA" ON CANCELLATION LEVEL

4.1.3 Potential Benefits

In order to quantify the benefits for the space and ground stations, a typical land-mobile system is used as an example.

Multiple spot-beam coverage of the CONUS can be provided through use of a large satellite antenna in a land-mobile system. A seven-horn cluster provides a typical spot beam coverage as shown in Figure 4.1-4. The satellite antenna can be a center-fed reflector antenna or an offset-fed reflector antenna. The offset-fed reflector normally has a higher efficiency and a lower sidelobe due to elimination of signal blockage. However, the design of an offset reflector is normally more complex than that of a center-fed reflector. We assume the satellite antenna uses an offset reflector antenna and a typical beam of the antenna has a peak gain of 48 dBi with a 20 dB sidelobe. Tables 4.1-1 and 4.1-2 summarize a typical nominal link budget for uplink and downlink, respectivley, of such a system.

Table 4.1-1 Mobile to Satellite Link Budget (826 MHz)

Transmit Power/Channel, dBw	4.8 (3 W)
Line Loss, dB	-1.0
Transmit Antenna Gain, dB	9.0
Ground EIRP, dBw	12.8
Multipath Loss, dB	-5.0
Path Loss	-182.6
Pointing Loss, dB	-4.0
Beam Jitter, dB	-1.0
Polarization Loss, dB	-0.5
Receive Antenna Gain, dB	47.7
Circuit Loss, dB	-1.0
Received Carrier Power, dBw	-133.6
Receive System Noise Temperature, dB-k	26.8
Boltzman's Constant	-228.6
Carrier Noise Bandwidth	40.4
Received Noise Power, dBw	-161.4
C/N, dB	27.8

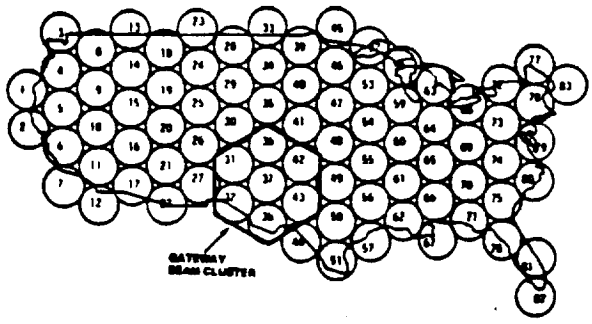

FIG. 4.1-4. TYPICAL CONUS-COVERAGE PATTERN

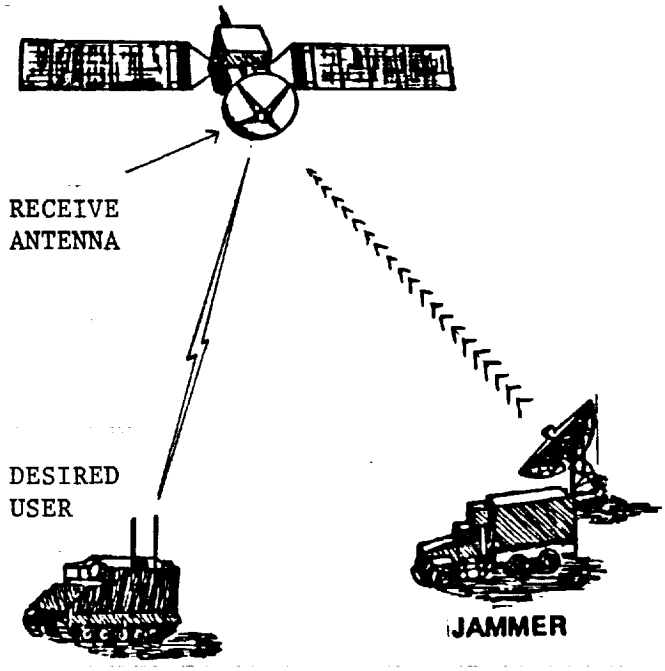

FIG. 4.1-5. JAMMING SCENARIO

Table 4.1-2 Satellite-to-Mobile Link Budget (871 MHz)

Transmit Power/Channel, dBw	-7.7 (0.17 W)
Circuit Loss, dB	-1.0
Transmit Antenna Gain, dB	48.1
Satellite EIRP, dBw	39.4
Pointing Loss, dB	-4.0
Beam Jitter Loss, dB	-1.0
Path Loss, dB	-183.0
Multipath Loss, dB	-5.0
Polarization Loss, dB	-0.5
Receive Antenna Gain, dB	9.0
Line Loss, dB	-1.0
Received Carrier Power, dBw	-146.1
Receive System Noise Temperature, dB-k	27.6
Boltzman's Constant, dBw/K-Hz	-228.6
Carrier Noise Bandwidth, dB-Hz	40.4
Received Noise Power, dBw	-160.6
C/N, dB	14.5

Assume a strong jamming signal interferes with the uplink channel and the received power at the satellite due to this jammer is -113.6 dBw. (See Figure 4.1-5). This jamming signal would degrade the satellite G/T as well as the uplink C/N (carrier-to-noise ratio). In order to restore the nominal C/N, the conventional approach is to increase the ground EIRP to overpower the jamming signal. The disadvantage of this approach is the tremendous extra power margin required; this additional power increase may be beyond the capability of the existing ground terminal design. With an adaptive antenna system, the power of the jamming signal can be significantly reduced before it enters the satellite receiver. This system therefore is able to improve the satellite G/T and the uplink C/N. The additional ground EIRP required in order to maintain the nominal C/N could also be significantly reduced or completely avoided. Table 4.1-3 summarizes the satellite G/T, the uplink C/N and the ground EIRP required in order to maintain the nominal C/N for the system with a conventional antenna and with an adaptive antenna system in the jamming environment.

Table 4.1-3 Performance Comparisons Between Conventional Antenna & Adaptive Antenna

Jammer Cancellation Parameters	Nominal Link	with -113.6 dBw Jammer	10 dB Jammer Cancel	20 dB Jammer Cancel	30 dB Jammer Cancel	40 dB Jammer Cancel	50 dB Jammer Cancel
Satellite G/T (dB/k)	20.9	-26.9	-16.9	-6.9	3.0	12.4	20.1
Uplink C/N (dB)	27.8	-20.0	-10.0	0.0	9.9	19.3	27.0
Ground EIRP required to maintain nominal C/N (dBw)	12.8	60.6	50.6	40.6	30.7	21.3	13.6
Additional Ground EIRP (dB)	0	47.8	37.8	27.8	17.9	8.5	0.8

Table 4.1-3 shows that with a conventional antenna, the jammer would degrade the satellite G/T from 20.9 dB/k into -26.9 dB/k, the uplink C/N from 27.8 dB into -20.0 dB and a huge 47.8 dBw additional ground EIRP is required in order to maintain the nominal uplink C/N. With an adaptive antenna system, both the satellite G/T and the uplink C/N improve and the additional ground EIRP decreases. With a 50 dB jammer cancellation, both the satellite G/T and the uplink C/N almost recover to their nominal values and the additional ground EIRP required in order to maintain the nominal C/N is only a modest 0.8 dB.

The above example demonstrates how an adaptive antenna system could benefit the space and ground stations in terms of satellite G/T improvement and decrease in ground EIRP margin requirement in a jamming environment. Although the above example uses a land-mobile system, the same conclusions directly apply to the multiple shaped beam systems and the scanning/fixed spot beam systems except that the extent of improvements would vary.

We have not addressed the issue of how to implement the adaptive nulling system in order to achieve the desired jamming cancellation. The implementation depends on several factors such as the type of communication system, the jamming scenario, the format of multiple-access, the system bandwidth, and the hardware limitations. The selection of a particular adaptive antenna

system includes the selection of the antenna design, the selection of adaptive algorithms, and the selection of the microprocessor.

A complete tradeoff study on this subject is highly complex and requires extensive computer simulation and hardware experiments, which is beyond the scope of this contract. However, it would be an important topic for follow-up efforts after this contract.

4.1.4 Hardware Requirements

The hardware requirements for an adaptive nulling system depend on the specific algorithm implemented in the nulling processor. There are many nulling algorithms available in the literature. However, most of them are derivatives of two major kinds - Howell-Applebaum algorithm and LMS algorithm. This report focuses on the hardware requirements of these two algorithms, Figures 4.1-6 and 4.1-7 illustrate the configurations of a typical Howell-Applebaum nulling system and a typical LMS nulling system, respectively. The figures indicate that the hardware common to both nulling systems is:

1. Sampling couplers on each antenna element channel and a separate coupler on the beamforming network output port.
2. A signal summer combining the signal in each element channel, which could be in the form of a hybrid.
3. Phase and amplitude controls for individual antenna elements.
4. A signal correlator.
5. A switch, switching each element channel to the input port of the correlator.
6. A microprocessor.
7. Connecting waveguides.

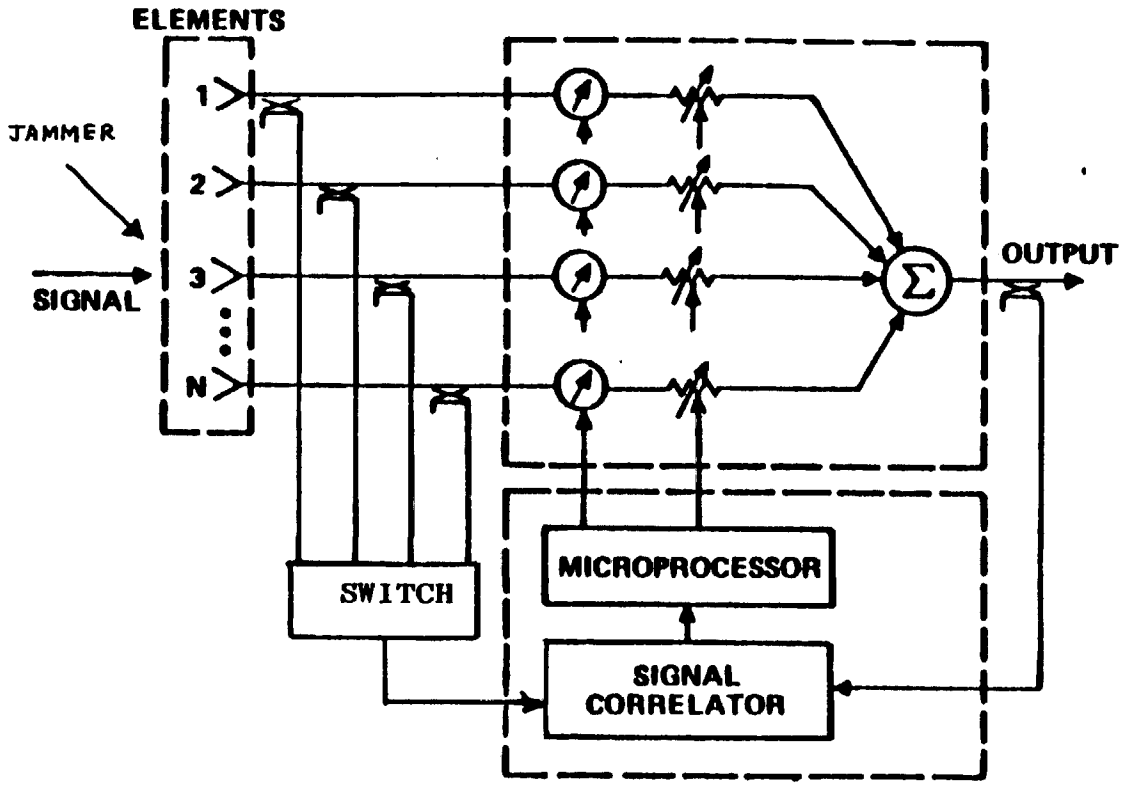

FIG. 4.1-6. CONFIGURATION OF TYPICAL HOWELL-APPLEBAUM ADAPTIVE NULLING SYSTEM

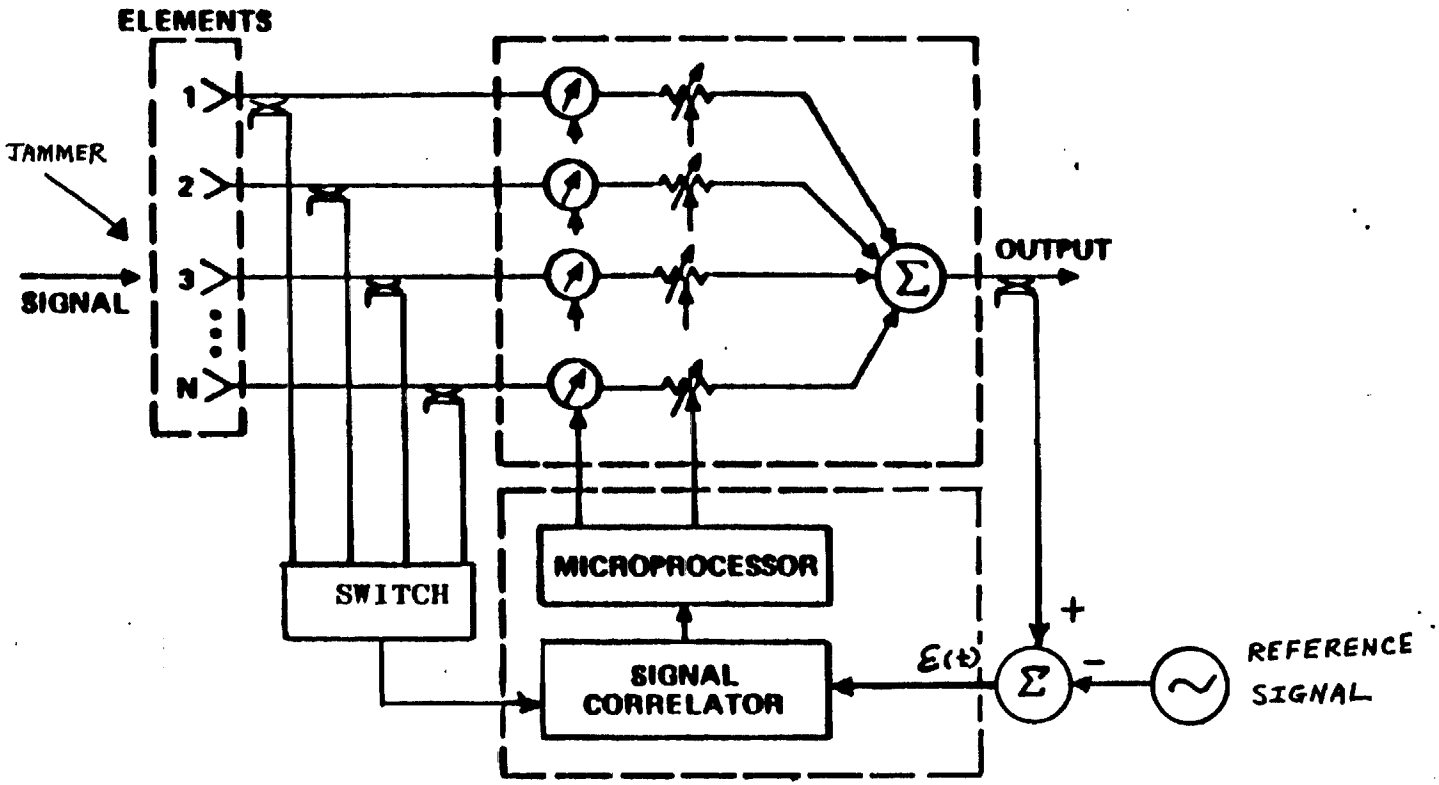

FIG. 4.1-7. CONFIGURATION OF TYPICAL LMS ADAPTIVE NULLING SYSTEM

The LMS system requires two additional pieces of hardware, i.e., an additional signal summer and a reference signal generation. The software codes implemented in the microprocessor are also different for each nulling system.

The signal correlator, which correlates the signal in the individual channel and the signal in the sum channel, is a very important component in the nulling system. Based on the correlator output, the microprocessor is able to carry out the nulling algorithm adaptively. Figure 4.1-8 shows the configuration of a typical correlator. The figure indicates that the correlator consists of four hybrids, four diodes, two video amplifiers, two integrators, and two analog-to-digital converters. The correlator accepts two signals of the same frequency and provides outputs with relative phase and amplitude information. Two RF input signals of amplitude A and phase α, amplitude B and phase β provide four video output signals V_1, V_2, V_3, and V_4. The video signals are given by the following expressions:

$$V_1 = |Ae^{j\alpha} + Be^{j\beta}|^2 = A^2 + B^2 + 2AB\,\mathrm{Cos}(\alpha-\beta)$$

$$V_2 = |Ae^{j\alpha} + Be^{j(\beta+\pi)}|^2 = A^2 + B^2 - 2AB\,\mathrm{Cos}(\alpha-\beta)$$

$$V_3 = |Ae^{j\alpha} + Be^{j(\beta+\pi/2)}|^2 = A^2 + B^2 + 2AB\,\mathrm{Sin}(\alpha-\beta)$$

$$V_4 = |Ae^{j\alpha} + Be^{j(\beta-\pi/2)}|^2 = A^2 + B^2 - 2AB\,\mathrm{Sin}(\alpha-\beta)$$

Each pair of two video signals is combined and amplified in an AC-coupled, low noise video amplifier. The outputs of the video amplifiers are integrated over a time period corresponding to the video bandwidth. The signals are then converted into digital numbers through two analog-to-digital converters. The final outputs of the correlator are the in-phase (I) and quadrature (Q) components of the two RF signals. I and Q are given by:

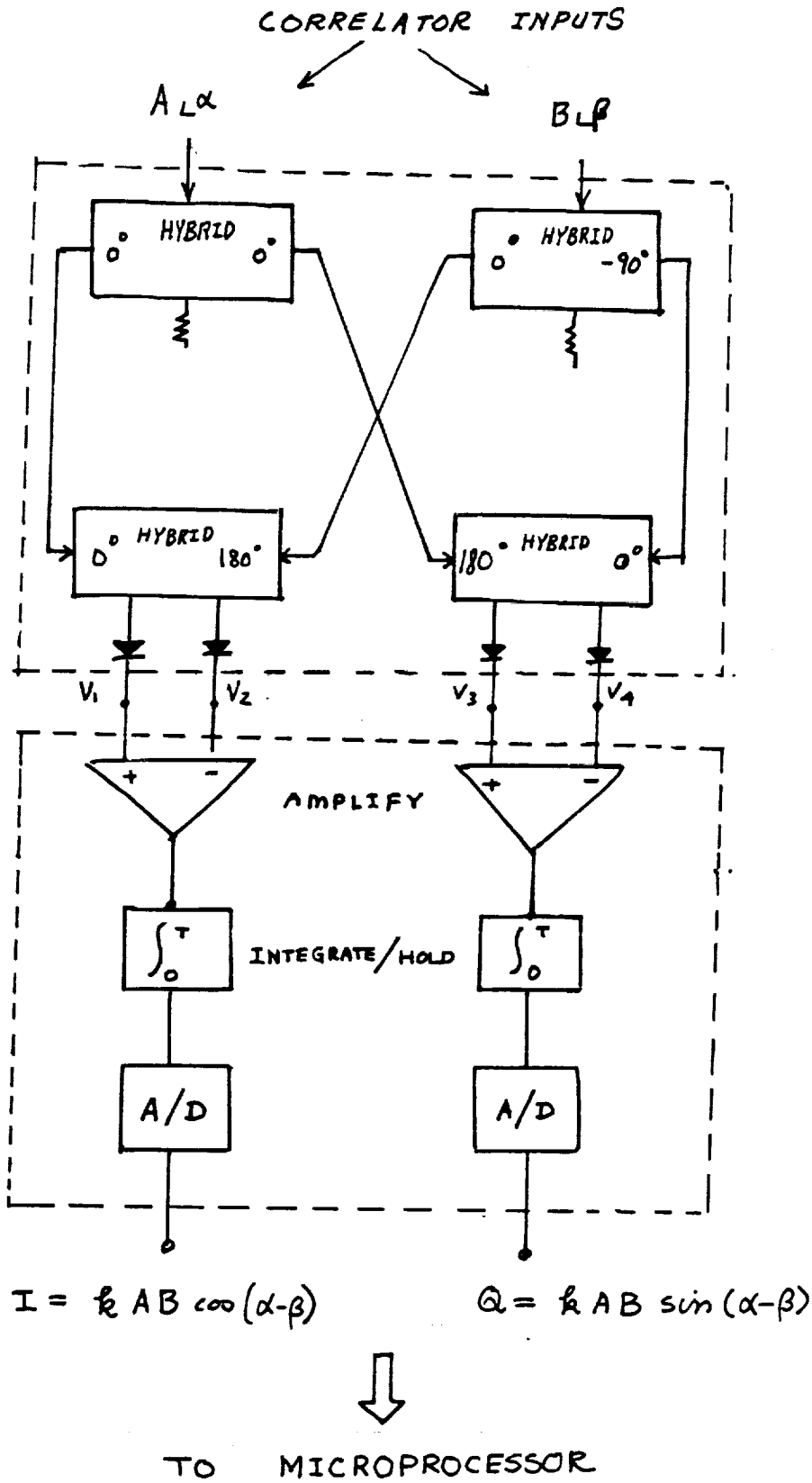

FIG. 4.1-8. CONFIGURATION OF A TYPICAL CORRELATOR

$$I = k\,AB\,\cos(\alpha-\beta)$$
$$Q = k\,AB\,\sin(\alpha-\beta)$$

where k is a constant.

The hardware requirements mentioned above are for a typical multiple shaped beam system. For a land-mobile system and a fixed/scanning spot beam system, additional hardware is required, as follows:

(1) Hardware for accurate tracking of users,

(2) Hardware for switching the number of feed elements.

4.2 Sidelobe Control

4.2.1 Applicability

An important constraint on the performance of multiple beam antenna systems with frequency reuse is the sidelobe isolation between beams. Typical antenna systems are designed with worst case edge-of-coverage gain and isolation specifications. Since the ground stations may not all be in use at one time, considerably relaxed overall specifications or much better particular specifications could be achieved for any one communications scenario if the antenna pattern were optimized for that scenario. An adaptive antenna system has the potential for so doing, given the inputs on the current ground stations in use.

For a multiple shaped beam system, adaptive sidelobe control implies that the excitation coefficients of those feed elements which directly affect that particular sidelobe requirement need to be adaptively adjusted. Since the number of feed elements whose excitation coefficients need to be significantly adjusted is relatively small compared to the total number of feed elements, the quiescent pattern is not expected to change very much.

On the other hand, for the land-mobile systems and the fixed/scanning spot beam systems, a typical spot beam is formed by a 7-horn cluster. Adaptive sidelobe control for certain coverage areas may jeopardize the gain

requirement and the sidelobe requirement for other coverage areas. The three measures suggested for interference control can also apply here. First, the spacecraft has to track the user accurately so that the antenna beam always provides sufficient gain towards the user. Second, we could dynamically steer the beam so that sufficient separation between two adjacent beams with the same polarization could be maintained. Last, we could dynamically vary the number of horns so that more degrees of freedom could be available for sidelobe control. Apparently, when sidelobe isolation becomes insufficient, polarization diversity has to be used in order to achieve the required beam isolation.

4.2.2 Potential Benefits

In order to quantify the potential benefits of this function for the space and ground stations, we use the same land-mobile system described in the previous section as an example. Again, we focus on the uplink channel. The nominal uplink budget is summarized in Table 4.1-1. The nominal satellite receive antenna has a 47.7 dB gain and a 20 dB sidelobe.

Assume an adjacent mobile station also transmits with the same ground EIRP (12.8 dBw). This signal would enter the satellite receiver through sidelobes and interfere with the nominal uplink communication. In order to reduce this sidelobe interference the 7-horn cluster beam could be reconfigured to provide a lower sidelobe at the expense of a slightly reduced gain. Table 4.2-1 summarizes a typical tradeoff between gain and sidelobe of a satellite receive station.

Table 4.2-1 A Typical Tradeoff Between Gain and Sidelobe

GAIN (dB)	SIDELOBE (dB)
48.6	15
47.7	20
46.8	25
45.9	30

On the other hand, if there is no adjacent mobile station transmitting, we could reconfigure the 7-horn cluster beam to provide a higher gain at the expense of a slightly higher sidelobe. Based on the assumed relation between the gain and sidelobe of Table 4.2-1 the satellite G/T, the uplink C/N, and the ground EIRP required in order to maintain the nominal C/N for the systems are summarized in Table 4.2-2 for various sidelobe levels.

Table 4.2-2 Performance Summary for Various Sidelobe Levels

Jammer Cancellation Parameters	Nominal Link	with SL Interfer. 20 dB SLL	with SL Interfer. 25 dB SLL	with SL Interfer. 30 dB SLL	with no SL Interfer.
Satellite G/T (dB/k)	20.9	12.4	15.4	18.3	21.8
Uplink C/N (dB)	27.8	19.3	22.3	25.2	28.7
Ground EIRP required to maintain nominal C/N (dBw)	12.8	21.3	18.3	15.4	11.9
Additional Ground EIRP (dBw)	0	8.5	5.5	2.6	-0.9

Table 4.2-2 indicates that the sidelobe interference would degrade the satellite G/T from 20.9 dB/k to 12.4 dB/k, the uplink C/N from 27.8 dB to 19.3 dB, and requires 8.5 dB additional ground EIRP in order to maintain the nominal uplink C/N. With sidelobe control capability, both satellite G/T and uplink C/N improve, and the additional ground EIRP decreases. If there is no adjacent station transmitting, we could reconfigure the beam to obtain a higher gain at the expense of a slightly higher sidelobe. In that case, we would actually increase the satellite G/T from 20.9 dB/k to 21.8 dB/k, the uplink C/N from 27.8 dB to 28.7 dB, or decrease the ground EIRP margin by 0.9 dB. The above example demonstrates how adaptive sidelobe control systems could benefit the space and ground stations in terms of satellite G/T improvement and decreases in ground EIRP margin requirements. These conclusions also apply to the multiple shaped beam systems and the fixed/scanning beam systems except that the extent of improvement would vary.

4.2.3 Hardware Requirements

The application of sidelobe control requires inputs from ground stations. For uplink channels, the ground station transmits; the satellite antenna then measures the sidelobe level and proceeds to adjust its excitation coefficients. For downlink channels, the satellite antenna transmits; the ground station measures the sidelobe and then gives the command to reconfigure the excitation coefficients of the satellite transmit antenna. The scenarios are shown in Figures 4.2-1 and 2.

Based on the discussions above, the necessary hardwares to implement adaptive sidelobe control are:

1. Instruments for sidelobe level measurements.
2. Sidelobe level comparators, which compare the measured sidelobe level to the desired sidelobe level.

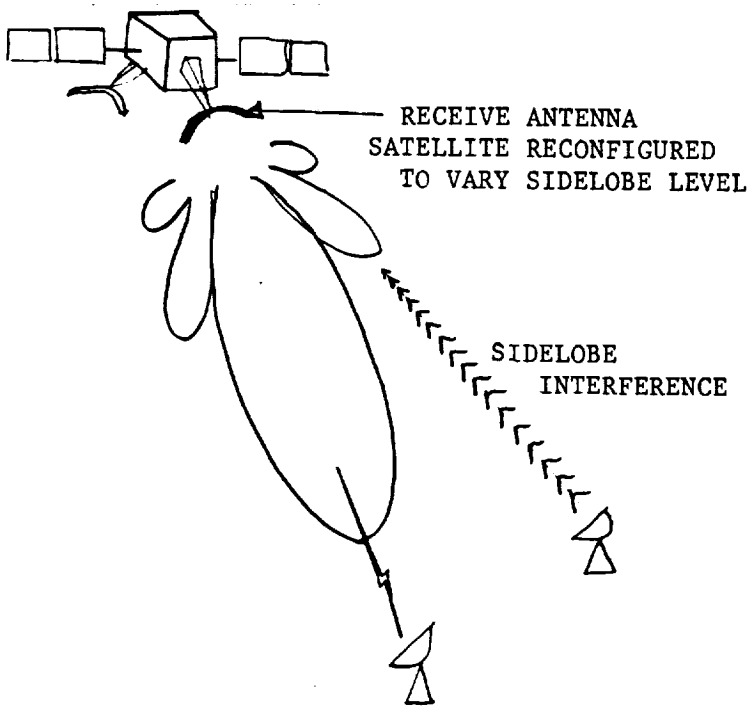

FIG. 4.2-1. SIDELOBE CONTROL (SATELLITE RECEIVES)

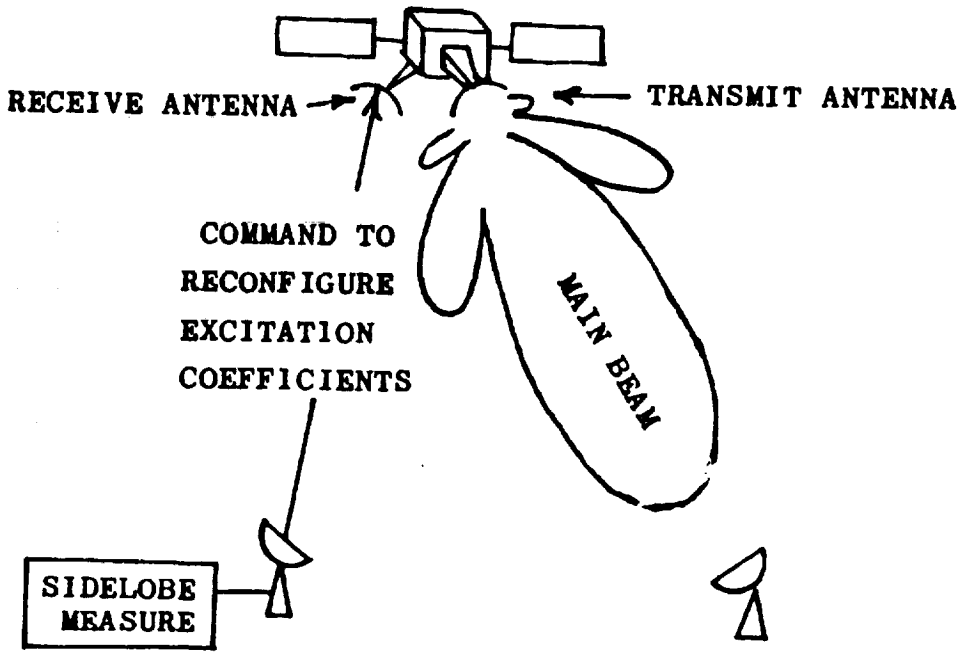

FIG. 4.2-2. SIDELOBE CONTROL (SATELLITE TRANSMITS)

3. A microprocessor to reoptimize the excitation coefficients in order to generate the desired sidelobe level.
4. Phase and amplitude controls for individual antenna elements.

The hardware requirements mentioned above are for a typical multiple shaped beam system. For a land-mobile system and a fixed/scanning spot beam system, additional hardware are required, which are:

1. Hardware for accurate tracking of users,
2. Hardware for switching the number of feed elements.

4.3 Precision Beam Forming

4.3.1 Applicability

Accurate antenna beam pointing is always an important issue for satellite communication systems. The pointing errors could be due to the setting uncertainty in the beamforming network. A number of sources of error may contribute to the setting uncertainty. These errors may be due to incorrect calibration, limited setting accuracy, temperature variation, or component failure. An adaptive antenna system with an on-board reference signal could detect the setting error and correct that error automatically through a feedback control loop. The pointing errors could also be due to antenna attitude changes relative to the spacecraft, antenna misalignment, or reflector surface deformation. Each of these cases would require a ground based referenced signal for the feedback control. The detection and correction of the errors in the beamforming network will be discussed in the next section. This section focuses on the errors caused by antenna mechanical or thermal changes.

Accurate beam pointing can be accomplished through an open-loop or a closed-loop algorithm. A closed-loop algorithm for accurate beam pointing is described in Section 5.4 of this report. This section focuses on the open-loop algorithms.

The open-loop algorithm is a two part process which requires detection of the pointing errors and correction for those errors. The detection part of the process requires beacon signals transmitted from ground stations. The antenna then determines the directions of the beacon signals through some direction finding techniques. The difference between the measured direction-of-arrival (DOA) and the desired DOA is the amount of pointing error.

The detection part of the process is essentially a direction-finding problem. One approach to solving this problem is introduced in Section 5.1. This approach determines the direction of arrival of a signal by comparing relative amplitudes of voltages in each of three adjacent horns in a single cluster. The particular cluster to be chosen would be the one whose horns receive the most power in the entire array. This approach is shown to have an accuracy better than 0.03 beamwidth, depending on the feed configuration utilized. This technique is good only for locating a single beam signal in a multiple beam antenna system.

Another approach to solving the direction-finding problem is the popular multiple signal characterization (MUSIC) algorithm (see references). This approach can provide estimates of:

1. number of signals (up to [N-1] signals, where N is the number of feed elements);
2. directions of arrival (DOA);
3. strengths and cross correlations among the directional waveforms;
4. polarizations;
5. strength of noise/interference.

The technique is shown to have good accuracy and is applicable for both multiple beam antennas and phased arrays. It is based on the eigen-analysis of the measured correlation matrix R. Each element r_{ij} of the matrix R

represents the cross correlation between the output at ith feed element and the output of jth feed element. The basic technique works as follows:

1. the correlator produces the cross correlation of the ith channel output and the jth channel output through quadrature detection;
2. the correlation matrix R is formed and the eigen structure computed to decide the number of sources;
3. the DOA spectrum is computed to find the peaks;
4. the source parameters are calculated to determine strength, polarization, and correlation.

The technique relies heavily on computations. Since we are interested only in the directions of arrival of beacon signals, step 4 is not required, avoiding some additional computation.

After the detection part of the process is completed, the microprocessor measures the amount of pointing error and compensates for it through resetting the excitation coefficients. The above-mentioned measures for accurate beamforming apply to all three communication systems.

4.3.2 Potential Benefits

In evaluating an antenna coverage gain, we normally have to include the antenna pointing error loss. The size of the pointing error is typically on the order of $\pm 0.1^{o}$ seen from synchronous orbit. This size of pointing error will result in an additional EOC (edge of coverage) gain reduction, the amount of which depends on the gain slope at each particular coverage point. For example, the nominal uplink budget summarized in Table 4.1-1 already includes a 4 dB pointing loss. If the system has an adaptive accurate beamforming capability, the pointing error loss can be reduced or completely eliminated. Suppose we reduce the pointing loss from 4 dB to 0.5 dB by accurate beamforming. This loss reduction would improve the uplink C/N by 3.5 dB. Equivalently, we could lower the ground EIRP or spacecraft G/T by

3.5 dB and still maintain the nominal uplink C/N. Similarly, the nominal downlink budget summarized in Table 4.1-2 also includes a 4 dB pointing loss. The same adaptive accurate beamforming mechanism could reduce the pointing error loss from 4 dB to 0.5 dB. By the same token, this loss reduction could improve the downlink C/N by 3.5 dB. The benefits of accurate beamforming for the space and ground stations in terms of reduced margin requirements in EIRP or G/T can be significant. These conclusions also apply to the multiple shaped beam systems and the fixed/scanning spot beam systems.

4.3.3 Hardware Requirements

The configuration and the hardware associated with the open-loop algorithm based on amplitude comparison are described in Section 5 of this report. The configuration of the MUSIC algorithm is shown in Figure 4.3-1. The figure indicates that the required hardwares to implement this algorithm are:

1. Sampling couplers on each antenna element channel.
2. A signal summer combining the signal in each element channel, which could be in the form of a hybrid.
3. Phase and amplitude controls for individual antenna elements.
4. A signal correlator.
5. A switch, switching each element channel to the input port of the correlator.
6. A microprocessor.
7. Connecting waveguide.

Note that the hardware requirements for this algorithm are similar to those for interference control except that the software implemented in the microprocessor would be different. The hardware requirements mentioned above are the same for all three communication systems.

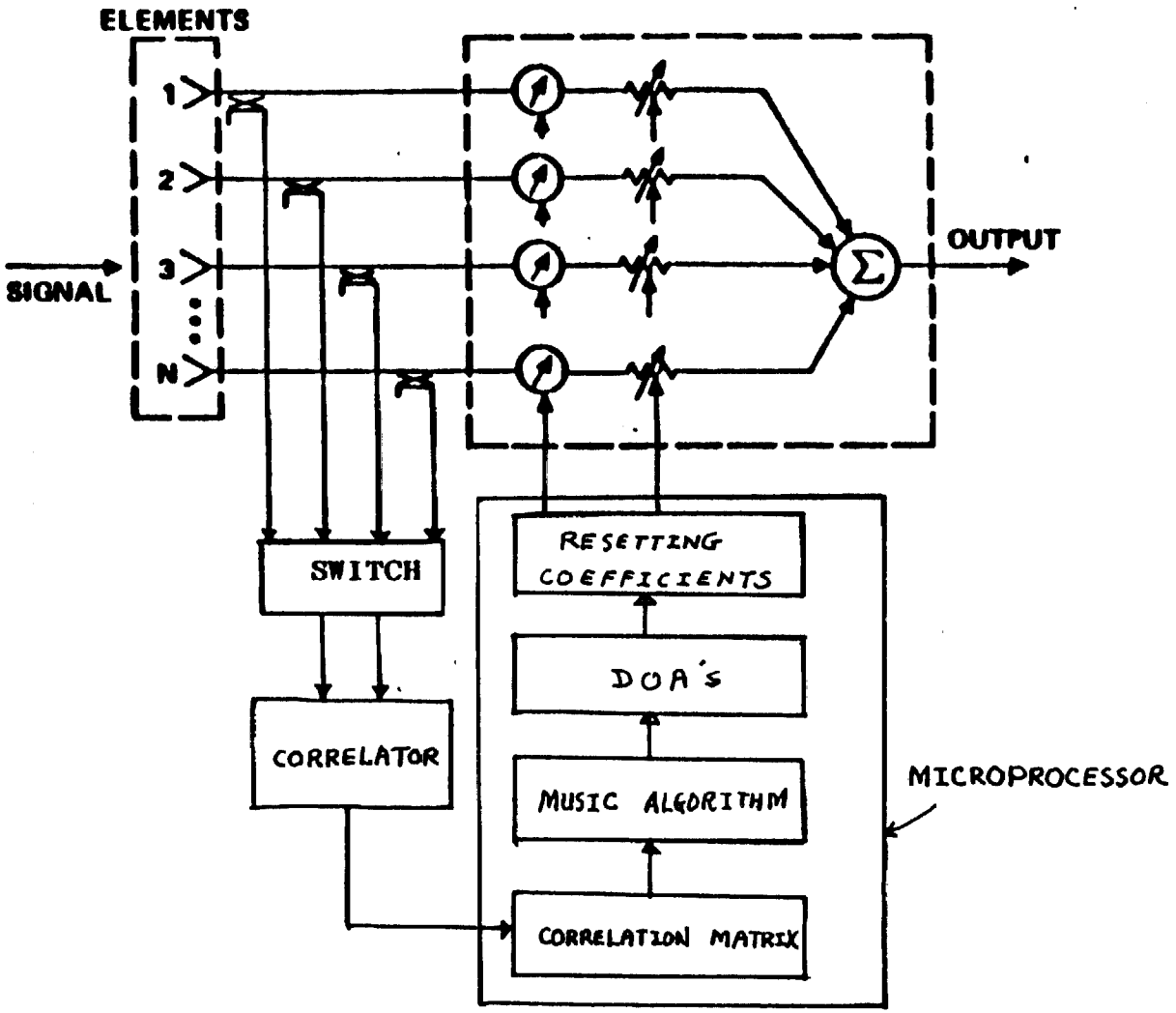

FIG. 4.3-1. HARDWARE IMPLEMENTATION FOR MUSIC ALGORITHM

4.4 In-Orbit Adjustment and Testing of Antenna Systems

4.4.1 Applicability

In order to design an advanced antenna system and verify its performance, complex range testing is normally required. Limitations on range accuracy in assessing several key parameters, such as sidelobe requirements in excess of 30 dB, may result in increased margin requirements (i.e. <-33 dB sidelobes) for testing, which in turn may lead to overdesigned systems. Additionally, in spite of all ground testing, the testing range environments are still different from the true space environments. Furthermore, vibrations during the satellite launch process could cause certain antenna structures or components to deviate from their designed conditions. All these considerations could make the antenna performance in space different from the predicted performance based on the range test results. Therefore, in-orbit testing and subsequent adjusting of the antenna pattern are very desirable. An adaptive antenna has the potential for such an application. A special algorithm could be used to adjust the complex weight of each antenna element based on an earth-based or a space-based reference signal. Such an adaptive algorithm for in-orbit adjustment and testing applies to all three communication systems.

4.4.2 Potential Benefits

The purpose of in-orbit testing and adjustments is to detect and correct any antenna performance deterioration due to errors in the beamforming network. The sources of errors in the beamforming network include coefficient setting uncertainty and component aging or failure. Any combination of these errors could result in beam shift, alteration in the pattern shape, or high sidelobe levels. With the capability of in-orbit testing and adjustments, such performance deterioration can be reduced significantly or completely eliminated. In order to quantify the benefits for the space and

ground stations, we use the same land-mobile system described in the previous section as an example.

Suppose there is a coefficient setting error in the beamforming network of the satellite receive antenna. We assume this error would result in a 2 dB antenna gain reduction and an additional 2 dB pointing loss. In order to maintain the nominal uplink carrier-to-noise ratio (C/N), an additional 4 dB ground EIRP would be required to compensate for the loss. With the capability of in-orbit testing, the setting error in the beamforming network could be detected and corrected; consequently, nominal operation could be maintained. Similar arguments could apply to the downlink communication. The benefits of in-orbit testing for the space and ground stations in terms of reduced margin requirements in EIRP are obvious. The capability of in-orbit testing apparently also enhances the system reliability and prolongs the satellite life span. The economical implications of these benefits is significant. These conclusions also apply to the multiple shaped beam systems and the fixed/scanning spot beam systems.

4.4.3 Hardware Requirements

In-orbit testing can be accomplished by multiple ground station sampling or by scanning the spacecraft and measuring the signals at a single station. In-orbit testing can also be accomplished by on-board processing. Figures 4.4-1a and 4.4-1b show the configurations of on-board beamforming test units. Individual feed coefficients are measured by signal injection for the receive antenna and by signal sampling for the transmit antenna. The measured coefficients are compared to the desired coefficients in the microprocessor. The deviations between the two sets of coefficients are detected and corrected accordingly.

The figures indicate that the required hardware is as follows:

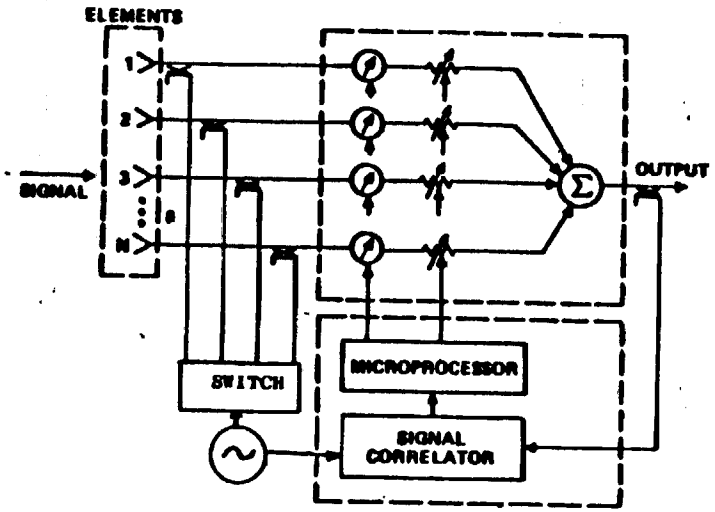

(a) SATELLITE RECEIVES

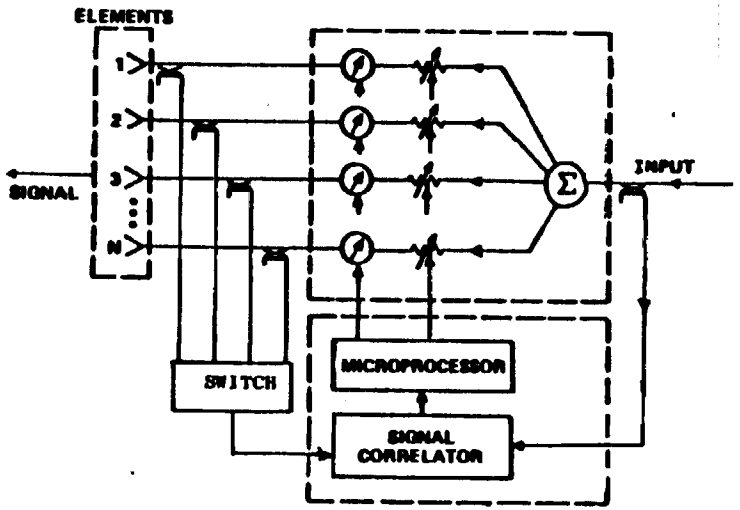

(b) SATELLITE TRANSMITS

FIG. 4.4-1. HARDWARE IMPLEMENTATION FOR IN-ORBIT TESTING

1. Sampling couplers on each antenna element channel and a separate coupler on the beamforming network output port.
2. A signal summer combining the signal in each element channel, which could be in the form of a hybrid.
3. Phase and amplitude controls for individual antenna elements.
4. A reference signal generator.
5. A signal correlator.
6. A switch, switching each element channel to the input port of the correlator.
7. A microprocessor.
8. Connecting waveguide.

The hardware requirements mentioned above are the same for all three communication systems.

4.5 Compensation_for_Transient_Propagation_Effects

4.5.1 Applicability

Dynamic pattern reconfiguration in orbit can partially compensate for spatially selective fading, such as thunderstorm activity, which may affect small areas. The adaptive system could sense decreased signal strength from the rain-affected stations and redirect a small percent of the power over a broad area to compensate the EIRP loss in the affected areas. For a multibeam antenna, the shaped beam is formed by a large number of feed elements and normally covers a large area. Since the rain-affected area is small compared to the whole coverage area, only the excitation coefficients for a small number of feeds need to be adjusted. These adjustments should not significantly change the desired coverage gain and isolation requirements. On the other hand, for the land mobile systems and the fixed/scanning spot beam systems, a typical 7-horn spot beam covers a small area. If the rain affected area is small compared to the spot beam coverage area, the same

principle discussed above for the multiple shaped beam systems can apply here. However, if the rain affected area is comparable to or larger than the spot beam coverage area, other measures need to be taken. First, we may have to increase the number of feed elements in the feed cluster. Second, certain transmit power control algorithms need to be implemented. Third, certain forward-error-correction coding may be required in order to improve the bit-error-rate.

4.5.2 Potential Benefits

At frequencies above 1 GHz, rain causes significant signal fading. For the land-mobile system described in the previous section, the frequencies are below 1 GHz; therefore, rain attenuation is not significant and the rain attenuation loss is not included in the link budgets (See Tables 4.1-1 and -2). In the 4/6 GHz band, the signal loss in a severe thunderstorm is about 4 dB, which increases to about 10 dB in the 12/14 GHz band. In the 20/30 GHz band, the signal fading due to thunderstorm activity could be as much as 15 to 30 dB. One of the conventional ways to deal with this problem is to allocate sufficient power margins to compensate for the rain attenuation loss. Clearly, a significant power margin is required in the 20/30 GHz band by using this approach. Another alternative, called site diversity, is to use multiple satellite terminals located sufficiently far apart that both should not be affected simultaneously by the same storm. This method clearly requires an extra investment in ground terminals.

With the capability of adaptive weather compensation, the system could redirect a small percent of the power from over a broad area to compensate the EIRP loss in the affected area by readjusting the antenna excitation coefficients. This adaptive capability therefore enables the system to maintain the nominal communication link without additional power margin or additional investments in ground terminals.

4.5.3 Hardware Requirements

Figure 4.5-1 demonstrates how the system works. The rain-affected station sends the path loss information to a ground control center. The control center then sends a command to reconfigure the antenna excitation coefficients so as to compensate the attenuation loss in that particular communication channel. This procedure would continue until acceptable compensation is completed.

The figure indicates that the following additional hardware is required for this adaptive function:

1. Equipments for measuring signal attenuation.
2. A control center.
3. Data links between the control center and each ground station.

The hardware requirements mentioned above are for a typical multiple shaped beam system. For a fixed/scanning spot beam system, additional hardware is required, which includes hardware for switching the number of feed elements. The function is not required for land-mobile systems.

5.0 POINTING ERROR COMPENSATION STUDY FOR A MULTIPLE SCANNING/FIXED SPOT BEAM REFLECTOR ANTENNA SYSTEM

5.1 Study Methods for Determining Pointing Error Size and Direction for Multiple Scanning/Fixed Beam Reflector Antenna System (ACTS) (SOW 2.2.1)

5.1.1 Multiple Beam Antenna Systems

The antenna system under consideration for the pointing error compensation study is the multiple scanning/fixed beam reflector antenna configuration as described in Section 3.0 above. This system is also referred to as the Advanced Communications Technology Satellite (ACTS). Both Ford Aerospace and TRW developed antenna system concepts for this application, on contracts NAS3-22498 and NAS3-22499, respectively. This work has been continued by RCA on the current ACTS contract. Both of the original concepts utilized an offset-fed dual reflector, illuminated by an array of 260 to 500 contiguous

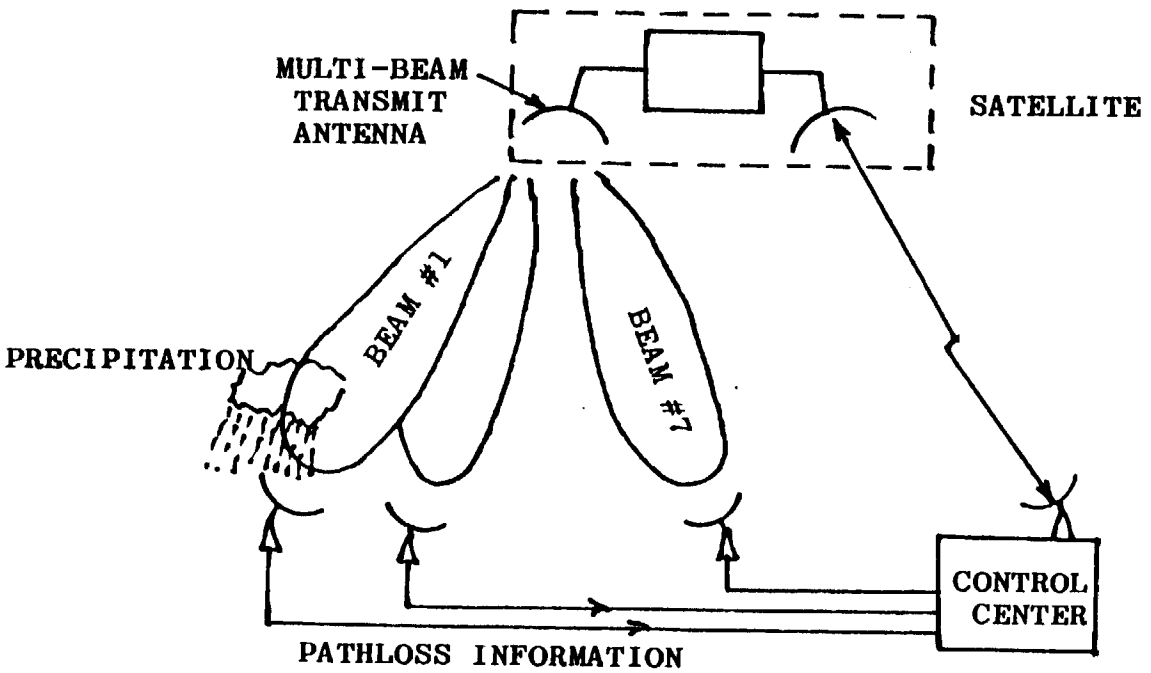

FIG. 4.5-1. ADAPTIVE WEATHER COMPENSATION SCHEMATIC

feeds arranged in a triangular lattice. The differences are due to the optical designs and feed horn sizes. Each feed element produces a spot beam in a different direction, depending upon its location in the array.

Two slightly different configurations are possible for the FACC design, as shown in Figure 5.1-1, depending upon the orientation of the array with respect to the offset-fed reflectors, which introduces an assymmetry to the system. Because of this assymmetry, beams are not spaced the same distance apart for the two cases, as seen in Figure 5.1-1, which pictures the approximate 3 dB contours of adjacent beams, spaced 0.15° apart in the plane of symmetry of the reflectors, and 0.2° apart in the assymmetric plane. These values correspond with measured results on the referenced contract. Normally seven adjacent elements were illuminated together with proper amplitudes and phases to produce a low sidelobe spot beam.

The TRW design consists of an array of 260 3-wavelength square feed horns (for CONUS coverage) illuminating a Cassegrain dual reflector to create scan beams. Each scan beam can be formed either from a single feed horn, or by any combination of two or three adjacent horns (as shown in Figure 5.1-2), through an adjustable beam forming network (BFN). The particular combination chosen depends upon the desired center of the scanning beam. The fixed beams are formed either through a set of large multimode horns, or by combining sets of the scan beam horns for cities in close proximity (Boston, New York, Washington, etc.). Predicted beam patterns did not show the assymetry measured on the Ford antenna, and so the TRW design should produce singlet patterns as depicted in Figure 5.1-3. The singlet beamwidth is approximately 0.233°, while the beam separation is 0.25° in both azimuth and elevation.

5.1.2 Pointing Error Determination

Pointing "errors" cannot normally be determined directly, but only the actual pointing direction of an antenna, from which errors may be calculated

FIG. 5.1-1. FEED ARRAY SINGLET BEAMS, FORD AEROSPACE ANTENNA

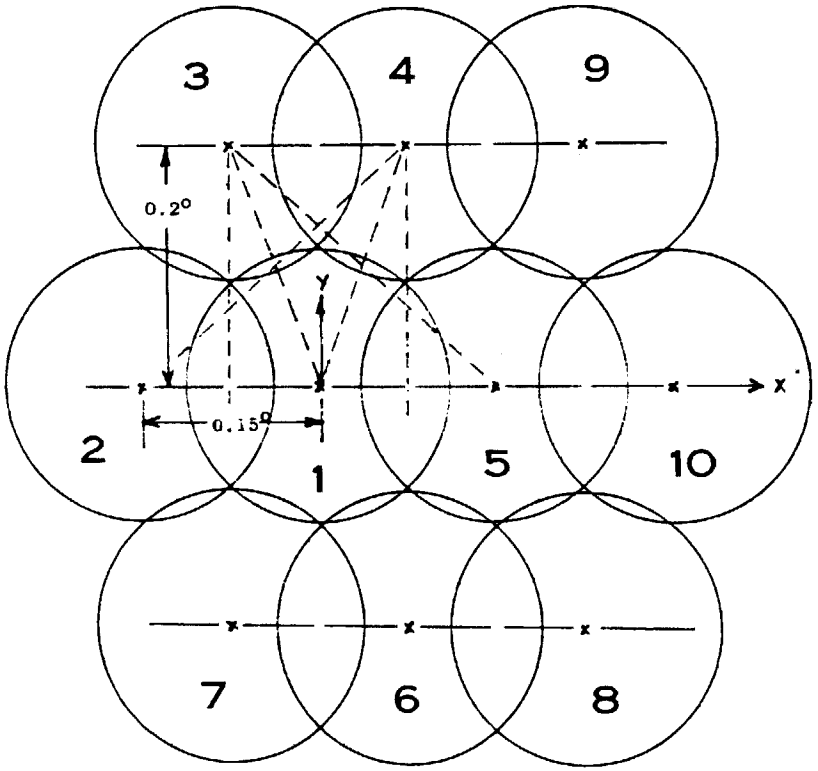

CONFIGURATION #1

BEAMWIDTHS = 0.225°

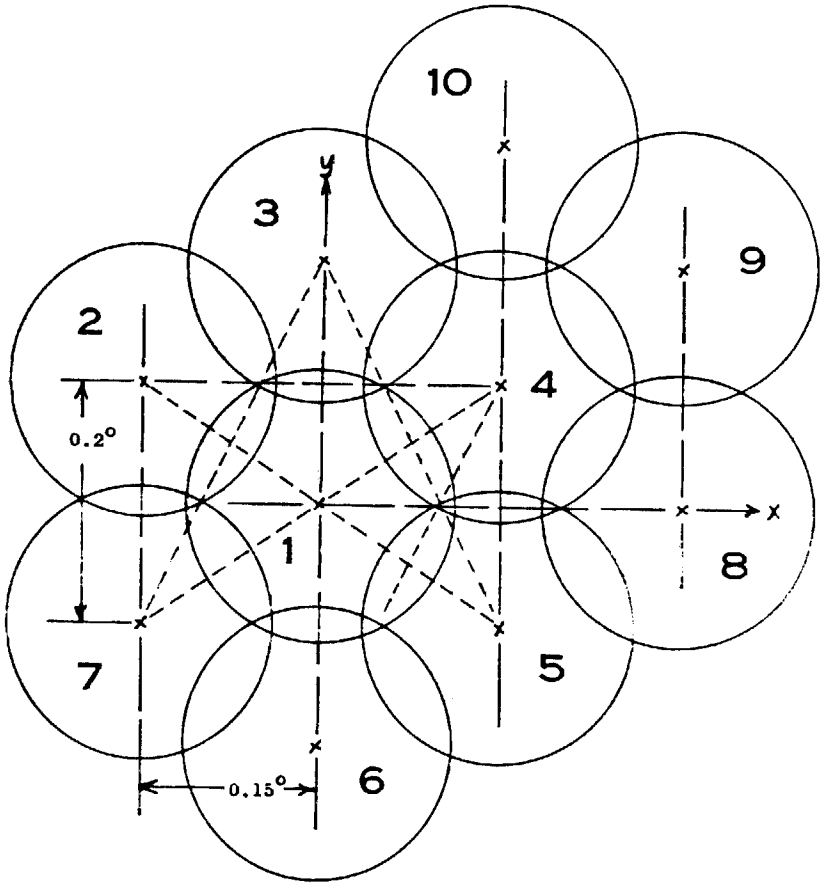

CONFIGURATION #2

BEAM SPACINGS: 0.15° x 0.20°

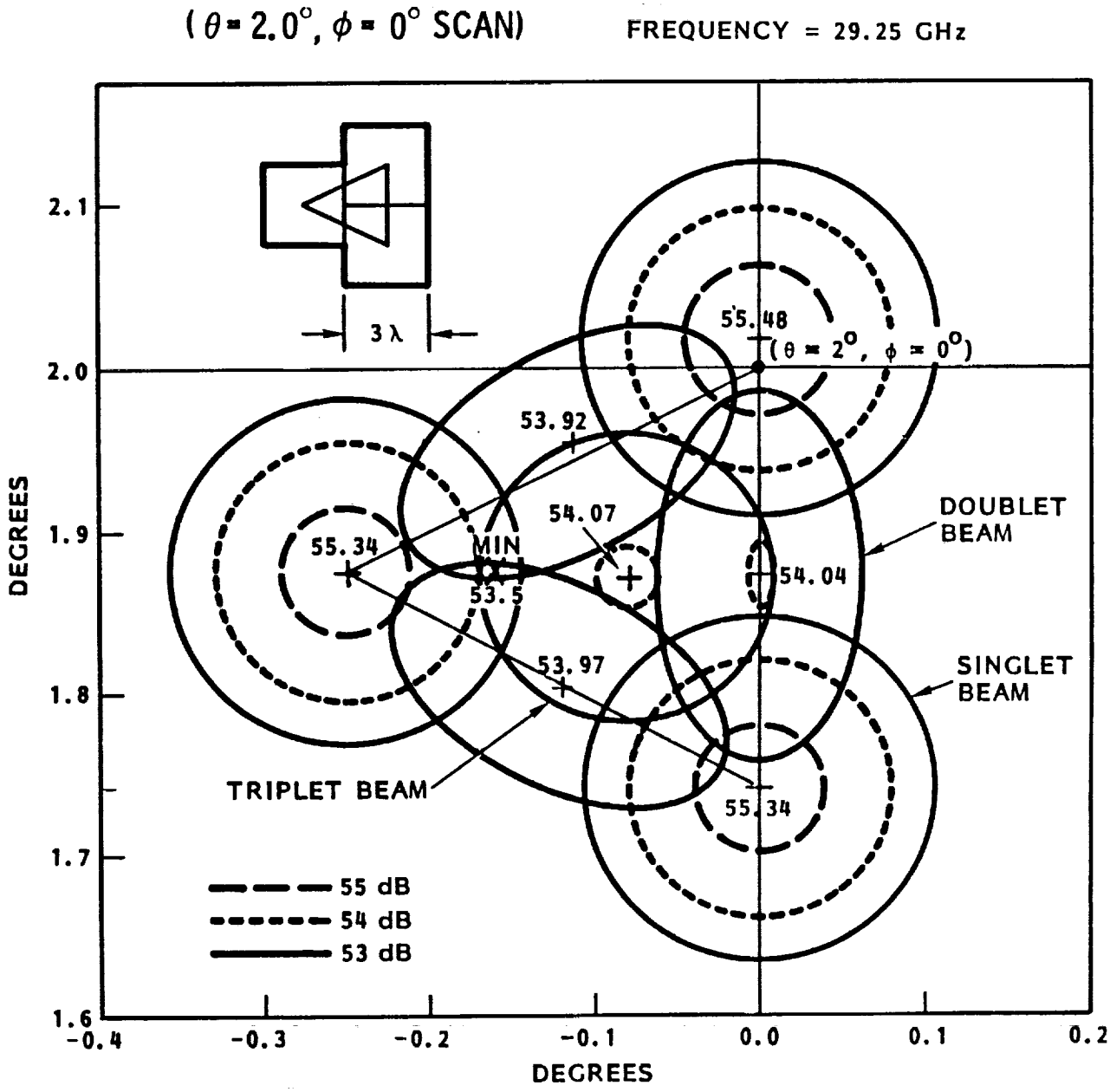

FIG. 5.1-2. GAIN CONTOURS FOR SINGLET, DOUBLET AND TRIPLET BEAMS, TRW ANTENNA

FIG. 5.1-3. FEED ARRAY SINGLET BEAMS, TRW ANTENNA

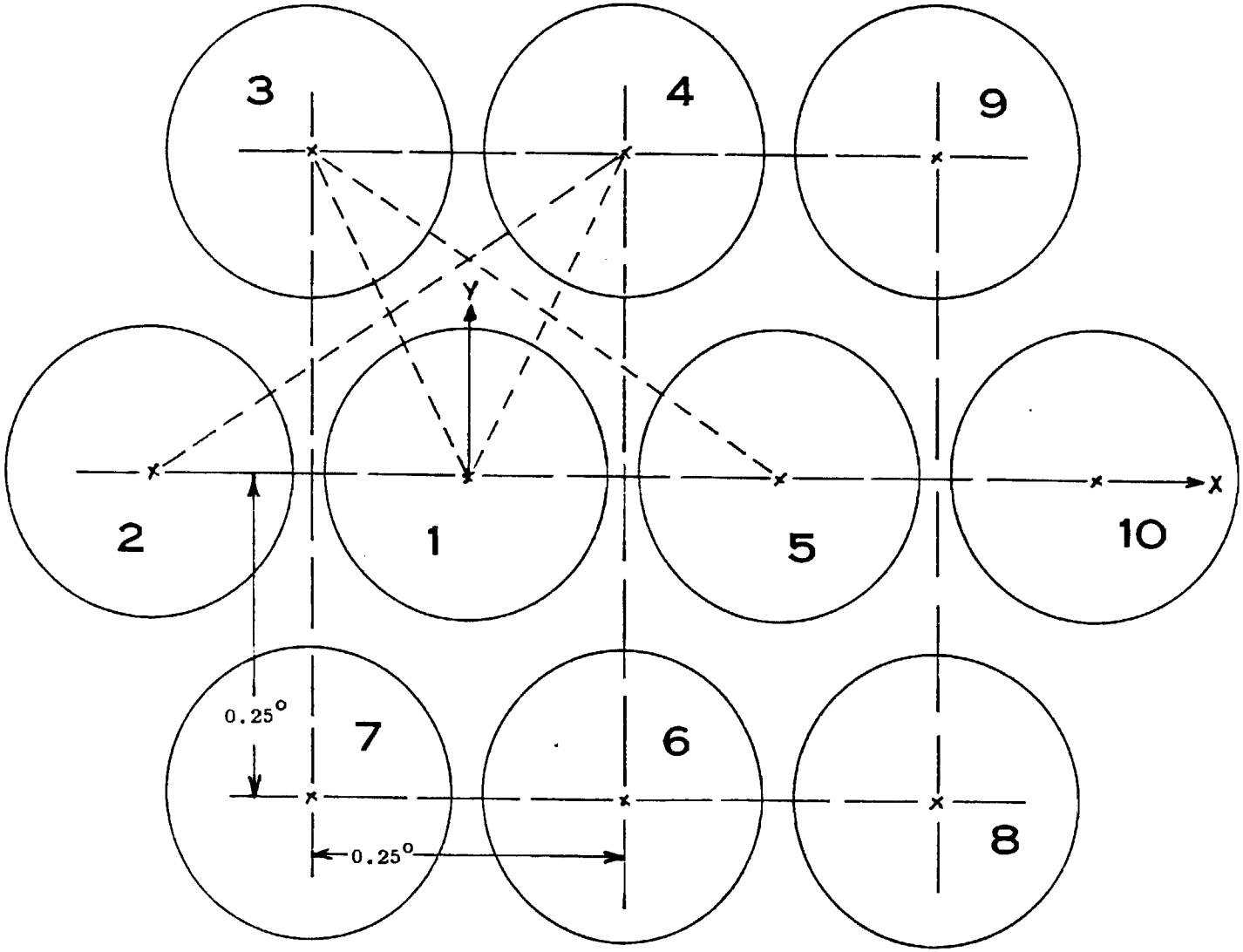

CONFIGURATION #3 BEAMWIDTHS = 0.233° BEAM SPACINGS: 0.25°

by comparison with desired pointing. Determining the direction of arrival of a signal with either of the above antennas can be accomplished by comparing relative amplitudes of voltages induced in each of the three to seven horns in a typical cluster feed. The particular cluster to be chosen would be the one which receives the strongest signals in the entire array. Both the Ford and the TRW designs will be analyzed with reference to three different beam configurations: #1 and #2, representing the two orientations of the Ford design shown in Figure 5.1-1, and #3 representing the TRW design of Figure 5.1-3.

The pointing direction can be determined from the measured voltage amplitudes in various array elements by comparison with patterns produced by the elements singly. For such analyses, it is convenient to use a mathematical model for the individual beam shapes. A different model was selected for the Ford and TRW antennas, by utilizing a curve of the form:

$$V(\theta) = -3\,(\theta / \theta_3)^n \ \text{dB}$$

where θ_3 is half the half-power beamwidth (HPBW). Coefficients for a best fit to measured data for the two antennas were determined, and a change of scale for the angle variable adopted for convenience. With these modifications, the beam shapes adopted (assumed to be circularly symmetric) were of the form:

$$V(R) = -K R^n \quad \text{where} \quad R^2 = X^2 + Y^2$$
$$X = 40\,\theta_x$$
$$Y = 40\,\theta_y$$

The units for the variables x and y are thus $.025^\circ$, or roughly a tenth of a beamwidth. Resulting coefficients are:

Antenna	θ_3	K	N
Ford Aerospace	0.225	.0651	2.5
TRW	0.233	.1381	2.0

These relations were used to predict relative amplitudes of voltages induced in each horn of a 7-element cluster for signals arriving from a variety of directions (x,y) relative to the center of horn #1, for each of the three configurations. These values (in dB) are given in Table 5.1-1 for values (x,y) in one sector of the array only - other sectors would show similar values because of symmetry of the array, while a signal outside the set of sectors would induce similar voltages in a different cluster of horns.

Examination of Table 5.1-1 shows that the range of signal variations is roughly 0 to -20 dB for Configurations #1 & #2, and 0 to -30 dB for Configuration #3. Direction finding using these voltages and a "look-up" table, with interpolation, should be possible with an accuracy of at least $.01^{o}$ (40% of the step size evaluated). Actually, only three elements are needed for signal direction determination normally, the three closest to the actual signal direction, which would thus exhibit the largest signals. For the sector evaluated in Table 5.1-1, these would be elements #1, 4, and 5. For these, it is seen that the levels over the sector vary over the range 0 to -10 dB for Configuration #1 & #2, and 0 to -17 dB for Configuration #3. Use of these horns would afford some advantage in signal detectability because of their greater amplitudes. Others could be added to improve accuracy, if necessary.

Table 5.1-1 Voltages Induced In Various Horns For Three Different Configurations
$\theta_x = 0.025x$ $\theta_y = 0.025y$

CONFIGURATION #1

X	Y	V-1	V-2	V-3	V-4	V-5	V-6	V-7
0	0	0	-5.33	-10.81	-10.81	-5.33	-10.81	-10.81
0	1	-0.15	-5.48	-8.59	-8.59	-5.48	-13.33	-13.33
0	2	-0.59	-5.93	-6.67	-6.67	-5.93	-16.15	-16.15
0	3	-1.33	-6.67	-5.04	-5.04	-6.67	-19.26	-19.26
0	4	-2.37	-7.70	-3.70	-3.70	-7.70	-22.66	-22.66
1	0	-0.15	-7.26	-11.85	-10.07	-3.70	-10.07	-11.85
1	1	-0.30	-7.41	-9.63	-7.85	-3.85	-12.59	-14.37
1	2	-0.74	-7.85	-7.70	-5.92	-4.30	-15.41	-17.18
1	3	-1.48	-8.59	-6.07	-4.30	-5.04	-18.52	-20.29
2	0	-0.59	-9.48	-13.18	-9.63	-2.37	-9.63	-13.18
2	1	-0.74	-9.63	-10.96	-7.41	-2.52	-12.15	-15.70
2	2	-1.18	-10.07	-9.04	-5.48	-2.96	-14.96	-18.52
2	3	-1.93	-10.81	-7.41	-3.85	-3.70	-18.07	-21.63
2	4	-2.96	-11.85	-6.07	-2.52	-4.74	-21.48	-25.03
3	0	-1.33	-12.00	-14.81	-9.48	-1.33	-9.48	-14.81
3	1	-1.48	-12.15	-12.59	-7.26	-1.48	-12.00	-17.33
3	2	-1.93	-12.59	-10.67	-5.33	-1.93	-14.81	-20.14
3	3	-2.67	-13.33	-9.04	-3.70	-2.67	-17.92	-23.26

CONFIGURATION #2

X	Y	V-1	V-2	V-3	V-4	V-5	V-6	V-7
0	0	0	-7.70	-9.48	-7.70	-7.70	-9.48	-7.70
0	1	-0.15	-6.67	-7.26	-6.67	-9.04	-12.00	-9.04
1	0	-0.15	-9.63	-9.63	-6.07	-6.07	-9.63	-9.63
1	1	-0.30	-8.59	-7.41	-5.04	-7.41	-12.15	-10.96
1	2	-0.74	-7.85	-5.48	-4.30	-9.04	-14.96	-12.59
2	0	-0.59	-11.85	-10.07	-4.74	-4.74	-10.07	-11.85
2	1	-0.74	-10.81	-7.85	-3.70	-6.07	-12.59	-13.18
2	2	-1.18	-10.07	-5.92	-2.96	-7-70	-15.41	-14.81
3	0	-1.33	-14.37	-10.81	-3.70	-3.70	-10.81	-14.37
3	1	-1.48	-13.33	-8.59	-2.67	-5.04	-13.33	-15.70
3	2	-1.93	-12.59	-6.67	-1.93	-6-67	-16.15	-17.33

Table 5.1-1 (Continued)

CONFIGURATION #3

X	Y	V-1	V-2	V-3	V-4	V-5	V-6	V-7
0	0	0	-13.81	-17.27	-17.27	-13.81	-17.27	-17.27
0	1	-0.14	-13.95	-14.64	-14.64	-13.95	-20.17	-20.17
0	2	-0.55	-14.37	-12.29	-12.29	-14.37	-23.34	-23.34
1	0	-0.14	-16.71	-18.79	-16.02	-11.19	-16.02	-18.79
1	1	-0.28	-16.85	-16.16	-13.40	-11.33	-18.92	-21.69
1	2	-0.69	-17.27	-13.81	-11.05	-11.74	-22.10	-24.86
1	3	-1.38	-17.96	-11.74	-8.98	-12.43	-25.55	-28.32
2	0	-0.55	-19.89	-20.58	-15.06	-8.84	-15.06	-20.58
2	1	-0.69	-20.03	-17.96	-12.43	-8.98	-17.96	-23.48
2	2	-1.10	-20.44	-15.61	-10.08	-9.39	-21.13	-26.66
2	3	-1.80	-21.13	-13.54	-8.01	-10.08	-24.59	-30.11
2	4	-2.76	-22.10	-11.74	-6.22	-11.05	-28.32	-33.84
2	5	-4.01	-23.34	-10.22	-4.70	-12.29	-32.32	-37.85
3	0	-1.24	-23.34	-22.65	-14.37	-6.77	-14.37	-22.65
3	1	-1.38	-23.48	-20.03	-11.74	-6.91	-17.27	-25.55
3	2	-1.80	-23.90	-17.68	-9.39	-7.32	-20.44	-28.73
3	3	-2.49	-24.59	-15.61	-7.32	-8.01	-23.90	-32.18
3	4	-3.45	-25.55	-13.81	-5.53	-8.98	-27.63	-35.91
3	5	-4.70	-26.80	-12.29	-4.01	-10.22	-31.63	39.92
4	0	-2.21	-27.07	-25.00	-13.95	-4.97	-13.95	-25.00
4	1	-2.35	-27.21	-22.38	-11.33	-5.11	-16.85	-27.90
4	2	-2.76	-27.63	-20.03	-8.98	-5.53	-20.03	-31.08
4	3	-3.45	-28.32	-17.96	-6.91	-6.22	-23.48	-34.53
4	4	-4.42	-29.28	-16.16	-5.11	-7.18	-27.21	-38.26
5	0	-3.45	-31.08	-27.63	-13.81	-3.45	-13.81	-27.63
5	1	-3.59	-31.22	-25.00	-11.19	-3.59	-16.71	-30.53
5	2	-4.01	-31.63	-22.65	-8.84	-4.01	-19.89	-33.70
5	3	-4.70	-32.32	-20.58	-6.77	-4.70	-23.34	-37.16

Pointing direction information could be obtained from the TRW fixed beam multimode horns by incorporating mode couplers which would permit separate extraction of so called tracking modes (such as TE_{21}) from the multimode horns, as is being done by Ford for tracking on a number of ground antennas.

5.1.3 Pointing Direction Accuracy

In order to determine the relative accuracy with which the direction of an incoming signal can be determined, one need merely examine the differences

between dB levels of adjacent entries in the tables for pointing direction developed in the previous section, and relate to these the associated angle differences. Because of the regularity of the entries in Table 5.1-1, it is possible to derive a specific formula to represent this relationship, which can be differentiated to determine slopes and therefore accuracies.

The coordinate system for this analysis is given in Figure 5.1-4, which is scaled specifically for Configuration #3, but would also apply to the other configurations. A given set of three horns would be used for signal arrivals only over a triangular area between their centers, as shown. Analysis need be performed only over one-third of this area, since the other portions may be covered by symmetry. With the coordinate system shown, the x-direction of arrival can be from horns 1 and 5 only. The following relations may be derived from the differences shown in Table 5.1-1 for Configuration #1:

$$X = 3(1 - V_x / 5.33) \qquad Y = 4\{1 - [V_y + 0.88(x-1.5)] / 9.48\}$$

where $VX = V_1 - V_5$ in dB and $VY = V_1 - V_4$ in dB. The values of "x" and "y" are in units of 0.025 degrees. The accuracy of determining pointing direction can be ascertained by differentiation of the above expressions, as:

$$\frac{\delta X}{\delta V_x} = \frac{-3}{5.33} = -0.563 \text{ Units / dB or } -0.563 \cdot 0.025 = -0.0141^\circ / \text{dB}$$

$$\frac{\delta Y}{\delta V_y} = \frac{-4}{9.48} = -0.422 \text{ Units / dB or } -0.422 \cdot 0.025 = -0.0105^\circ / \text{dB}$$

$$\frac{\delta Y}{\delta V_x} = \frac{\delta Y}{\delta X}\frac{\delta X}{\delta V_x} = 0.209 \text{ Units / dB or } 0.209 \cdot 0.025 = 0.0052^\circ / \text{dB}$$

Total accuracies may be obtained from RSS'ing the above values, as:

$$\frac{\delta Y}{\delta (V_x, V_y)} = \sqrt{\left[\frac{dY}{dV_x}\right]^2 + \left[\frac{dY}{dV_y}\right]^2} = 0.0117^\circ / \text{dB}$$

$$\frac{\delta P(X,Y)}{\delta (V_x, V_y)} = \sqrt{\left[\frac{dX}{dV_x}\right]^2 + \left[\frac{dY}{d(V_x, V_y)}\right]^2} = 0.0183^\circ / \text{dB}$$

The final accuracy with which the pointing direction can be determined depends on how accurately the difference signals in the various horns can be measured. A reasonable accuracy for amplitude measurements for signals which are within 10 dB of each other is ±0.2 dB, which implies that the accuracy of direction determination should be 0.0183° x 0.2 dB = $\pm 0.0036^{\circ}$. This represents 1.6% of a beamwidth. Similar accuracy figures also apply to Configuration #2.

The accuracy of the triangular array developed by TRW for the ACTS program can be evaluated in a similar fashion. The relations between the corresponding horn voltage differences and the beam positions are as follows:

$$X = 5(1 - V_x / 13.81) \qquad Y = 5\{1 - [V_y + 1.38(x-2.5)] / 13.82\}$$

The corresponding slopes are:

$$\frac{\delta X}{\delta V_x} = \frac{-5}{13.81} = -0.3621 \text{ Units / dB or } -0.3621 \cdot 0.025 = -0.0091^{\circ} / \text{dB}$$

$$\frac{\delta Y}{\delta V_x} = -0.0091^{\circ} / \text{dB}; \qquad \frac{\delta Y}{\delta V_x} = \frac{\delta Y}{\delta X}\frac{\delta X}{\delta V_x} = 0.0045^{\circ} / \text{dB}$$

$$\frac{\delta Y}{\delta (V_x, V_y)} = 0.0102^{\circ} / \text{dB}; \qquad \frac{\delta P(X,Y)}{\delta (V_x, V_y)} = 0.0136^{\circ} / \text{dB}$$

Because the voltage differences in this case are generally greater than for Configurations #1 and #2, with differences as high as 20 dB, the accuracy of measurement will not be as great, perhaps as much as 0.5 dB. Thus the direction accuracies will be around $\pm .0068^{\circ}$, or about half the accuracy of Configurations #1 and #2 with more closely spaced beams.

5.2 Pointing Error Correction Mechanisms

In order to steer, or redirect, singlet beams in a multibeam array, such as the scanning or fixed beams in the ACTS system, it is merely necessary to

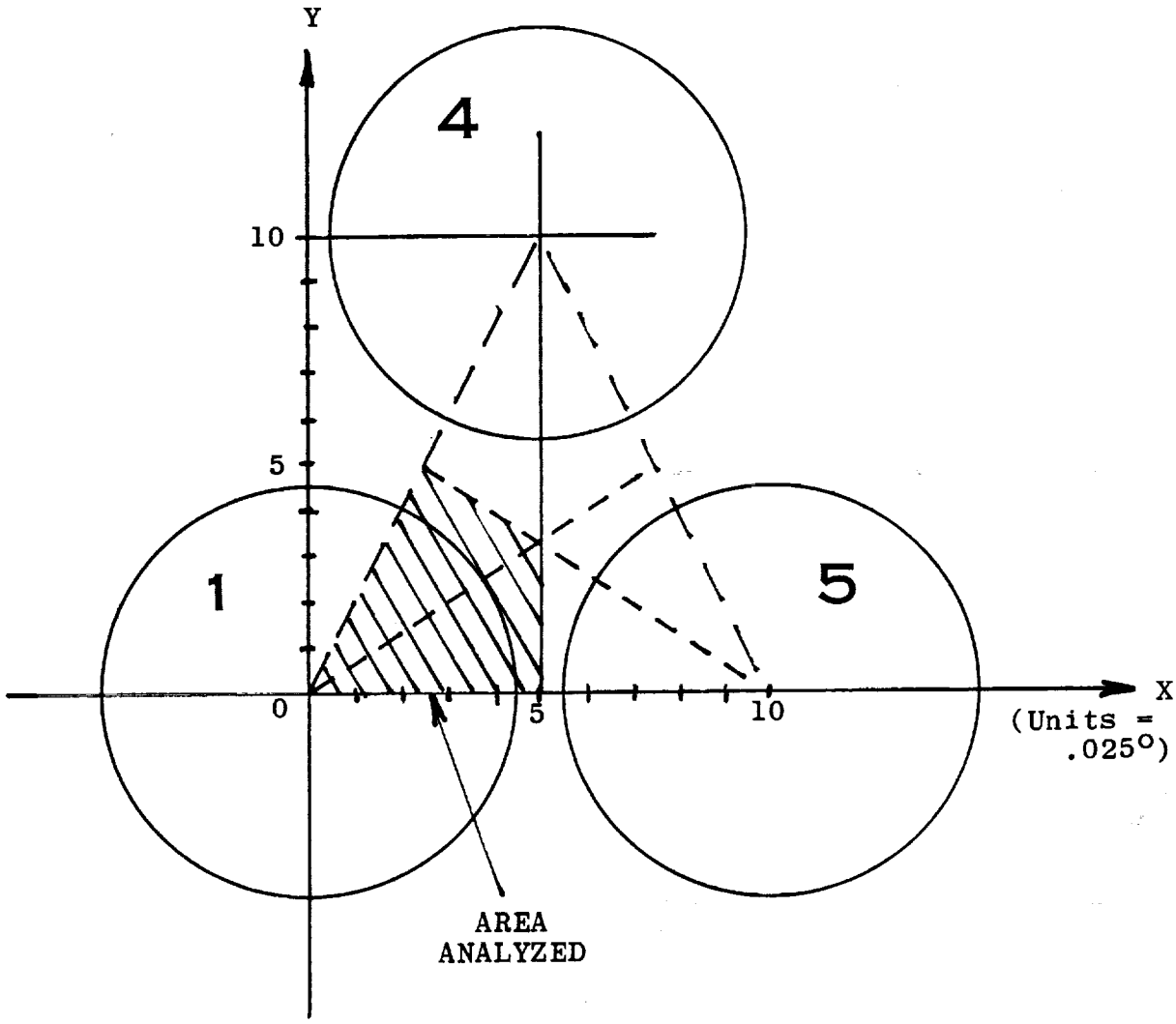

FIG. 5.1-4. COORDINATE SYSTEM FOR ANALYSIS

readjust the amplitude feed coefficients of the feed horns which produce the individual beams. In the TRW configuration, only three horns are normally excited for each scanning beam; in the FACC configuration, seven horns are usually excited, to produce low sidelobe beams, and because the singlet beams are closer together. Because of the difficulty of optimizing seven variable feed coefficients for steering a beam, let us consider first the simpler case of steering with three horns only, and address the optimization with additional horns later.

For a given feed horn configuration, a given set of feed excitations will produce a beam with a peak in an arbitrary direction. It is difficult to derive analytically the exact feed coefficients to produce a beam with a peak in a given direction. An easier approach is to calculate beam peaks produced by a large combination of excitation coefficients, from which some information as to what excitation coefficients are required to steer a beam in a given direction may be obtained. Accordingly, an iterative program was set up to locate beam peaks with a given set of excitation coefficients, for each of the three horn configurations analyzed above (two FACC and one TRW). To simplify calculations, singlet beams were considered circularly symmetric, and best fit power curves determined by comparison with measured data from prior programs, as discussed in the previous section.

Results of a large number of calculations for the two Ford Aerospace configurations are shown in Figures 5.2-1a and 1b. These represent contours of beam peaks at various levels above singlet beam excitations, for various combinations of horn excitations. They show that a beam peak up to 2.3 dB above that of a singlet beam may be produced in a given location, and that over most of the area for which the given three horns would be used to produce a steered beam, the gain is 1 to 2 dB above the singlet beam peak.

Steered beam peaks for TRW's Configuration #3 are shown roughly in Figure 5.2-1c. These peaks do not vary as much as for Configurations #1 and

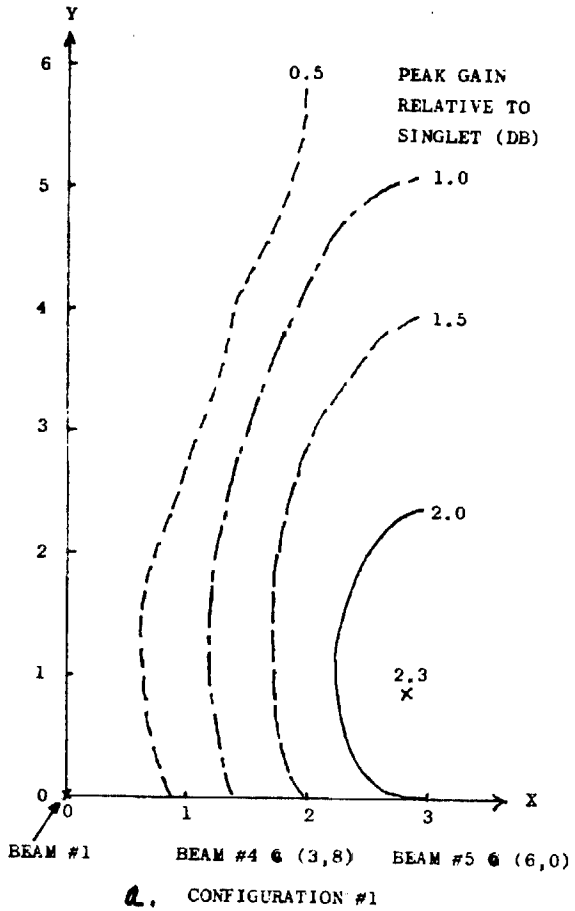

a. CONFIGURATION #1

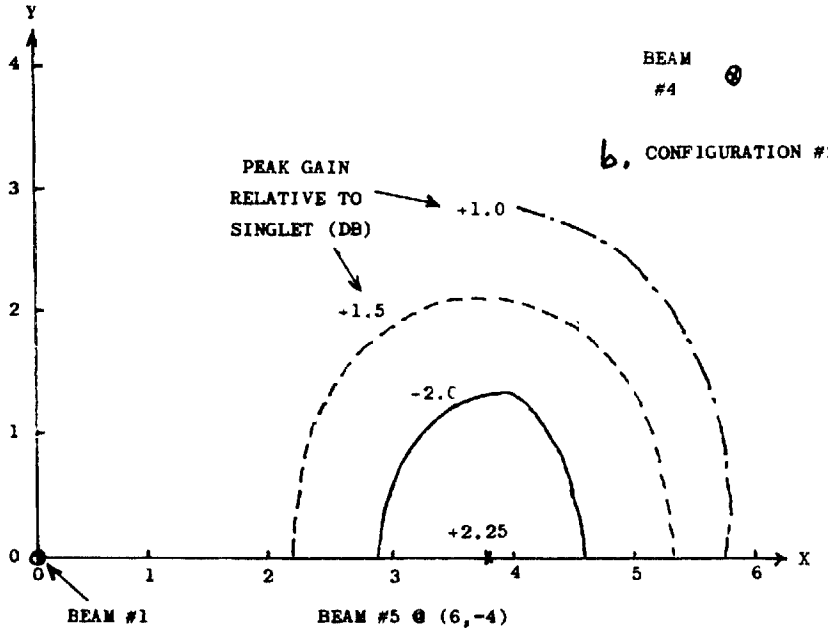

b. CONFIGURATION #2

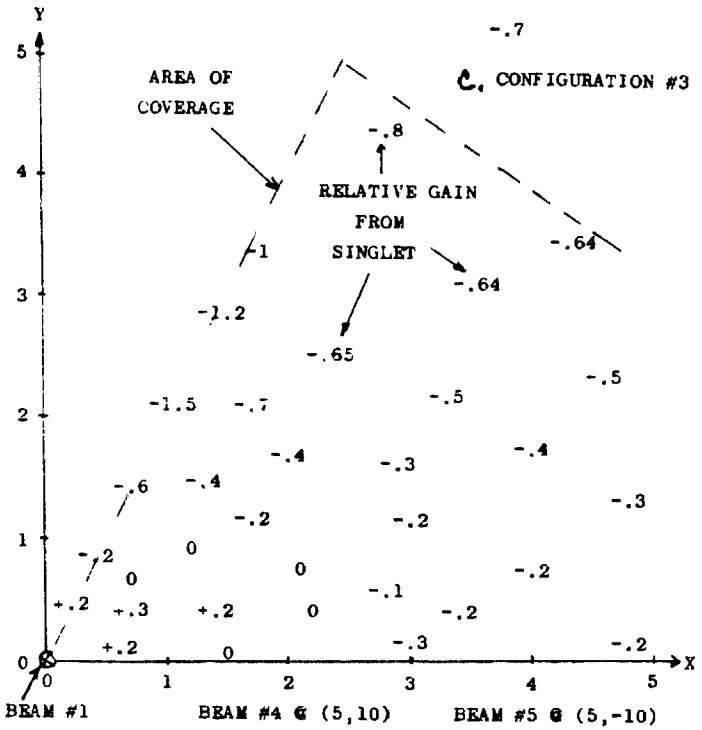

c. CONFIGURATION #3

FIG. 5.2-1. CONTOURS OF TRIPLET BEAM MAXIMA

#2, showing a maximum of only about 0.3 dB above the singlet, and up to 1 dB below the singlet, over the area of coverage for the given three beams.

Data derived for these curves could be used to determine excitation coefficients for steering to a given location. The effects of beam pointing corrections on antenna radiation characteristics are considered in the next section.

5.3 Methods for Correction Determination

An explicit relationship to determine feed coefficients to steer a beam in a given direction can be obtained by developing a formula for gain as a function of position, with feed coefficients as parameters, and setting the differentials of this expression equal to zero at the desired steering point to determine the necessary feed coefficients to maximize gain at this point. An auxiliary condition must also be imposed, that the sum of the voltage feed coefficients squared equal unity for conservation of power. This may be expressed as follows:

$$E_T(P_0) = \sum_{i=1}^{n} V_i P(r_i)$$

where: E_T is the total field strength at the given point, p_o

V_i is the voltage feed coefficient of the ith feed element

$P(r_i)$ is the pattern function of a typical element at a point p_o which is a distance r_i from the center of the element

The power conservation condition may be expressed as:

$$\sum_{i=1}^{n} V_i^2 = 1$$

For maximizing the field at p_o, the following relations must hold, subject to the conservation condition:

$$\frac{\delta E_T(P_0)}{\delta V_i} = 0 \qquad i=1,2,3,\ldots\ldots\ldots\ldots,n$$

The solution to this set of equations may be shown to be:

$$V_i = P_i / P_t$$

where $P_i = P(r_i)$ which is the pattern function for the ith element

and $P_t = \sqrt{\sum_i P_i^2}$

Furthermore, the maximum value of E_T is just P_t or:

$$E_T \text{ (max)} = P_t$$

These relations allow direct calculation of feed coefficients for steering a composite beam to any desired position, using as many feed elements as desired. Interestingly, this relation does not necessarily create a beam peak in the given direction, but maximizes the gain in that direction regardless of the location of the peak. For example, using FACC Configuration #1, and adjusting coefficients for elements 1, 4, and 5 for maximum gain at p_o = (1.5,4.0) results in optimized values of 1.46 dB above the singlet at p_o, but the peak of this beam is 1.83 dB, located at the point (2.6,2.8). In contrast, the maximum gain which can be produced at p_o with a beam whose peak is also at p_o is about 0.55 dB, as shown in Figure 5.2-1a.

These relations also allow direct evaluation of the effect of exciting additional elements for maximizing gain in a given direction, as each additional element contributes an additive factor of P_i^2 to the total P_t which represents the maximum gain. For example, adding three additional elements (#2, 3, and 9) to the three defined above (#1, 4, and 5) produces a maximum gain of 2.43 dB at p_o = (1.5,4.0). The corresponding voltages are: $V_1 = V_4 = .570$; $V_3 = V_5 = .3883$; and $V_2 = V_9 = .156$. All other elements represent values of P_i more than 25 dB below V_1 which would contribute less than an additional .002 dB to the total gain.

Using these relations, the maximum gains which can be produced at various points over the coverage areas defined for each of the three configurations (FACC #1 and #2 and TRW #3) defined previously, are shown in Figure 5.3-1. The number of elements required to produce this maximum are listed in Figure 5.3-2, for the corresponding points. Corresponding maximum gains using only three elements (#1, 4, and 5) are shown in parentheses in Figure 5.3-1; differences over 1.0 dB are noted at some places.

5.3.1 Pattern Shapes

The additional factor of interest in modification of feed coefficients to affect beam steering, is the effects which these modifications have on beam patterns - sidelobes, etc. Accordingly, a Cassegrain configuration similar to the TRW design, scaled to 19 GHz, and shown in Figure 5.3-3 was implemented for pattern calculations on the FACC computer, using our DPAT program. Two feed array configurations were considered, both using square feed horns in a triangular lattice structure, but differing in feed horn sizes (and thus spacings). The first used 1.00" square feed horns, corresponding to the FACC Configuration #1 (scaled slightly to produce the same beam separation as noted in the original FACC shaped-reflector design with a somewhat greater focal length). The second used 1.864" square feed horns, corresponding to the 3-wavelength TRW design in Configuration #3.

A set of patterns was calculated for each configuration, for various sets of feed coefficients corresponding to beam steering over a range of positions within the limits for which the chosen feed horns would be utilized. Various numbers of feed horns were also utilized, from a single to seven or eight, as prescribed for maximum gain in Figure 5.3-2. -3 dB contours for the individual beams are shown superimposed in Figure 5.3-4. These patterns show a displacement of about 0.05° (y =+2.0) from the optical antenna axis, probably because the feed array was located slightly off the

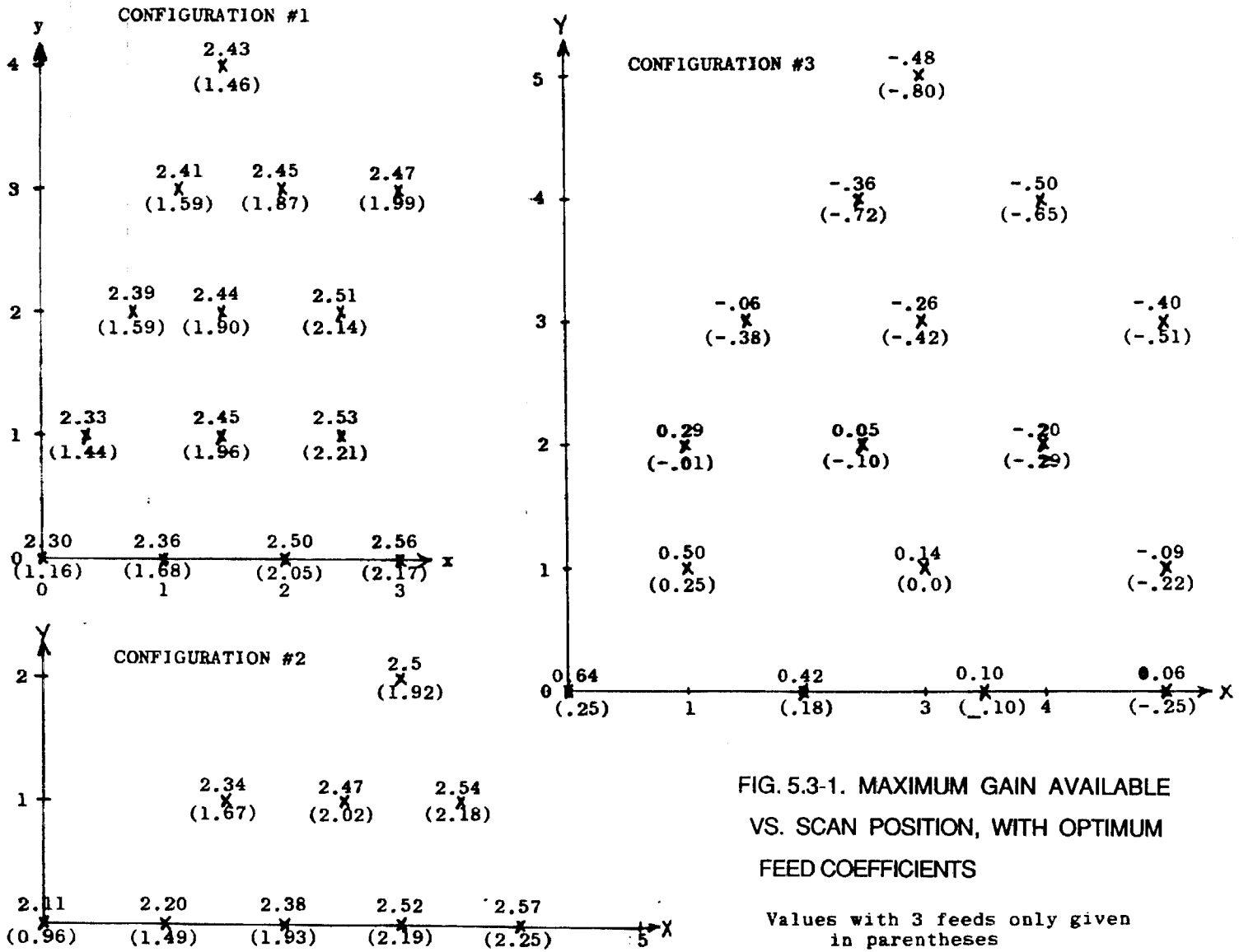

FIG. 5.3-1. MAXIMUM GAIN AVAILABLE VS. SCAN POSITION, WITH OPTIMUM FEED COEFFICIENTS

Values with 3 feeds only given in parentheses

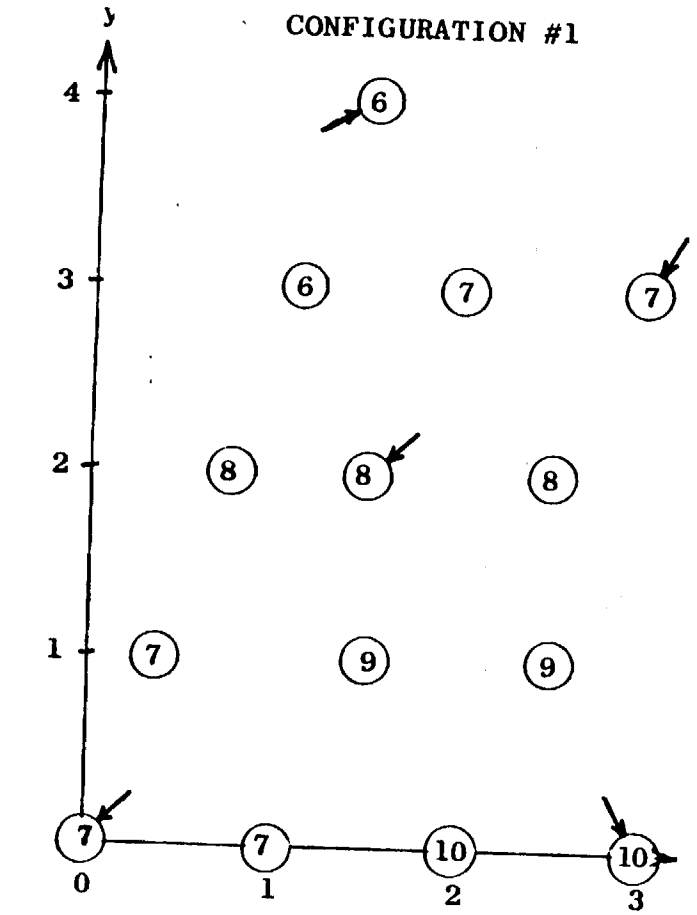

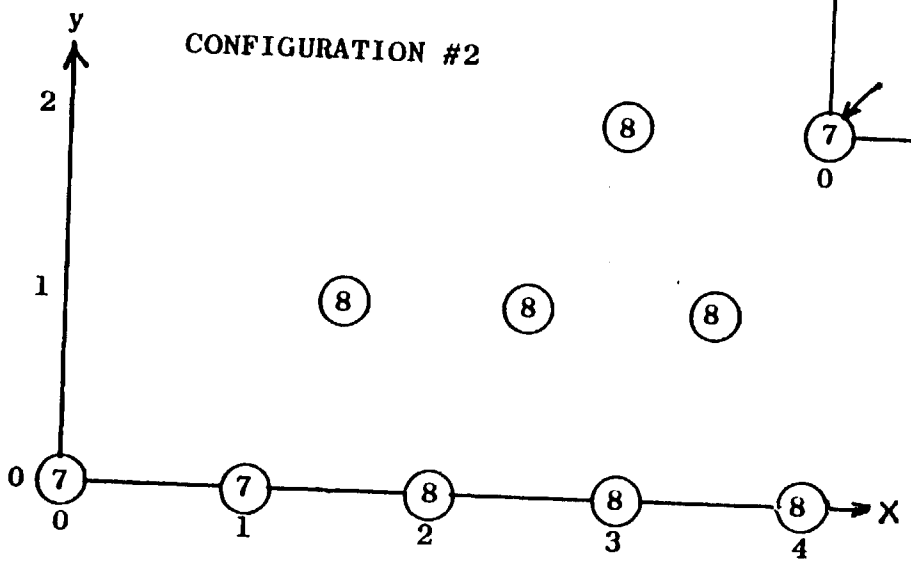

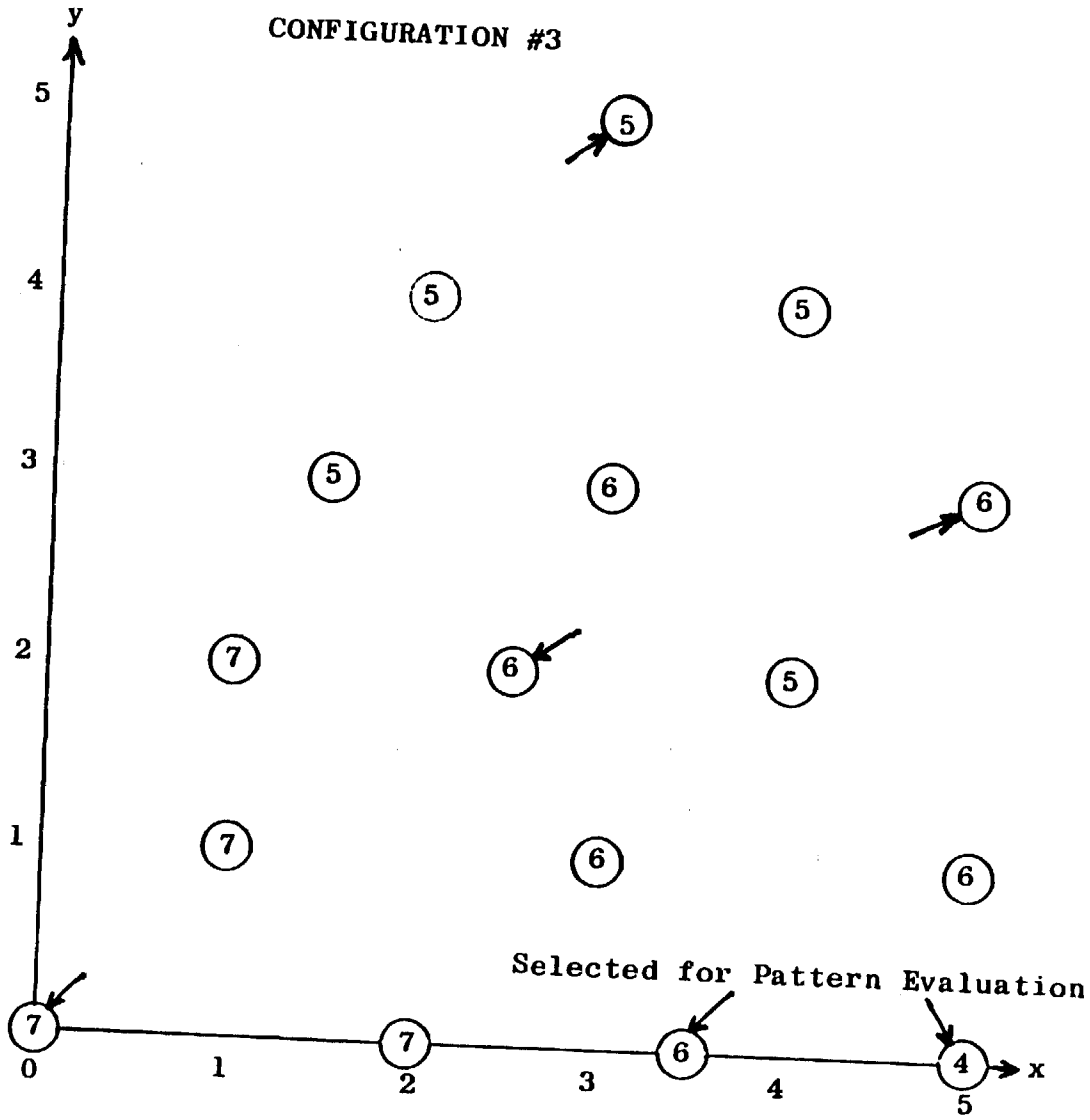

FIG. 5.3-2. OPTIMUM NUMBER OF FEED ELEMENTS FOR MAXIMUM GAIN

FIG. 5.3-3. OFFSET CASSEGRAIN REFLECTOR ANTENNA GEOMETRY

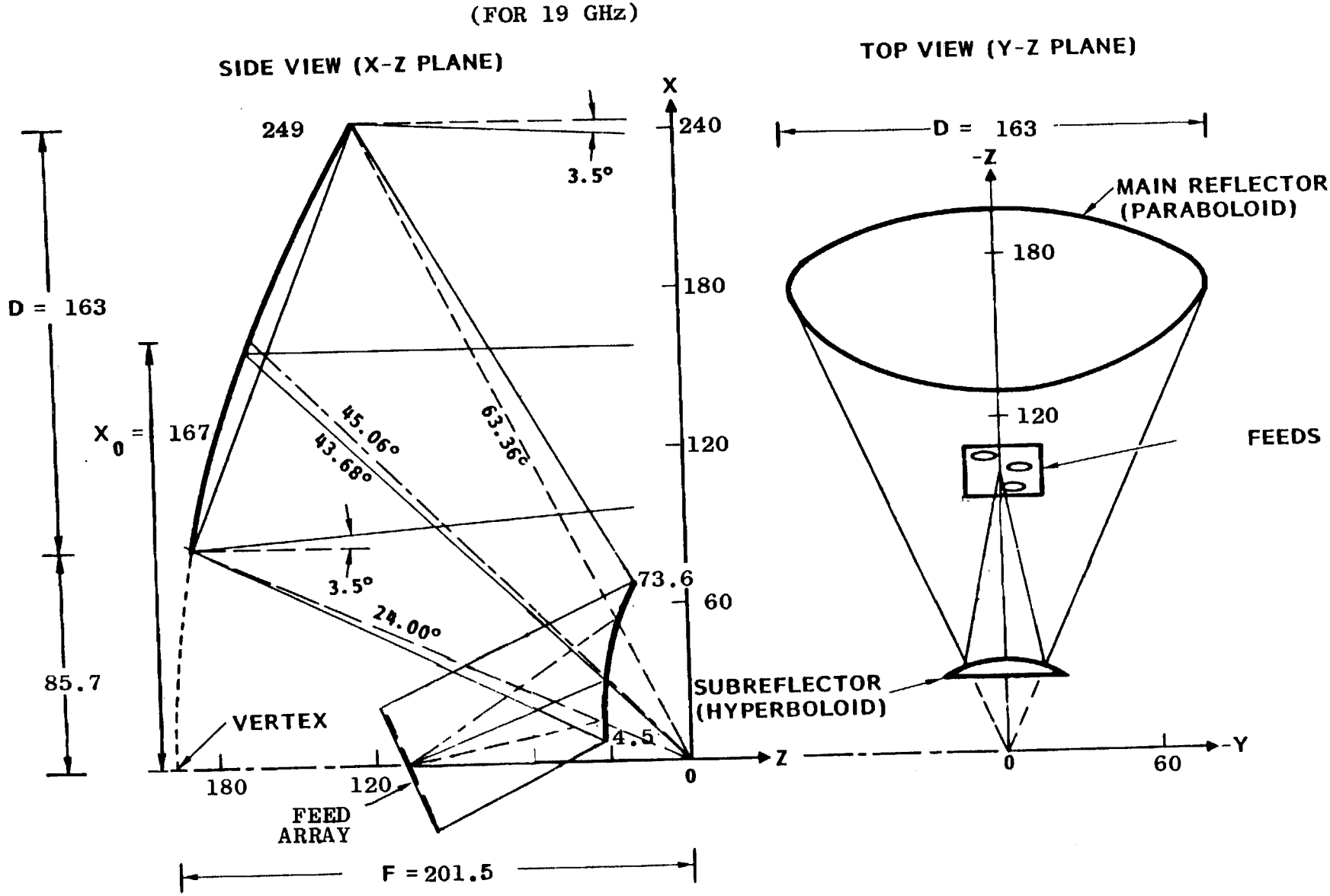

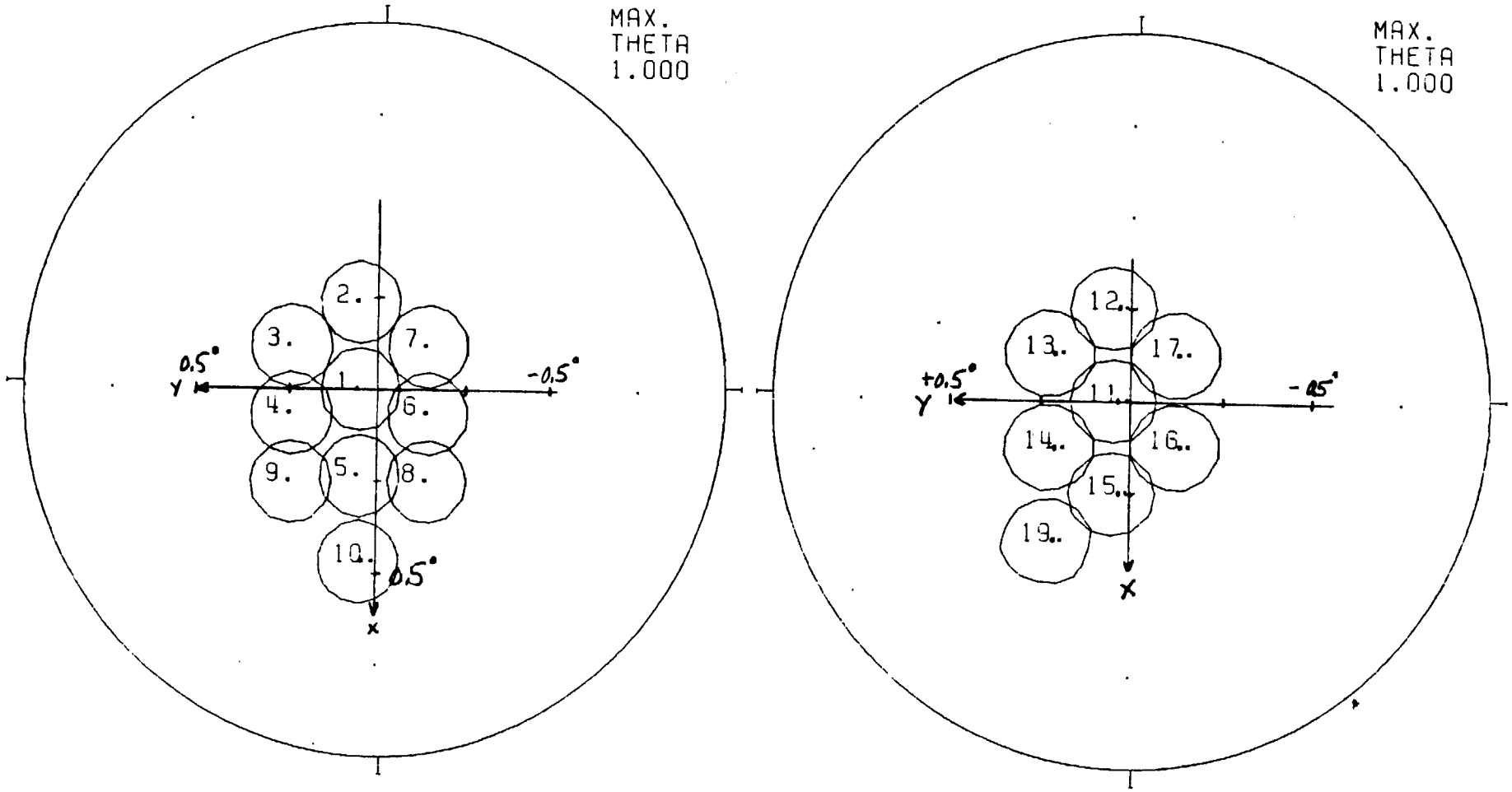

FIG. 5.3-4. FEED ARRAY BEAM POSITIONS

focal point. This displacement will be subtracted from results discussed in the following paragraphs.

Contour plots and x-y linear cuts for the on-axis beam of Configuration #1 are shown in Figure 5.3-5 for various sets of feed coefficients for a 7-element cluster, showing their effect on sidelobe structure. The list of contour levels for various symbols used on all contour plots is given in Table 5.3-1. It did not appear possible to reduce the first sidelobe level for this on-axis beam below about -20 dB except by raising the excitation levels of the peripheral beams in the 7-element cluster, which broadens the main beamwidth and reduces the peak gain. A list of various excitation options evaluated with their corresponding beamwidths and maximum sidelobe levels is given in Table 5.3-2. This performance is in contrast to the calculated and measured performance of the FACC design developed on NASA Contract NAS3-22498, which showed 30 dB sidelobes for 7-element cluster excitations. The explanation may lie in the fact that the design evaluated differed from the NAS3-22498 design in focal length, which was 290" for a 13.5 foot aperture, while the focal length of the scaled TRW design evaluated was 201" for the same diameter aperture.

Table 5.3-1 Contour Symbol Designations

CONTOUR SYMBOL	DATA LEVEL
A	0.000
B	-1.000
C	-2.000
D	-3.000
E	-4.000
F	-5.000
G	-10.000
H	-15.000
I	-20.000
J	-25.000
K	-30.000

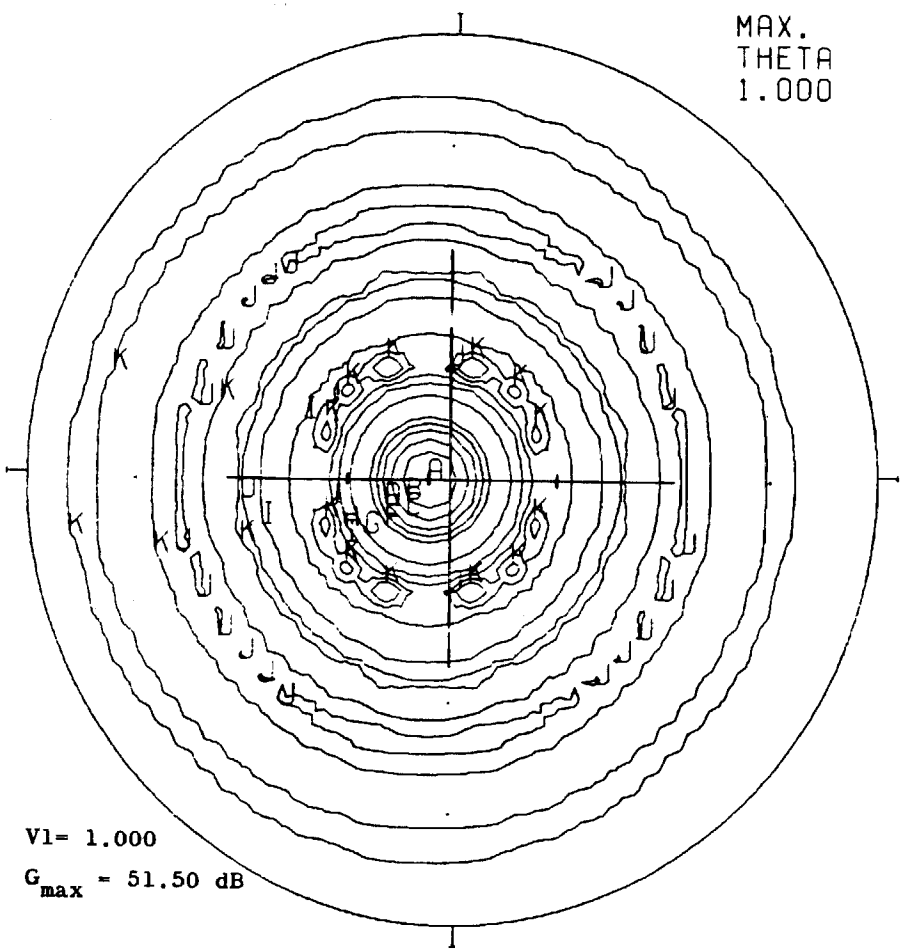

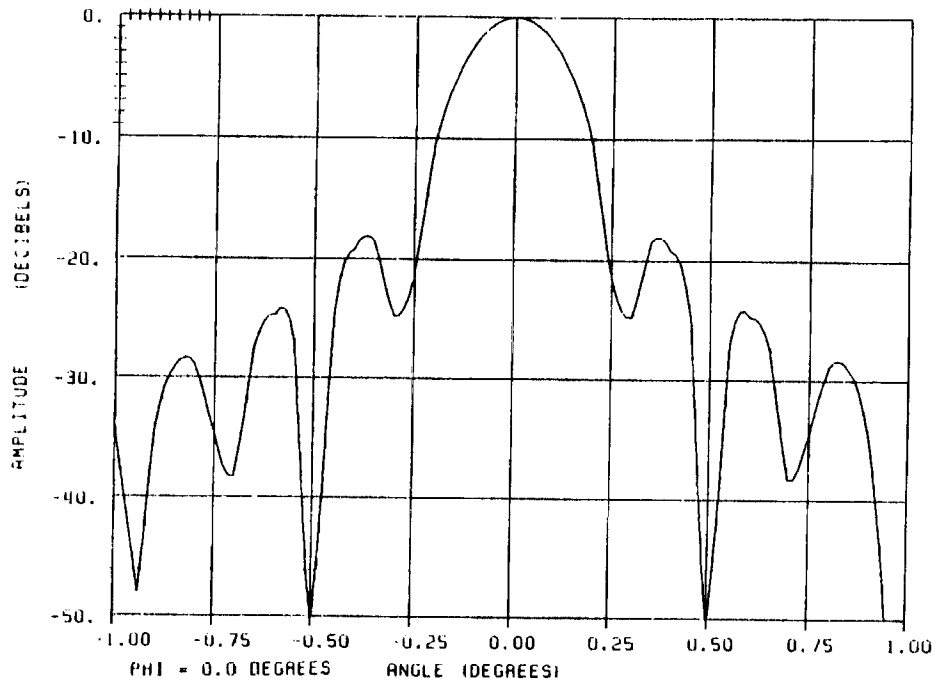

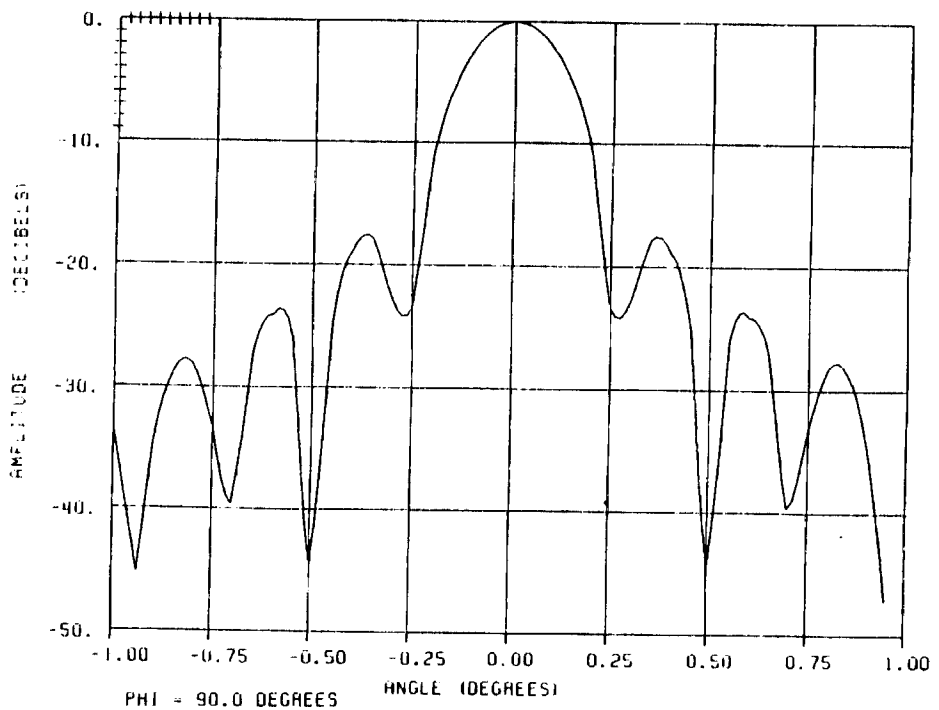

Fig. 5.3-5a. PATTERNS ON AXIS, SINGLE FEED ONLY

CONFIGURATION #1

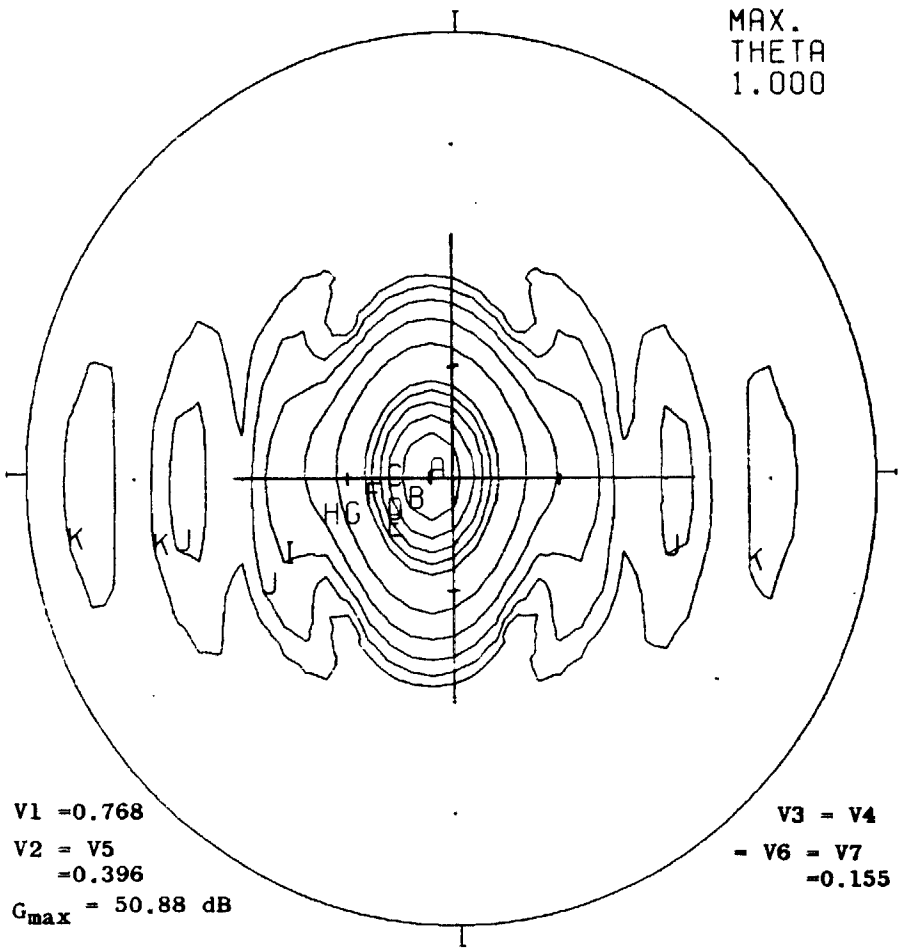

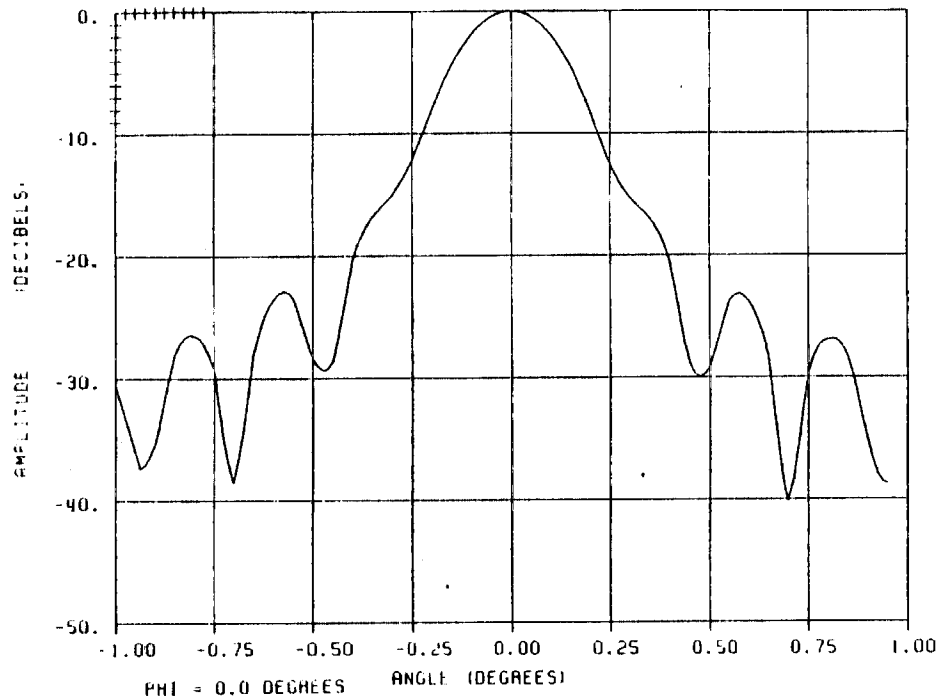

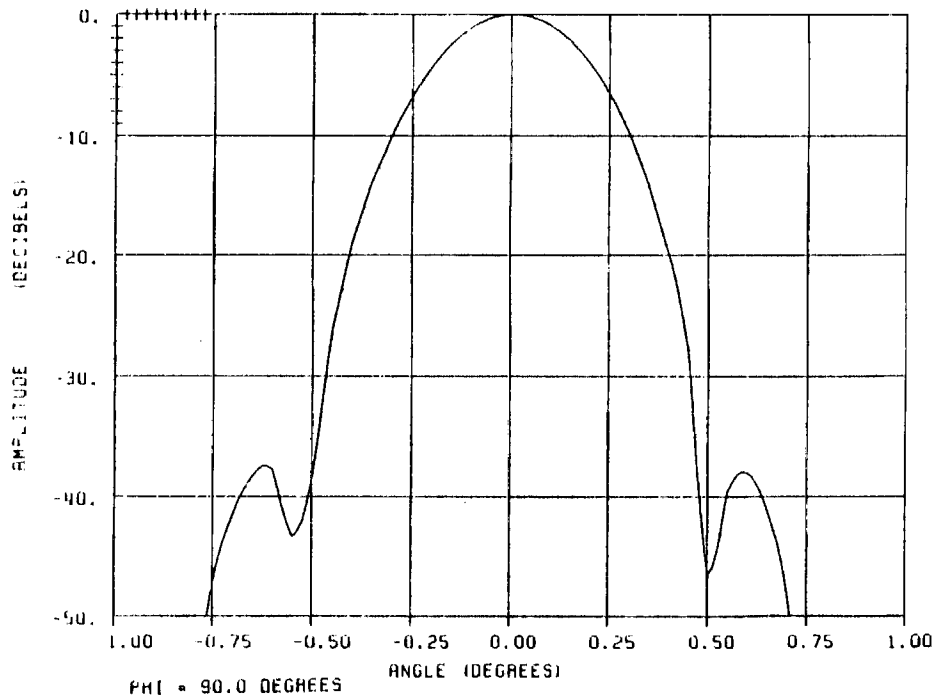

Fig. 5.3-5b. PATTERNS ON AXIS WITH SEVEN-ELEMENT CLUSTER CONFIGURATION #1

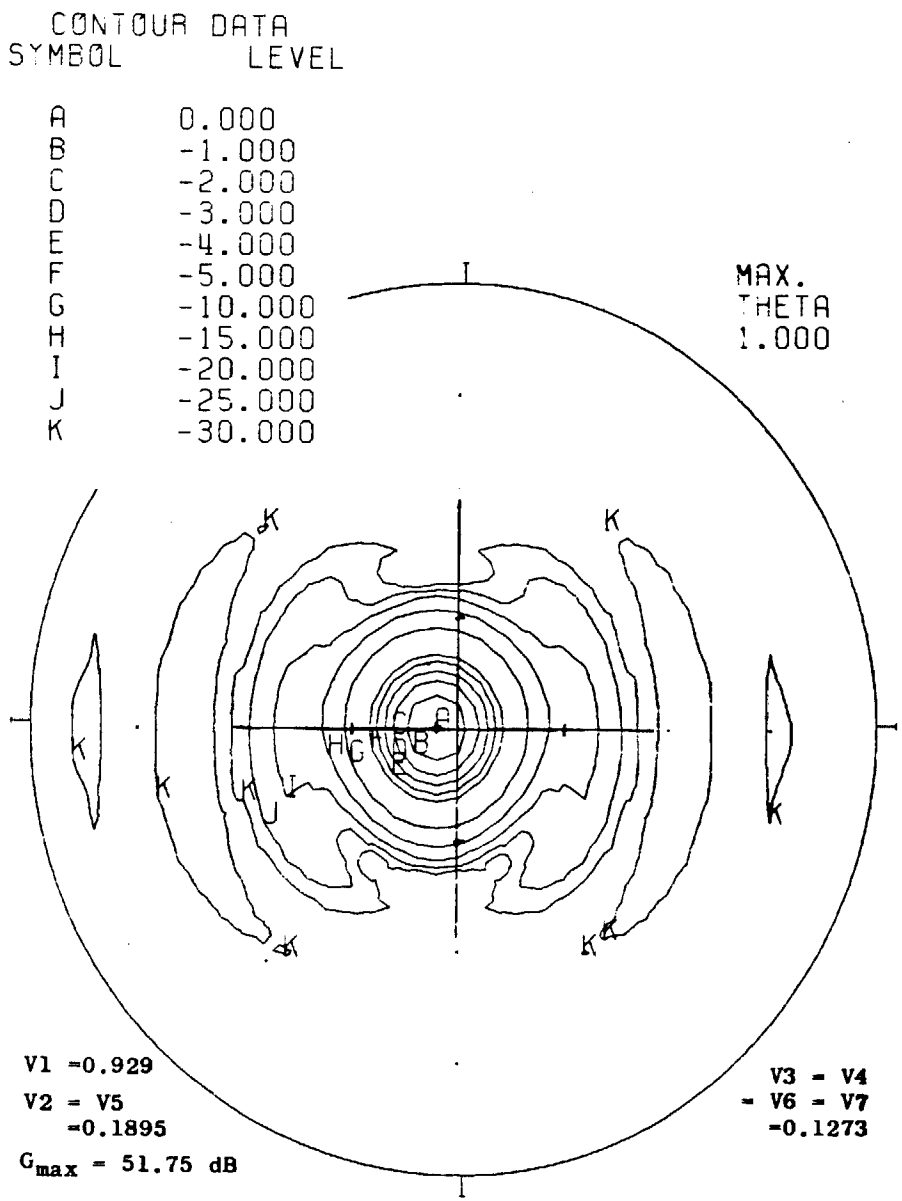

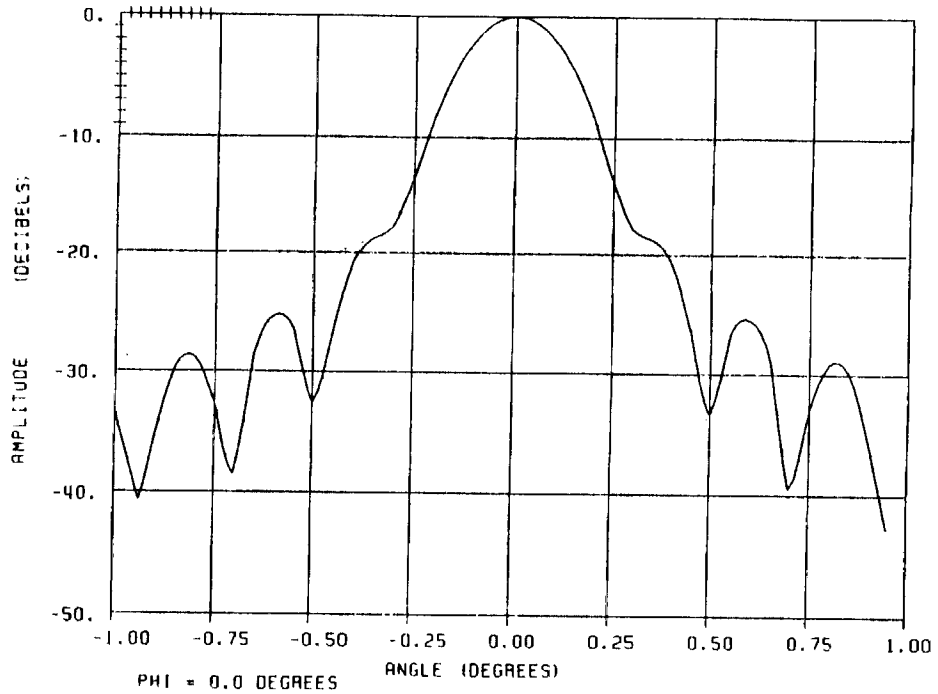

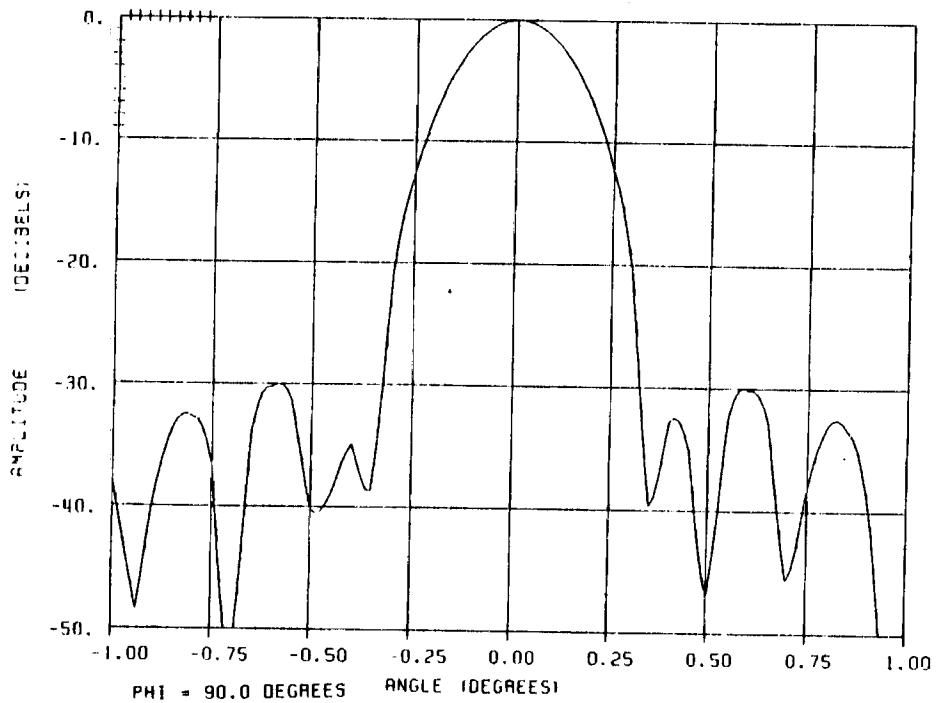

Fig. 5.3-5c. PATTERNS ON AXIS WITH ALTERNATE 7-ELEMENT COEFFICIENTS

CONFIGURATION #1

Table 5.3-2 On-Axis Beam Tradeoffs For Configuration #1

(Seven Element Excitation)

Adjacent* Horn Level dB	Edge** Horn Level dB	10 dB Beamwidth $\phi = 0$	10 dB Beamwidth $\phi = 90$	Max. Sidelobe dB	Max. Gain dB
Single Horn		0.39	0.39	-18	51.50
-1.11	-5.83	0.62	0.72	-23	49.08
-5.75	-13.89	0.45	0.61	-15	50.88
-12.63	-24.69	0.39	0.47	-17	51.68
-13.81	-17.25	0.43	0.45	-18	51.76
-14.63	-14.63	0.47	0.44	-17	51.7
-15.84	-21.30	0.40	0.44	-19	51.79
-17.68	-14.63	0.47	0.42	-21	51.73

* Adjacent Horns: Horns #2 and #5 in Figure 5.3-4
** Edge Horn: Horns #3, 4, 7 and 6 in Figure 5.3-4

Steered beam contour plots for a number of scan positions (designated by arrows in Figure 5-3-2) using this Configuration #1, are shown in Figure 5.3-6. These include cases with only three elements excited, as well as 6 to 10 elements (the maximum considered useful according to the criteria set up in the previous section, and listed in Figure 5.3-2). A summary of the scanning performance for this configuration is given in Table 5.3-3, which suggests a number of observations:

a. Steered patterns generally lose their symmetry, and the usual sidelobe structure gives way to a more gradual pattern drop-off in the direction of scan, generally known as a pattern "shoulder". Although this phenomenon is generally associated with beam broadening, such broadening is not apparent at levels above -10 dB.

b. The observed locations of actual beam peaks do not always coincide with the position to which the beam is being steered for maximum gain.

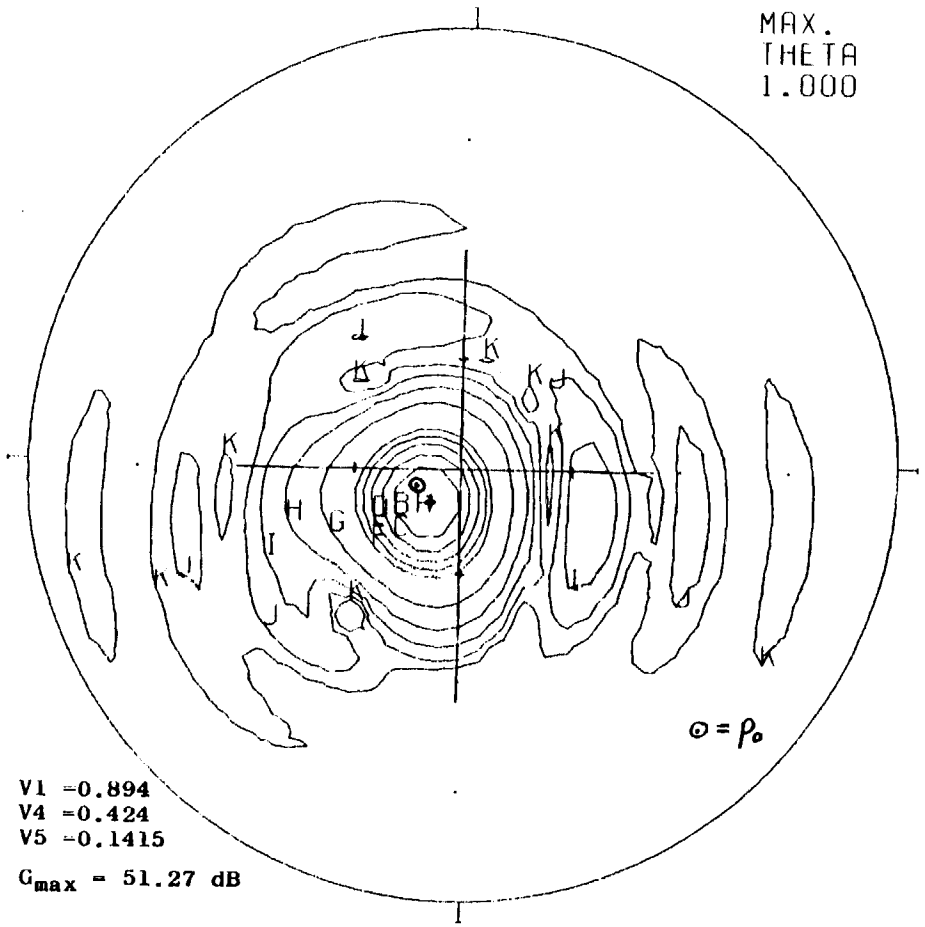

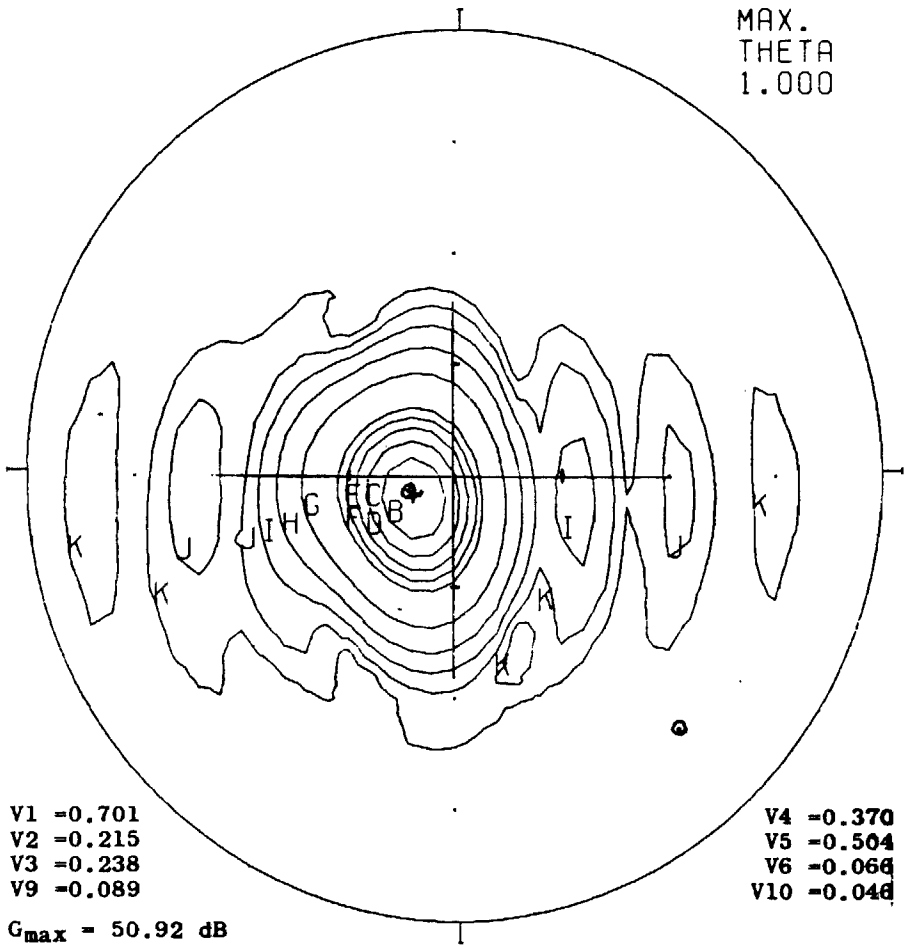

Fig. 5.3-6a. SCANNED BEAM PATTERNS, CONFIGURATION #1

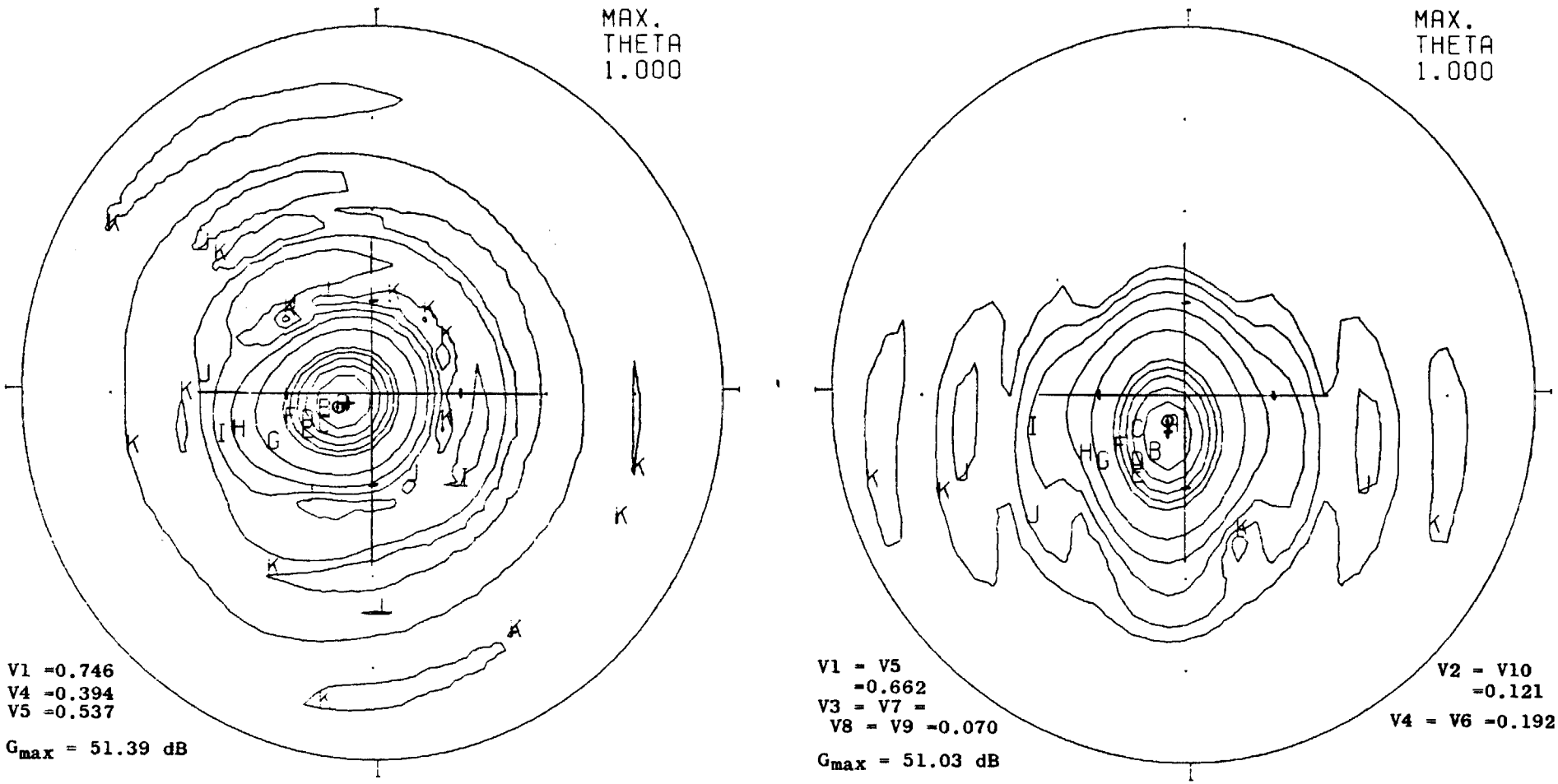

Fig. 5.3-6b. SCANNED BEAM PATTERNS, CONFIGURATION #1

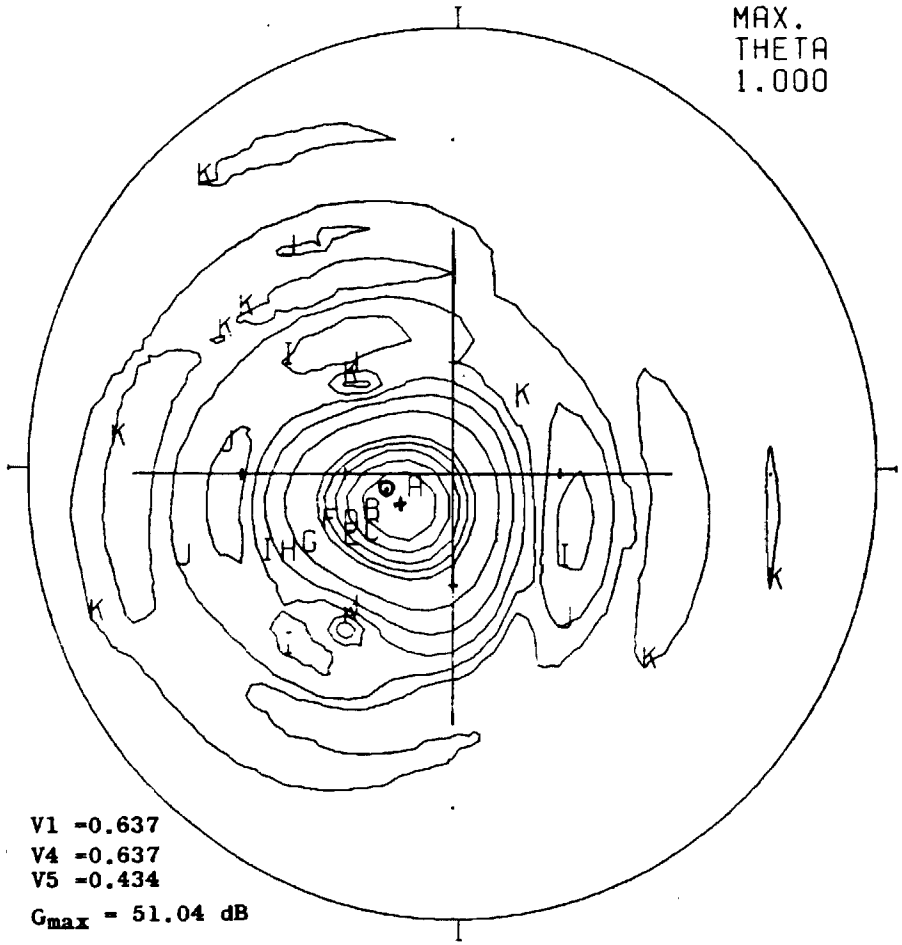

CASE CONFIG. NO 1.0, BEAM POS. = 1.5,4,

NO. ELMTS = 3

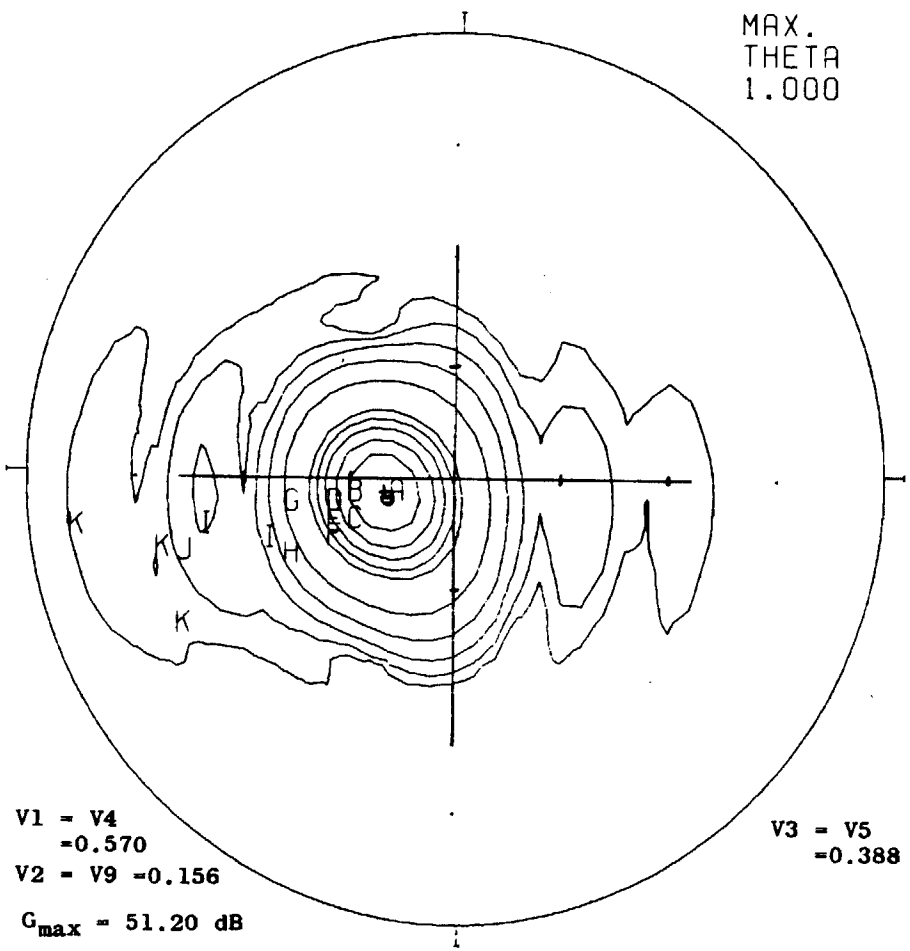

CASE CONFIG. NO 1.0, BEAM POS. = 1.5,4,

NO. ELMTS = 6

Fig. 5.3-6c. SCANNED BEAM PATTERNS, CONFIGURATION #1

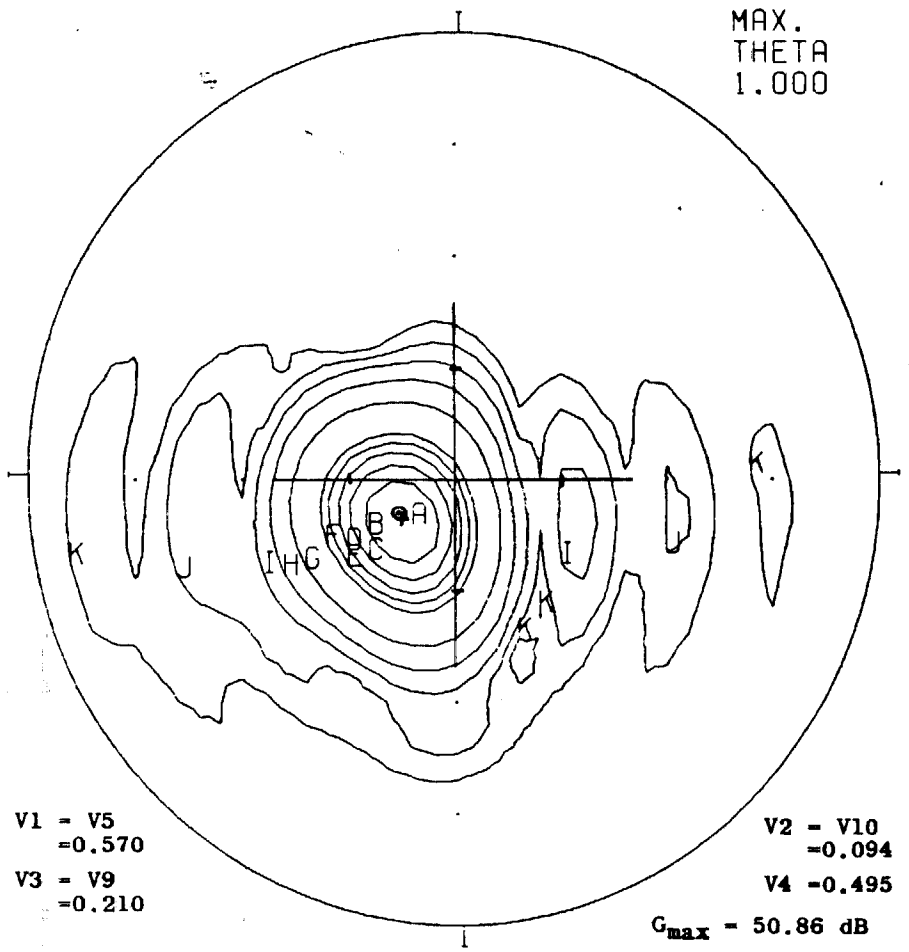

-50.856 WAS ADDED
TO INPUT DATA

CONTOUR DATA

SYMBOL	LEVEL
A	0.000
B	-1.000
C	-2.000
D	-3.000
E	-4.000
F	-5.000
G	-10.000
H	-15.000
I	-20.000
J	-25.000
K	-30.000

CASE CONFIG. NO 1.0, BEAM POS. = 3.3,NO. ELMTS = 7, FREQ = 19.0 GHZ

Fig. 5.3-6d. SCANNED BEAM PATTERNS, CONFIGURATION #1

However, the gain at the desired location is always greater with this optimized condition than if the beam peak were actually located at the desired position.

Table 5.3-3a Scanned Beam Summary, Configuration #1

Case	Desired Beam Pos (p_o)	Actual Peak Pos	No. Elem.	Peak Gain	Est. Gain @ p_o	Max. Sidelobe dB
1	0,0	0,0	1	51.50	51.50	-18
2	0,0	0,0	7	50.88	50.88	-15**
3	0,0	0,0	7	51.75*	51.75*	-18**
4	1.5,2	3.2,0.8	3	51.27	50.3	-18
5	1.5,2	2.0,2.0	8	50.92*	50.8*	-19
6	1.5,2	1.1,0.8	3	51.39	50.7	-19**
7	1.5,4	2.6,2.7	3	51.04	50.0	-18**
8	1.5,4	1.2,4.5	6	51.20*	51.2*	-19**
9	3,3	2.5,2.8	7	50.86*	50.8*	-18**
10	3,0	4.0,0	10	51.03*	50.8*	**

* Calculated value for maximum gain
** "Shoulder" effect rather than true sidelobe

Table 5.3-3b Scanned Beam Feed Voltages, Configuration #1

Case	V1	V2	V3	V4	V5	V6	V7	V8	V9	V10
1	1	0	0	0	0	0	0	0	0	0
2	.7677	.396	.155	.155	.396	.155	.155	0	0	0
3	.929	.190	.127	.127	.190	.127	.127	0	0	0
4	.894	0	0	.424	.1414	0	0	0	0	0
5	.701	.215	.238	.37	.504	.066	0	0	.089	.046
6	.746	0	0	.394	.537	0	0	0	0	0
7	.637	0	0	.637	.434	0	0	0		0
8	.57	.156	.388	.57	.388	0	0	0	.156	0
9	.57	.094	.21	.495	.57	0	0	0	.21	.094
10	.663	.121	.07	.192	.663	.192	.07	.07	.07	.121

c. Steering the beam anywhere within the prescribed coverage area for each 7 to 10-element cluster does not degrade gain performance by more than 1.0 dB. Maximum gain is generally achieved with a multi-element cluster of more than just three elements, since the desired steering can be accomplished more precisely (as evidenced by the closer proximity of actual beam peaks to the desired positions for the multi-element clusters, from Table 5.3-3).

Contour plots for Configuration #3, using larger 3-wavelength feed horns, are shown in Figure 5.3-7. The singlet on-axis beam shows a slightly wider beamwidth than Configuration #1 (with 1.6-wavelength horns), but comparable sidelobes. The chief difference is in calculated peak gain, which is some 4 dB higher than for Configuration #1, principally because of reduced spill-over with the larger feed horns. The on-axis beam produced by a 7-element cluster shows greatly improved sidelobes (around -21 dB in the assymetric plane), with about the same gain.

Upon examination of calculated on-axis patterns as shown in Figure 5.3-7, it was noted that the single-horn pattern of the TRW Configuration #3 did not match the assumed pattern shape used for coefficient determination of scanned beams, as reported in Section 5.2. This original pattern shape was taken from an early TRW report, and may not have corresponded to the final reflector configuration selected, which was scaled for the pattern calculations reported here. Accordingly, a new best-fit pattern function was chosen to correspond with the singlet patterns reported in Figure 5.3-7a, which is:

$$P(r) = -589.08\ r^{2.493}\ \text{(dB)}$$

where "r" is expressed in degrees. This corresponds to a 3 dB beamwidth of 0.24°. For "r" in units of $.025^{\circ}$ (as used in the analysis), the factor -589.08 should be replaced by -.059714. Single-element patterns for

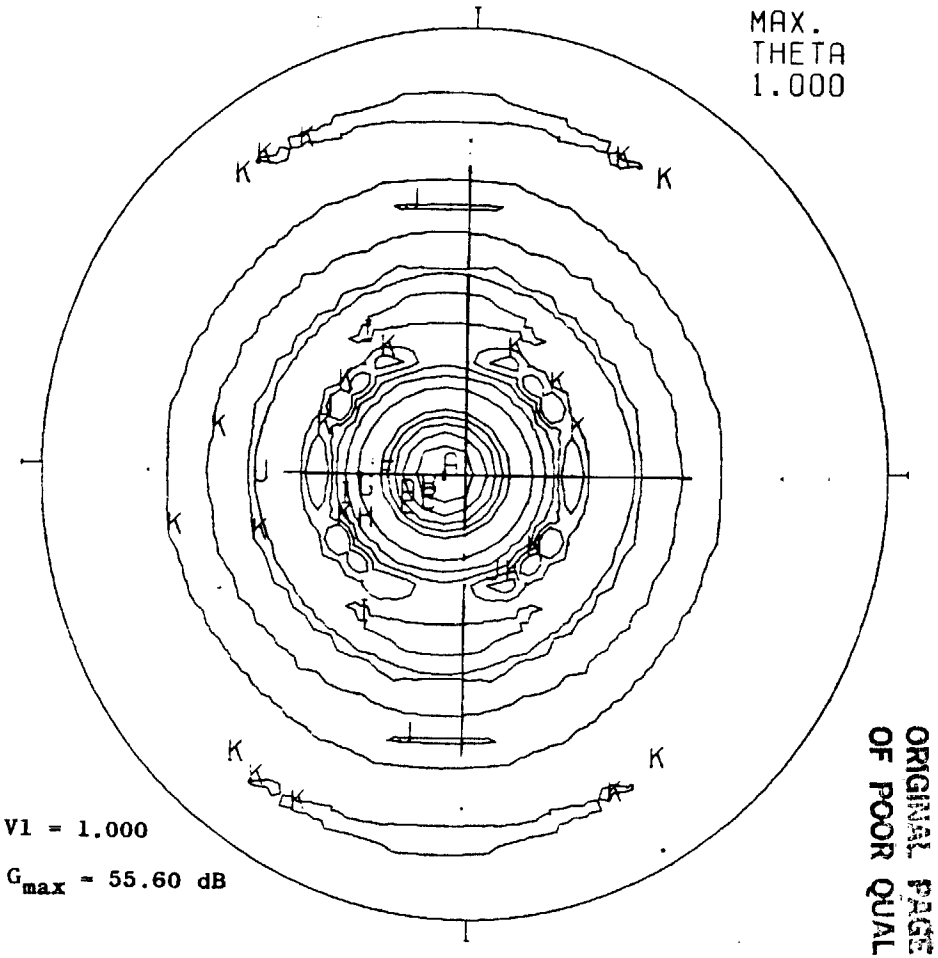

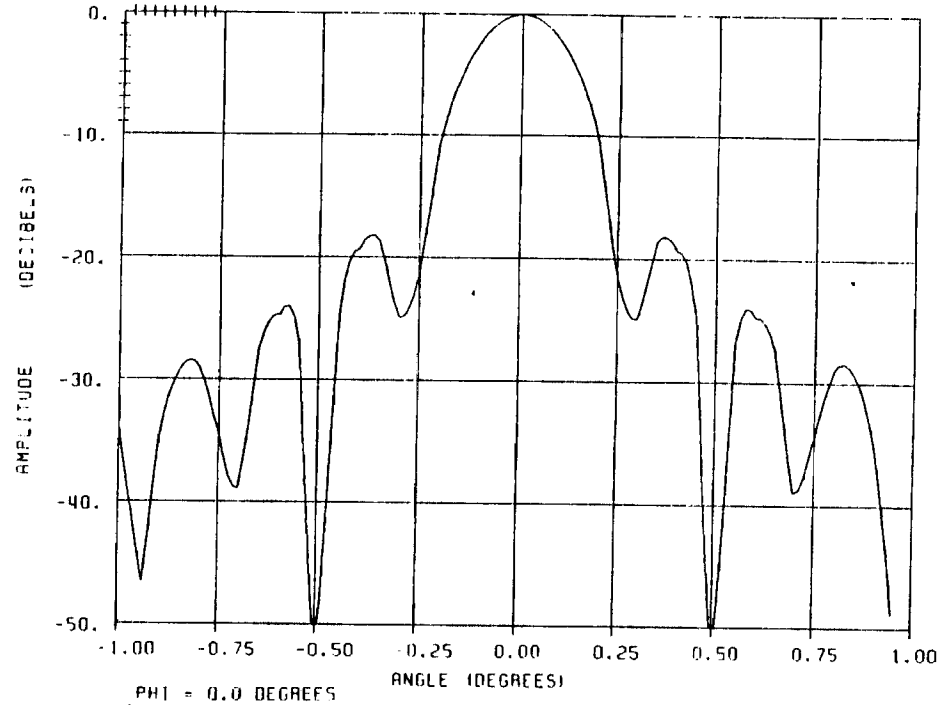

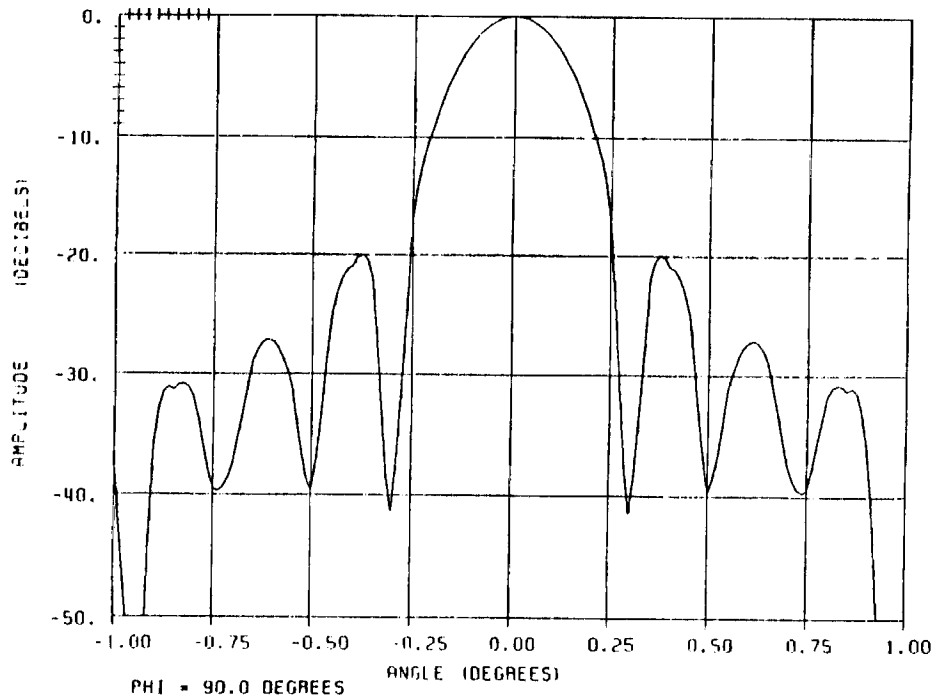

Fig. 5.3-7a. PATTERNS ON AXIS, SINGLE FEED ONLY CONFIGURATION #3

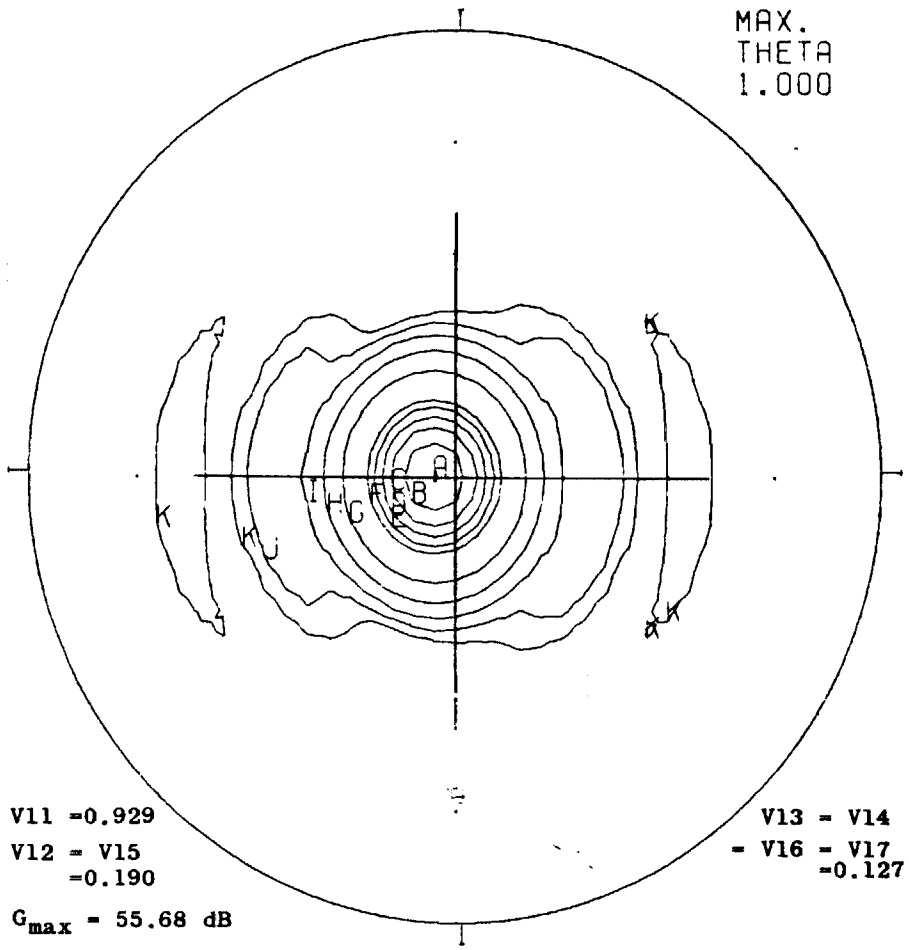

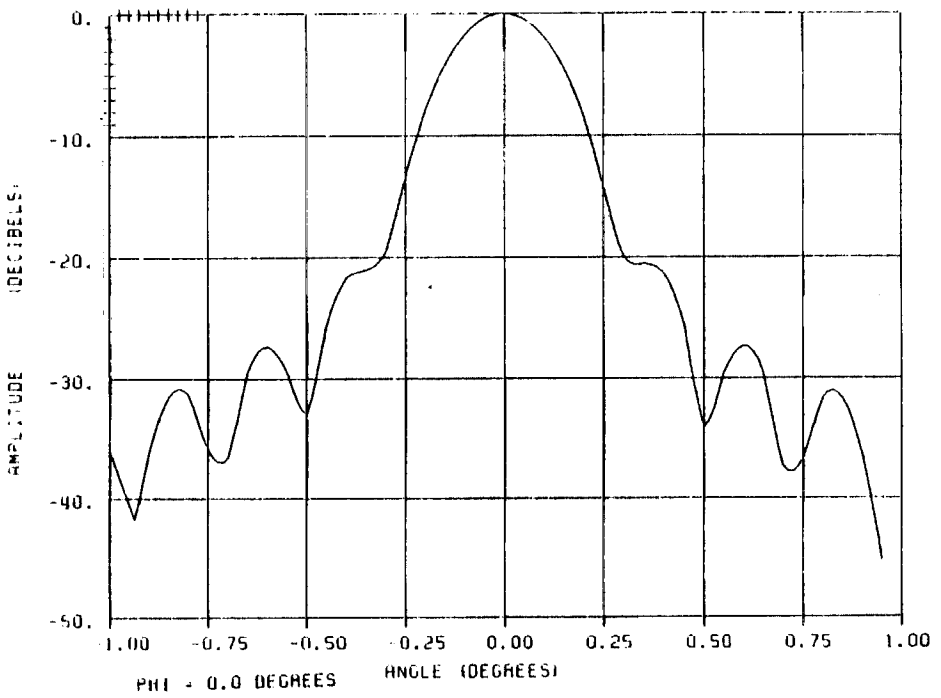

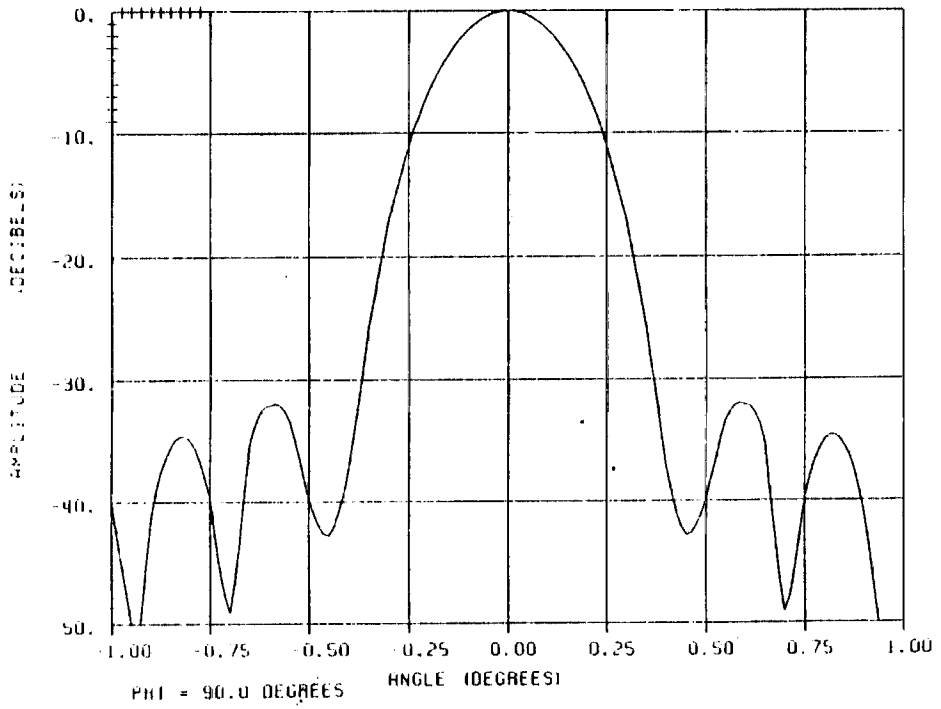

Fig. 5.3-7b. PATTERNS ON AXIS, SEVEN-ELEMENT CLUSTER CONFIGURATION #3

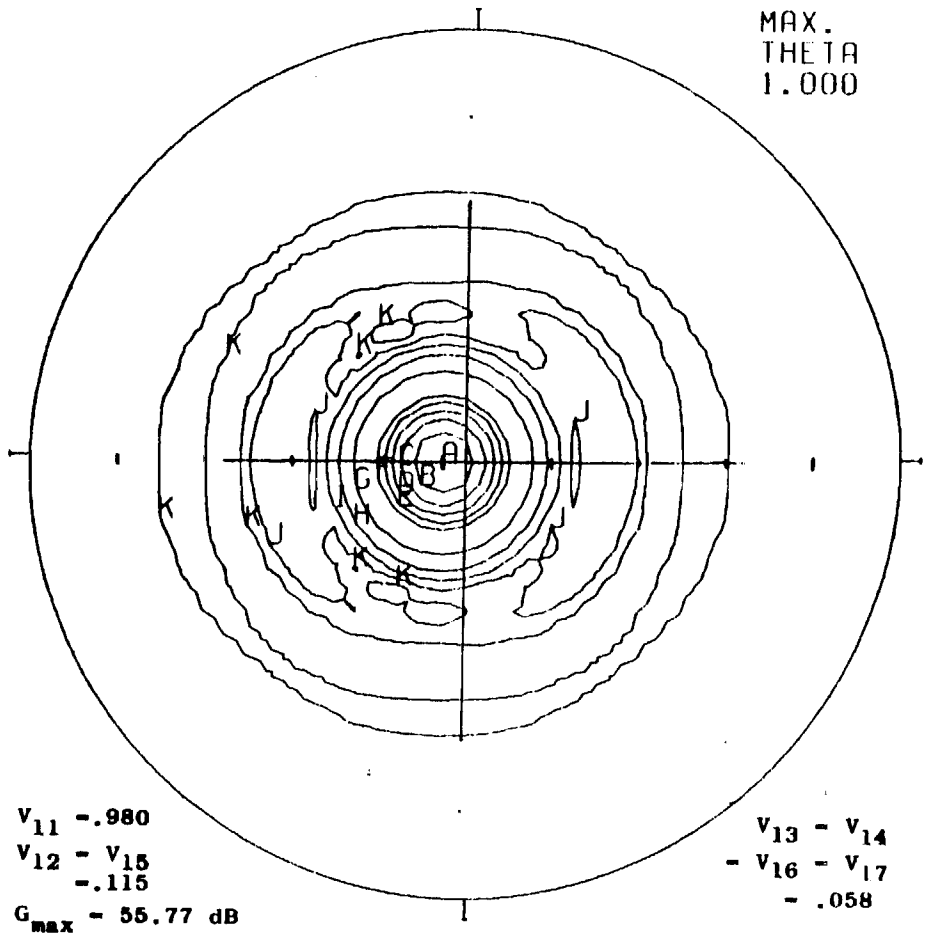

CASE CONFIG. NO 3.0, BEAM POS. = 0.0.
NO. ELMTS = 7, FREQ = 19.0 GHZ

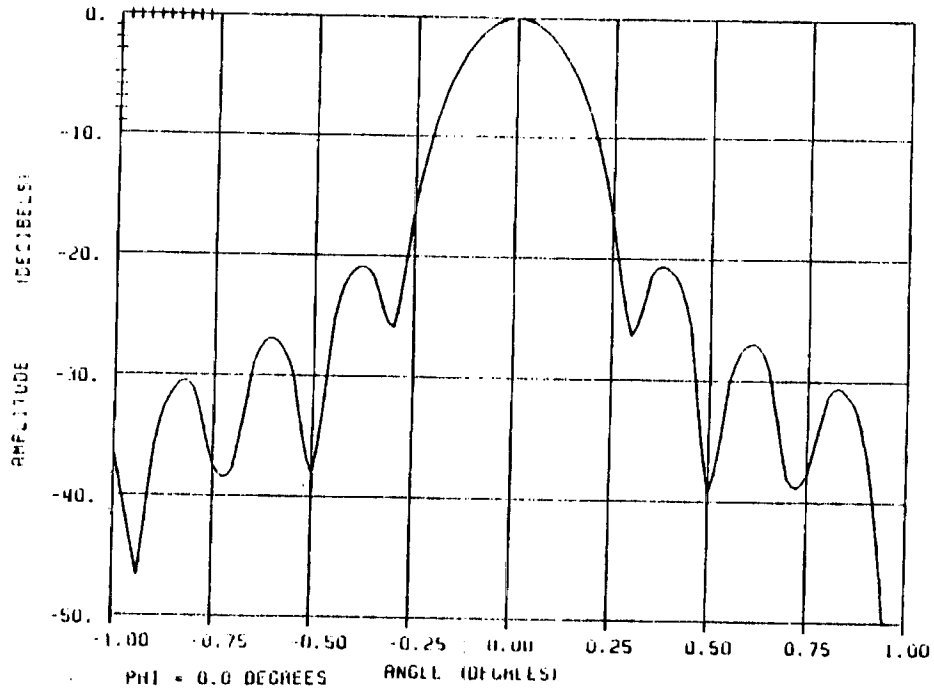

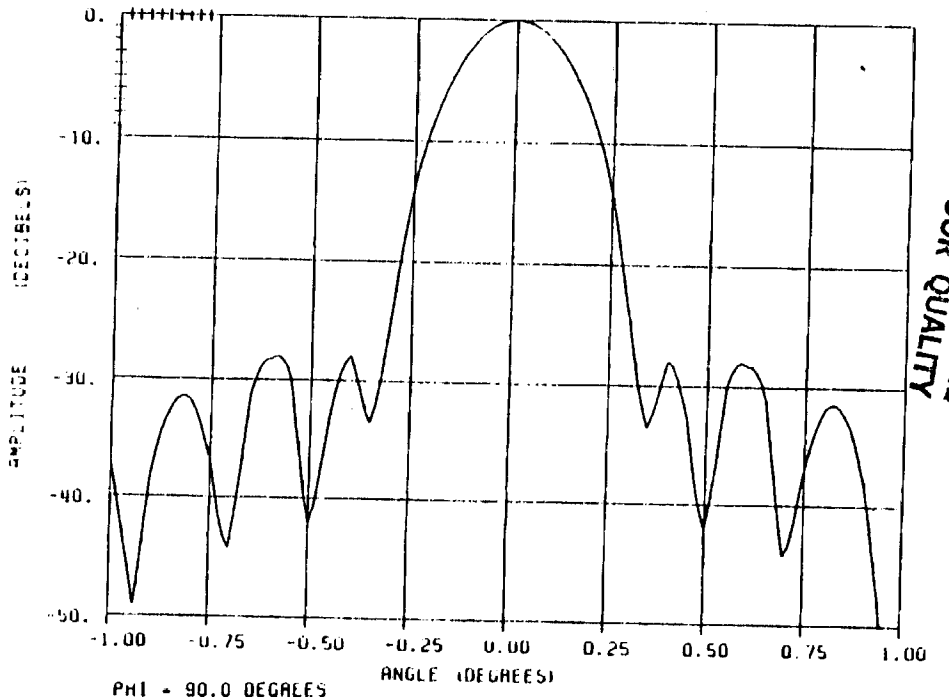

Fig. 5.3-7c. PATTERNS ON AXIS, SEVEN-ELEMENT CLUSTER, CONFIGURATION #3 NEW COEFFICIENTS

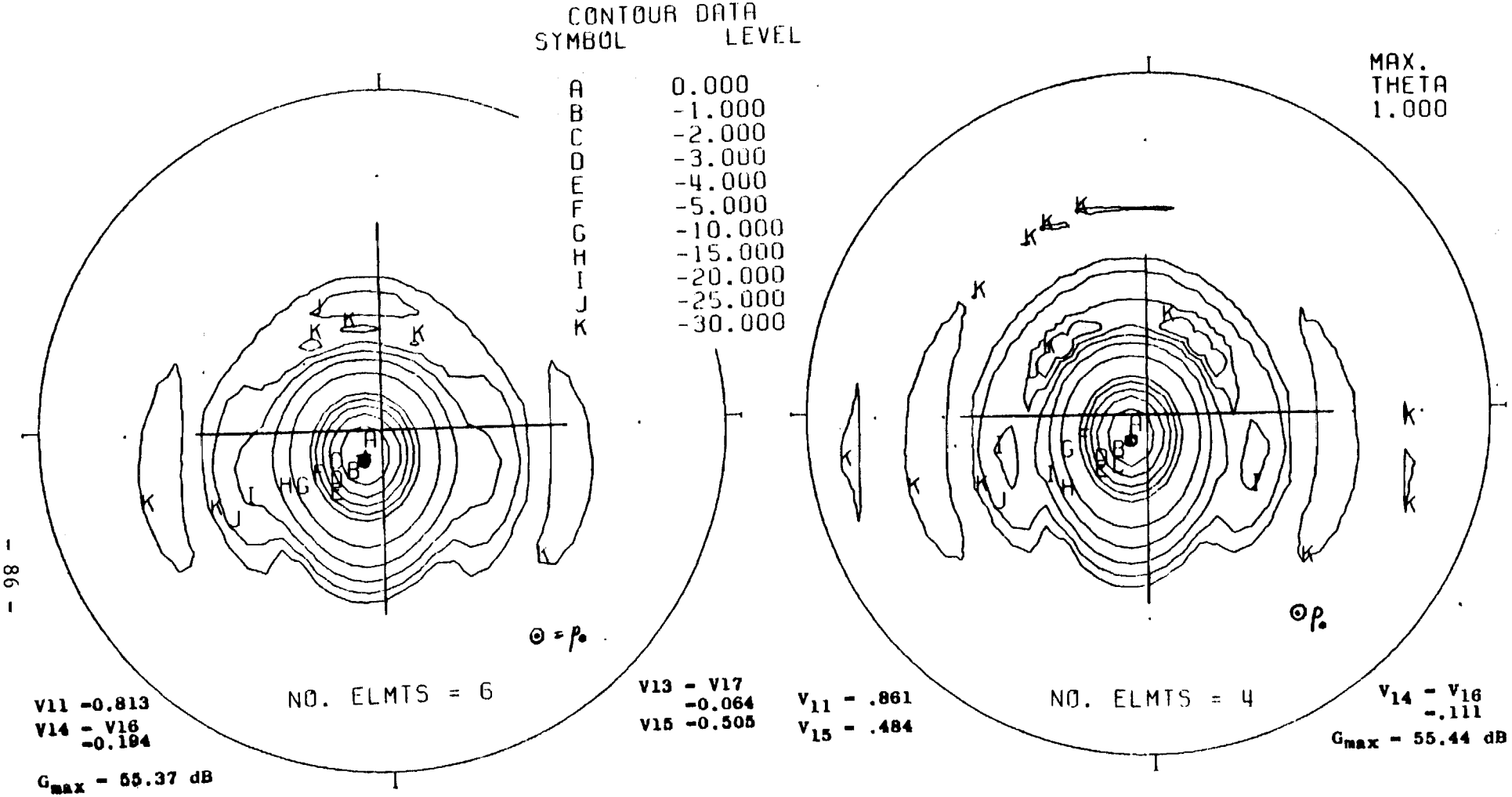

ORIGINAL COEFFICIENTS **NEW COEFFICIENTS**

Fig. 5.3-7d. SCANNED BEAM PATTERNS, CONFIGURATION #3

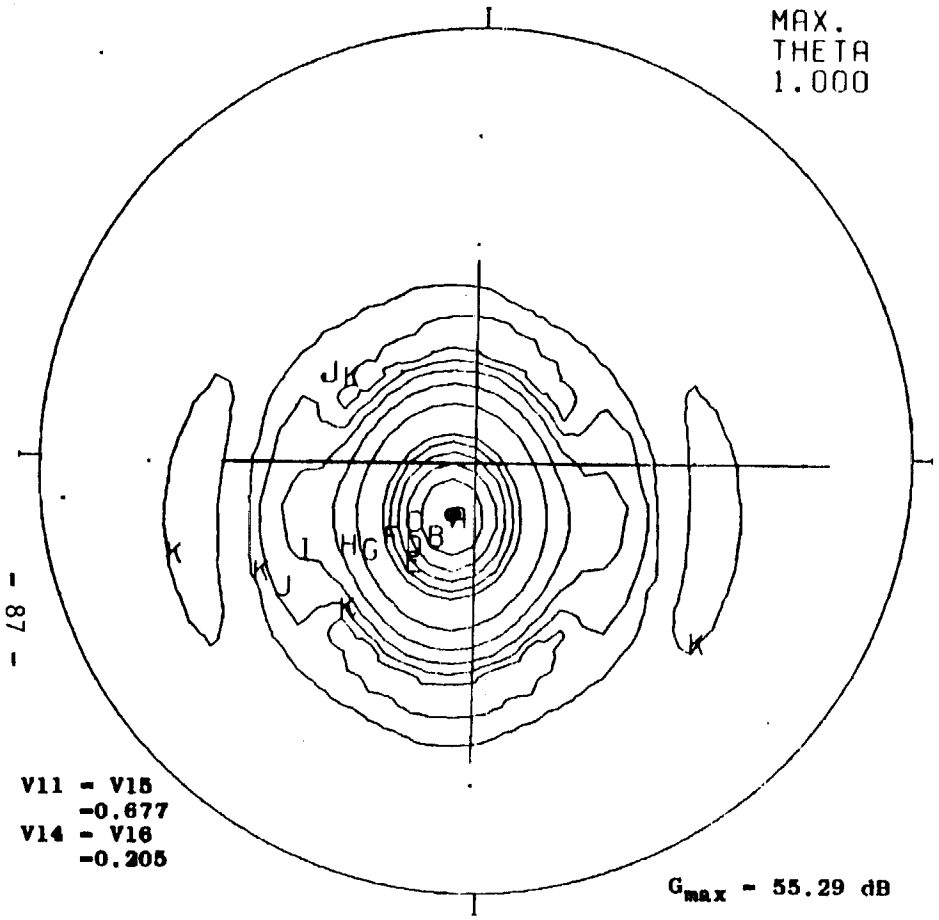

CASE CONFIG. NO 3.0, BEAM POS. = 5.0

ORIGINAL COEFFICIENTS

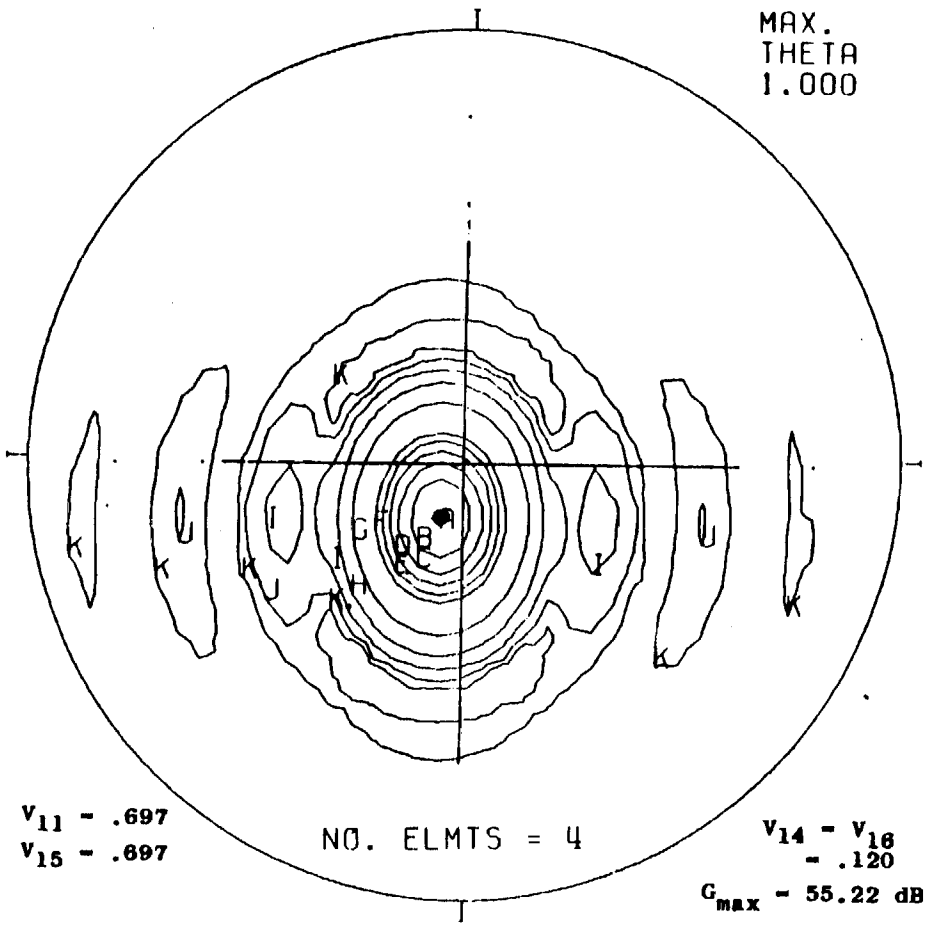

CASE CONFIG. NO 3.0, BEAM POS. = 5.0

NEW COEFFICIENTS

Fig. 5.3-7e. SCANNED BEAM PATTERNS, CONFIGURATION #3

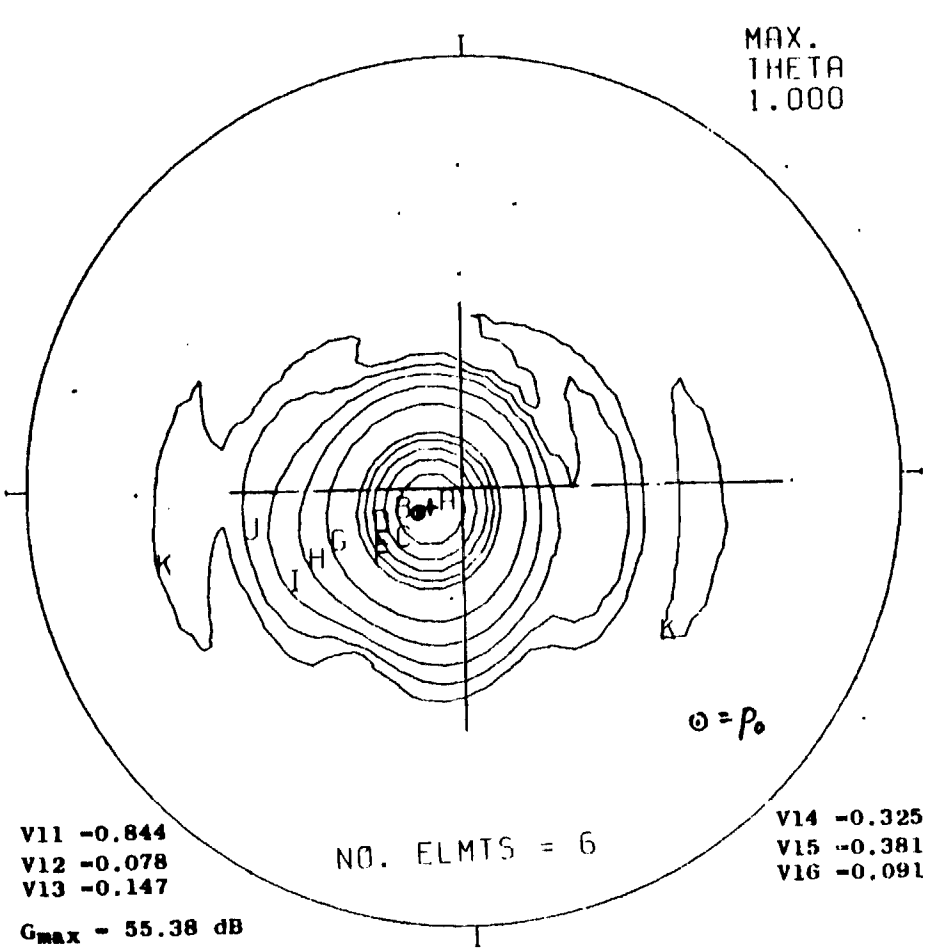

ORIGINAL COEFFICIENTS

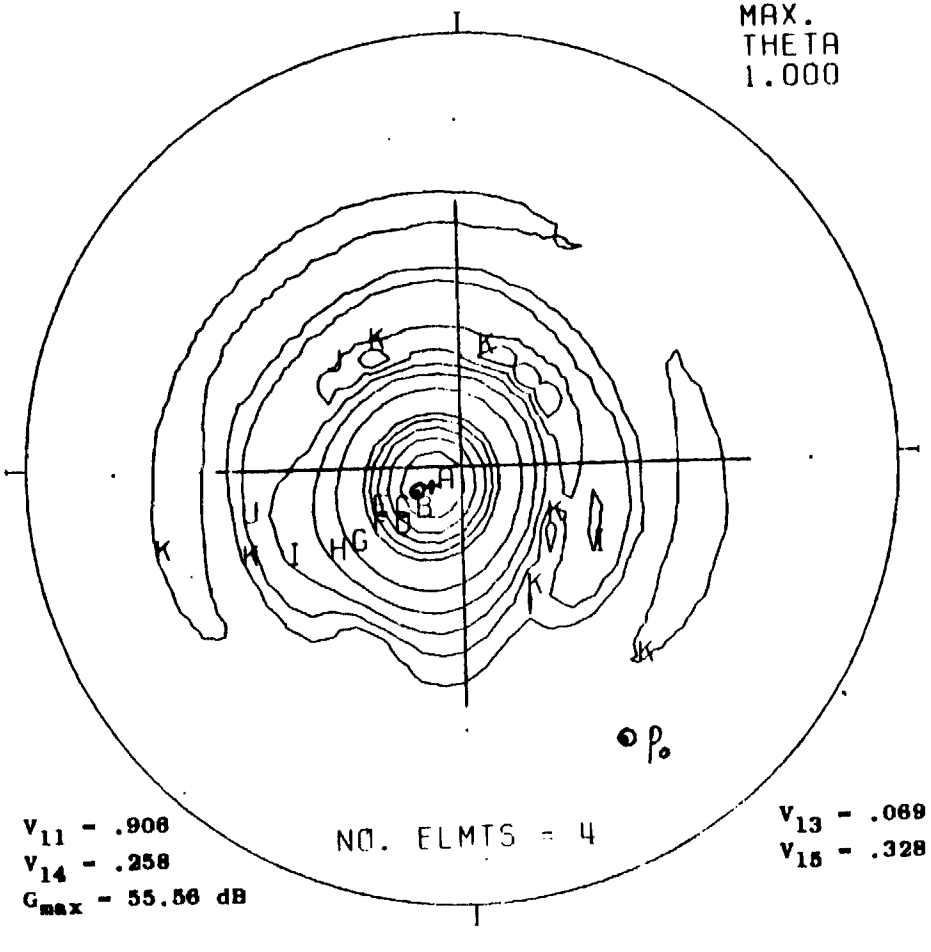

NEW COEFFICIENTS

Fig. 5.3-7f. SCANNED BEAM PATTERNS, CONFIGURATION #3

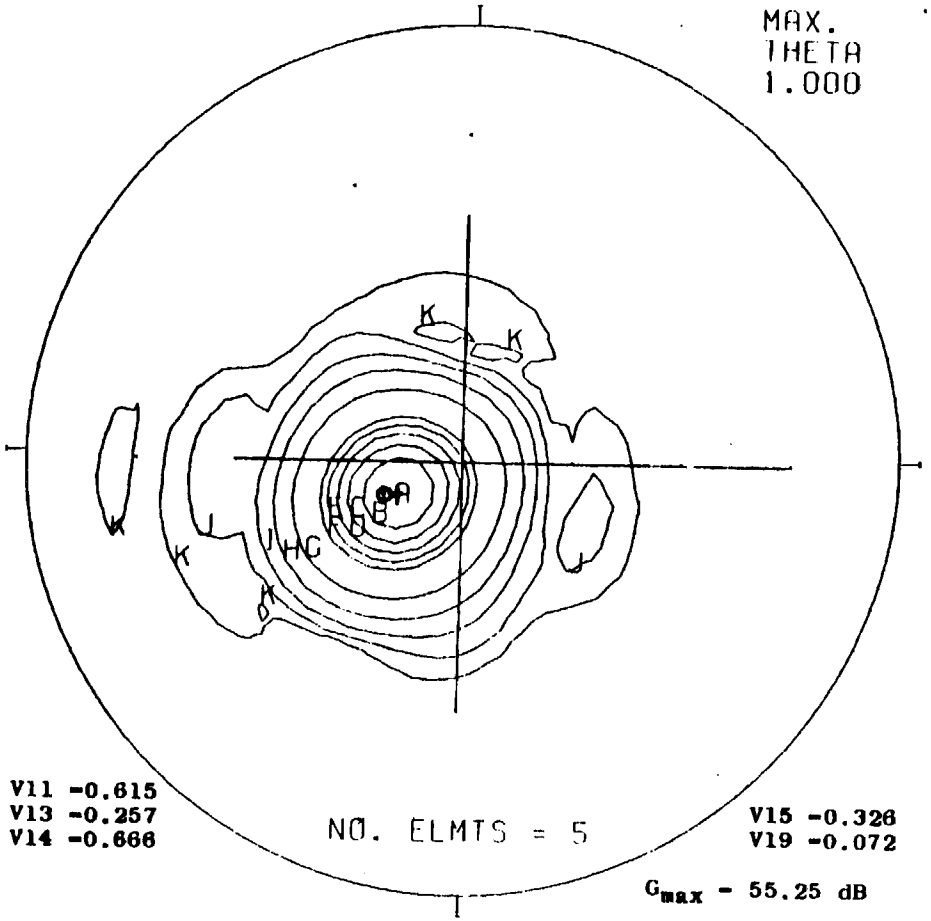

CASE CONFIG. NO 3.0, BEAM POS. = 3.5.

ORIGINAL COEFFICIENTS

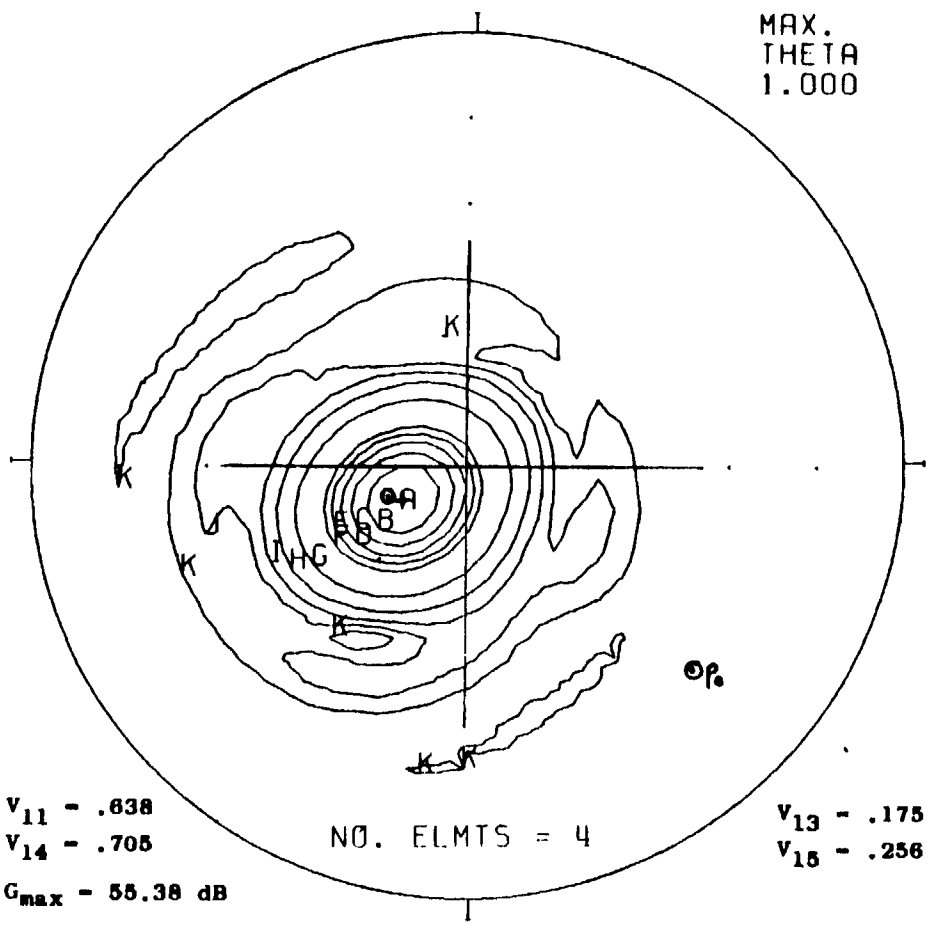

CASE CONFIG. NO 3.0, BEAM POS. = 3.5

NEW COEFFICIENTS

Fig. 5.3-7g. SCANNED BEAM PATTERNS, CONFIGURATION #3

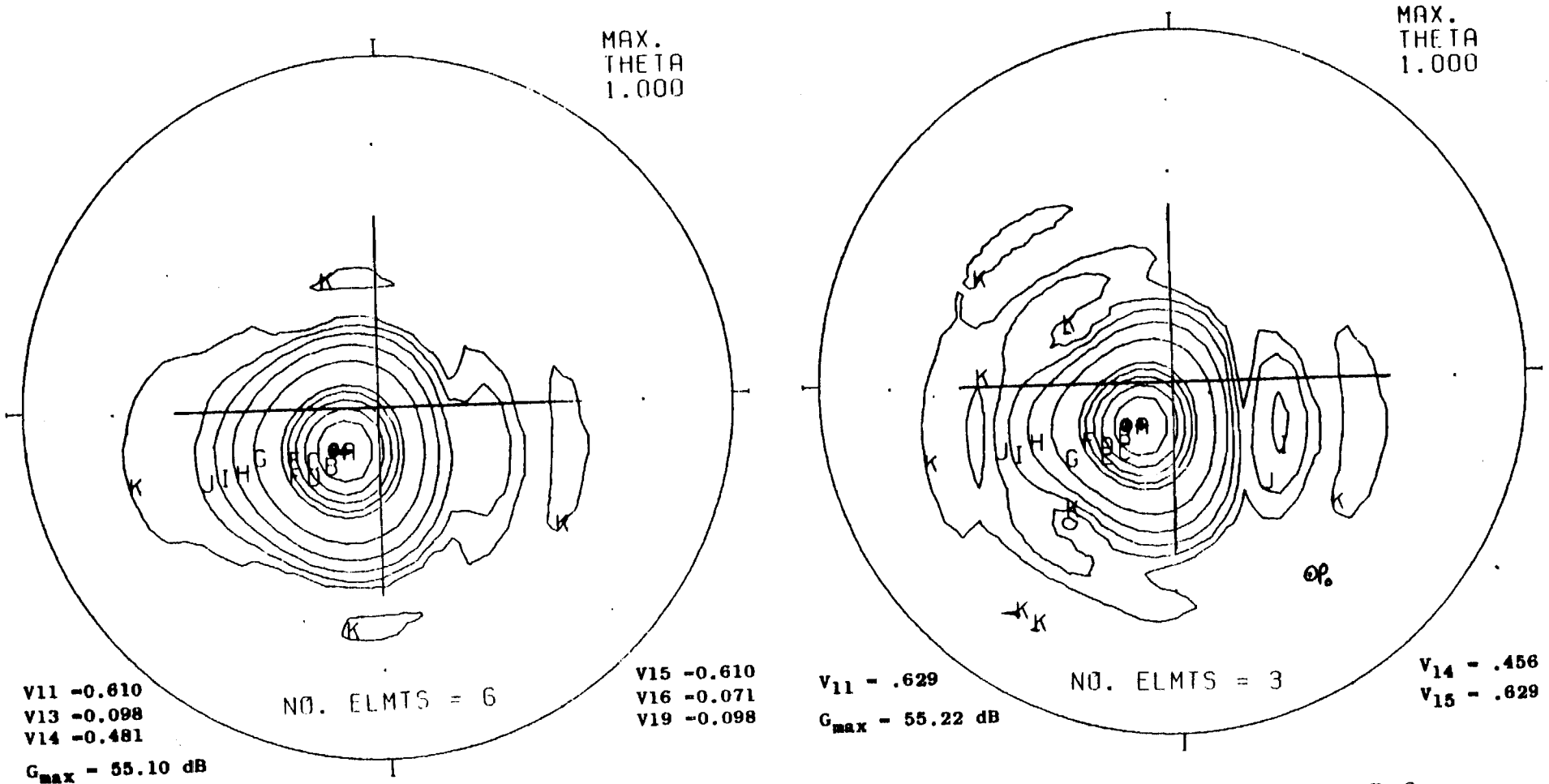

- 90 -

ORIGINAL COEFFICIENTS **NEW COEFFICIENTS**

Fig. 5.3-7h. SCANNED BEAM PATTERNS, CONFIGURATION #3

Configuration #1 were very close to the pattern function chosen earlier. Using this new pattern function for Configuration #3, new sets of feed coefficients were derived for steered beams as listed in Table 5.3-4b, and the composite patterns were calculated, with results listed in Table 5.3-4a. Calculated patterns for these steered beams are included in Figure 5.3-7, for positions designated by arrows in Figure 5.3-2. Again, there appears to be very little gain degradation with steering (less than 1.0 dB), and a beam broadening in the direction of scan, with no sidelobe degradation (even some improvement).

Prior to this observation concerning the discrepancy in assumed beam patterns for Configuration #3, steered beam patterns had been calculated for feed coefficients based on the original singlet pattern shape. These patterns are also shown in Figure 5.3-7 for comparison. In all but one case, the new coefficients resulted in higher gains than the original, but by only 0.1 to 0.2 dB. Thus we conclude that the optimization procedure used for maximizing gain at a given point is valid, and may be used for feed coefficient determination when steering a beam as part of a multibeam array.

One additional observation may be made from the patterns of Figure 5.3-7: the newly-formed optimum-gain beams generally have somewhat higher sidelobes, and a more complex sidelobe structure, than the beams formed from the original coefficients. This may be the result of the fact that the original patterns generally utilized more beams for their formation, which was the result of an arbitrary cut-off of beams whose excitation amplitudes were more than the 25 dB below the input level. If this level were reduced to -40 dB, several additional beams would be excited for the new set of coefficients, at levels indicated in parentheses in Table 5.3-4b. Although these additional beams would not contribute significantly to the overall gain, they may affect the sidelobe structure, and thus may be worthwhile implementing.

Table 5.3-4a Scanned Beam Summary, Configuration #3

Case	Beam Pos (p_o)	Peak Pos	No. Elem.	Peak Gain	Est. Gain @ p_o	Max. Sidelobe dB
1	0,0	0,0	1	55.60	55.6	-18
2	0,0	0,0	7	55.68*	55.7*	-21**
3	3.5,0	3,0	6	55.37	55.4	-21**
4	5,0	5.2,0	4	55.29	55.3	-21**
5	2.5,2.0	2.0,1.0	3	55.43	54.7	-20**
6	2.5,2.0	2.0,1.0	6	55.38*	54.7*	-21**
7	3,5	3,4	5	55.25	54.7	-23**
8	5,3	5,2	6	55.10	54.6	-23**

* Calculated value for maximum gain
** "Shoulder" effect rather than true sidelobe

Table 5.3-4b New Scanned Beam Feed Coefficients, Configuration #3

Case	V11	V12	V13	V14	V15	V16	V17/V19
1a	1	0	0	0	0	0	0
2a	.980	.115	.058	.058	.115	.058	.058
3a	.861	(0.11)	(.015)	.111	.484	.111	(.015)
4a	.697	0	0	.1195	.700	.1195	0
6a	.906	(.022)	.069	.258	.328	(.029)	0
7a	.638	0	.175	.705	.256	0	(.018)
8a	.629	0	(.032)	.456	.629	(.018)	(.032)

NOTE: Values in parentheses indicate coefficients more than 25 dB below input.

One factor to be remembered relative to the above steered beam evaluation is that the amount of steering is relatively small for a given set of beams, principally because the singlet beams are relatively close together. The maximum scan for Configuration #1 is only 0.11°, or 42% of the beamwidth; the maximum for Configuration #3 is only 0.15°, or 63% of a beamwidth. If

greater steering angles for the entire array are required, it is merely necessary to designate a different set of beams, within the limitations of the total feed array. This factor can be appreciated by comparing scan beam contours for different positions, and noting the relatively small deviations of the main beam.

5.4 Open and Closed-Loop Reconfigurable Systems

The methods discussed previously for pointing error compensation involved first a means of measuring the error, then determining a new set of feed coefficients to correct for the measured error, and setting these values into the feed network. This process, while designed to correct for any pointing errors measured, provides no assurance that such errors have been properly corrected - i.e., the process is basically open loop - no feedback is provided, which is a basic step in an adaptive control system. In addition, the process of error measurement entails considerable extra hardware, since a separate coupler-detector must be provided at each feed port to determine relative signal levels. In addition, these couplers introduce additional loss into the signal path, whose magnitude must be traded off against detectability in the error detectors. Such a system, nevertheless, could be implemented, as depicted in Figure 5.4-1.

An alternative to this process is to implement a truly adaptive pointing error correction system by providing some form of feedback. The simplest form of feedback is merely to sample the combined output of the antenna and to sense when this is maximized, which presumably is an indication that the antenna is pointed to the desired source. A simple random search could be implemented, perturbing all the feed coefficients randomly until the best combination for maximum output is found. However, a more orderly process (and undoubtedly faster) would be to try to determine how each feed coefficient should be changed to increase the total output. This is essentially

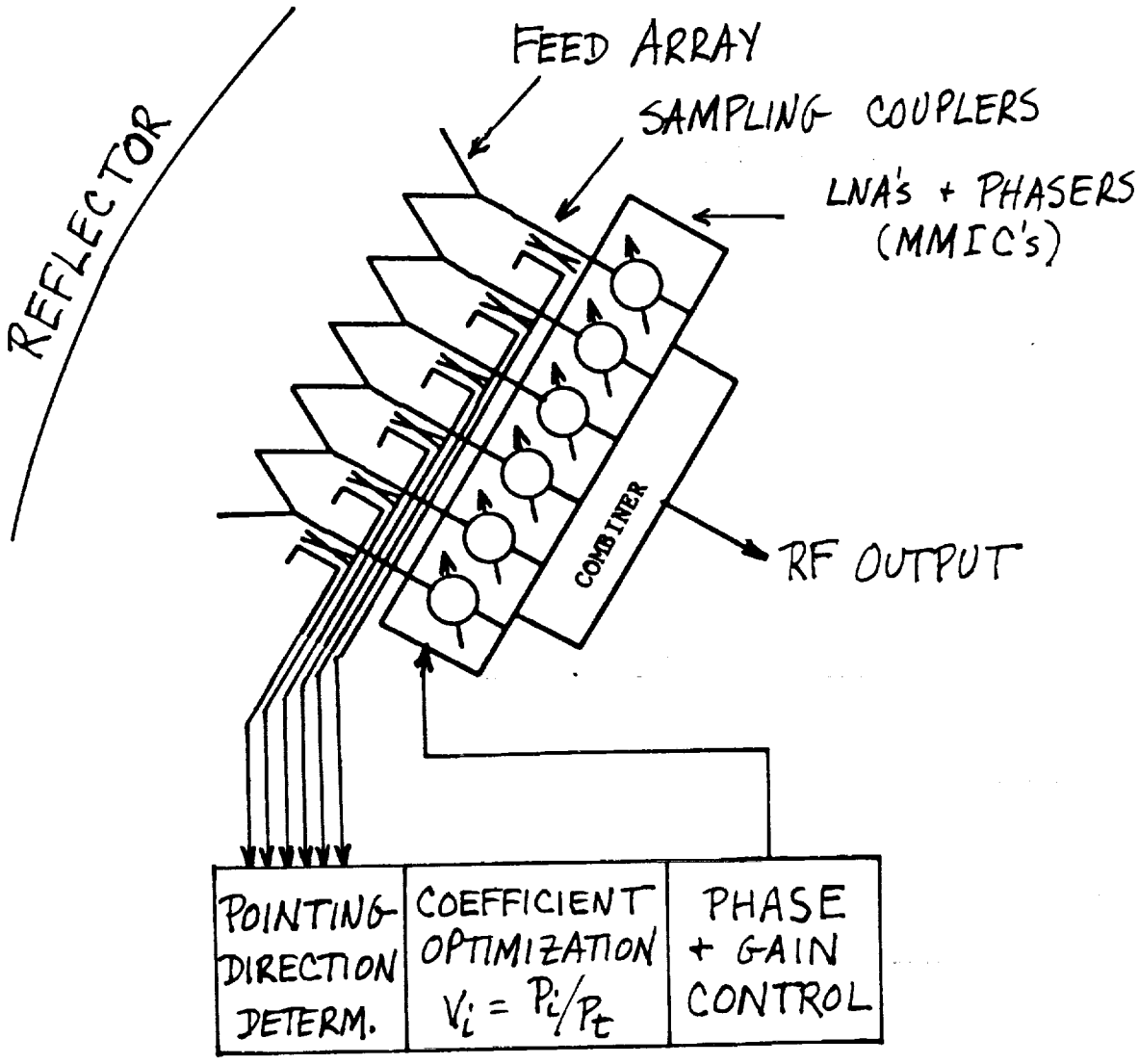

FIG. 5.4-1. OPEN-LOOP POINTING ERROR CORRECTION SYSTEM

the same process which was used for maximizing the output mathematically when searching for the best set of feed coefficients to correct for pointing errors which had been detected independently. This process is known as the gradient approach to optimization.

To implement this approach in a multibeam antenna system, two factors must be determined - first, the gradient at each feed port, and then how to vary each coefficient using this gradient to maximize the combined antenna output. The gradient could be determined by systematically perturbing each feed coefficient by a small amount and noting the effect on total output. This would be relatively simple in a spot beam system using only a few feeds (3 to 10) for each beam, and it would be easy to implement with an MMIC feed network by perturbing the gain of each amplifier in turn and noting its effect on total output. One particularly simple way to implement this detection would be to modulate the gain of each amplifier in turn at a low (audio) rate, and use a synchronous detector to determine the variations in output. The entire process could be achieved simultaneously by using different audio rates on each beam port amplifier, but the increase in hardware for such simultaneous detection may not be worth the time saved.

Changing the feed coefficients in response to the measured gradients is straightforward, and merely represents a compromise between speed of correction and stability. If a small correction in each coefficient is made in proportion to the size and direction of the gradient, the entire set of coefficients should converge slowly to the proper set to achieve the desired optimum pointing direction. If too large a set of corrections is implemented, the pointing direction may overshoot the desired location; thus there would appear to be an optimum size of correction for minimum settling time to the corrected position.

A block diagram of the adaptive system required to implement this correction scheme is presented in Figure 5.4-2. The only additional hardware

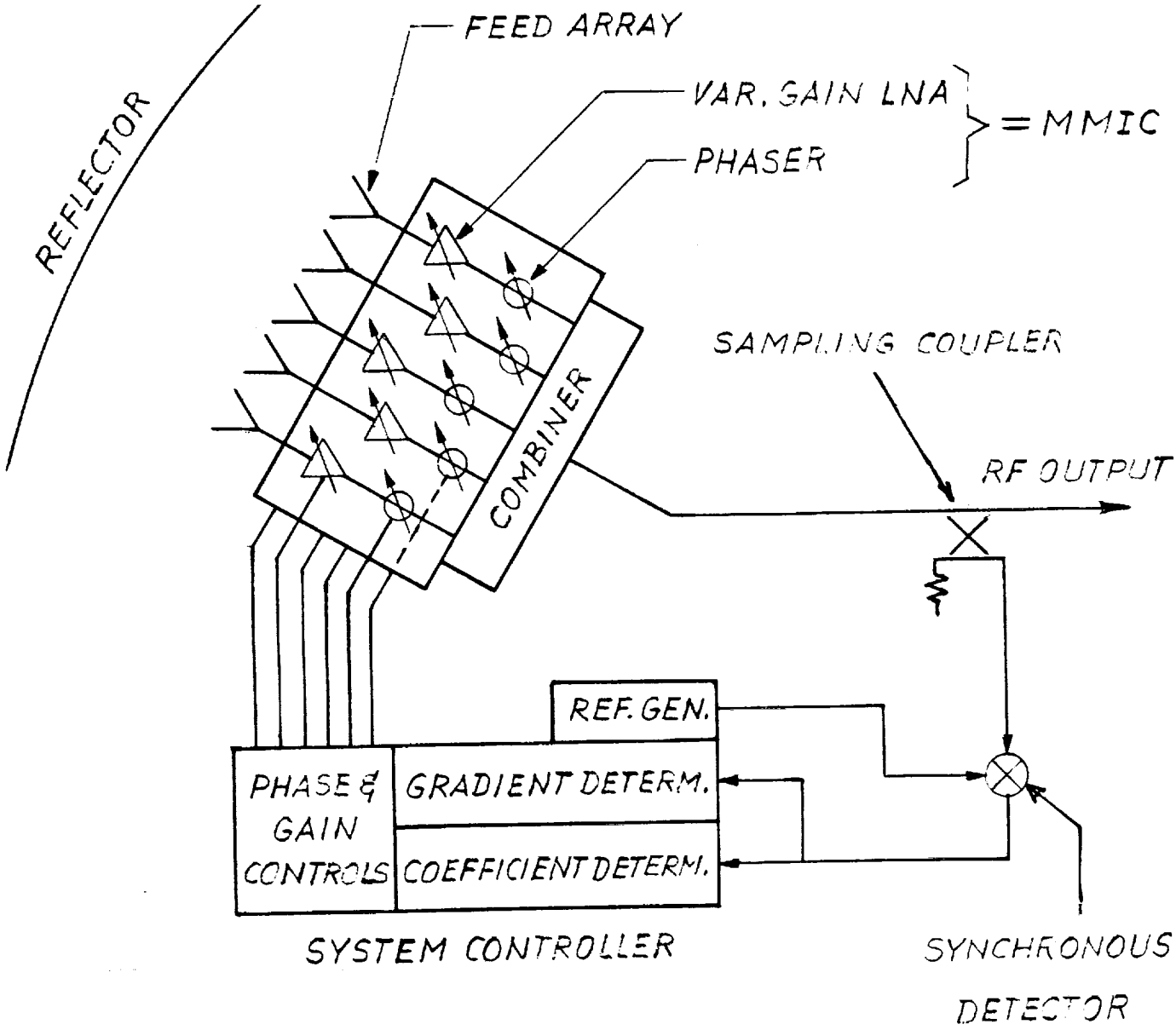

FIG. 5.4-2. CLOSED-LOOP POINTING ERROR CORRECTION SYSTEM

required is the sampling coupler, synchronous detector, and controller, which would probably represent only a modification to an existing unit required to control the MMIC modules without adaptive processing.

5.4.1 Simulated Adaptive Error Correction

In order to simulate the performance of the adaptive error correction scheme outlined above, a computer program was written using the basic correction techniques described, in addition to information generated on earlier tasks describing how the basic multibeam antenna system operates. Configuration #3 (the TRW ACTS beam configuration) was chosen for study because of its greater component beam separation, which represents a greater challenge for optimum control. An overlay of 3 dB beam contours of ten adjacent feeds is shown in Figure 5.1-3. Any or all of these feeds could be used to steer a beam anywhere near the center of the cluster. A simple elementary pattern shape of the form $P = -k\, r^{2.5}$ was used, where P is expressed in dB and "r" the angular distance from the center of the beam. This relation corresponds closely to calculated singlet patterns for the configuration chosen. Units for "r" were chosen as $.025^{o}$ for convenience in plotting; this was broken into orthogonal "x" and "y" components for analysis. The 3 dB beamwidth of the calculated beams was 0.24^{o}, corresponding to a value for "k" of .06.

The following steps were involved in the simulation:

1. Choose initial antenna position vector (x_o, y_o).
2. Calculate relative output from 10 horns at this position.
3. Calculate feed coefficients for maximum gain, and maximum gain from formulae developed in Section 5.3, as follows:

$$V_i = P_i / P_t \qquad P_t = \sqrt{\sum_i P_i^2}$$

These are the feed coefficients which presumably would be set into the antenna initially to maximize gain in the desired direction.

4. Choose new antenna position (x,y), representing some pointing error.
5. Calculate gain at this new position, using original set of feed coefficients.
6. Compute gradients for each feed at this new position, by increasing each a specified amount, re-normalizing the set of coefficients, and calculating the total output with these perturbed coefficients.
7. Choose a new set of feed coefficients by adjusting original coefficients in proportion to gradients (and re-normalizing).
8. Calculate gain with this new set of coefficients.
9. Compare new gain with old, and repeat process if there is significant improvement (more than approximately .001 dB).

This simulation program was tested for a number of cases, and the correction parameters were varied to find their effect on performance of the adaptive system. Typical outputs are given in Figure 5.4-3, and a listing of the program is included in Appendix A. Some indication of the convergence performance is given in Table 5.4-1, from a series of runs with this simulation program. Performance was measured in a number of ways - by the number of iterations required to reach maximum gain, by the difference between this maximum gain and the optimized value (unknown to the adaptive system, but calculated by the program at Step 5), and by the deviation of the final iterated feed coefficients from the optimized values (also calculated in Step 5). The parameter which was varied in the process was essentially the feedback gain, given by the parameter "Q" in the relationship to determine new feed coefficients, as:

$$V_i' = V_i + Q \cdot \Delta P / \Delta V_i$$

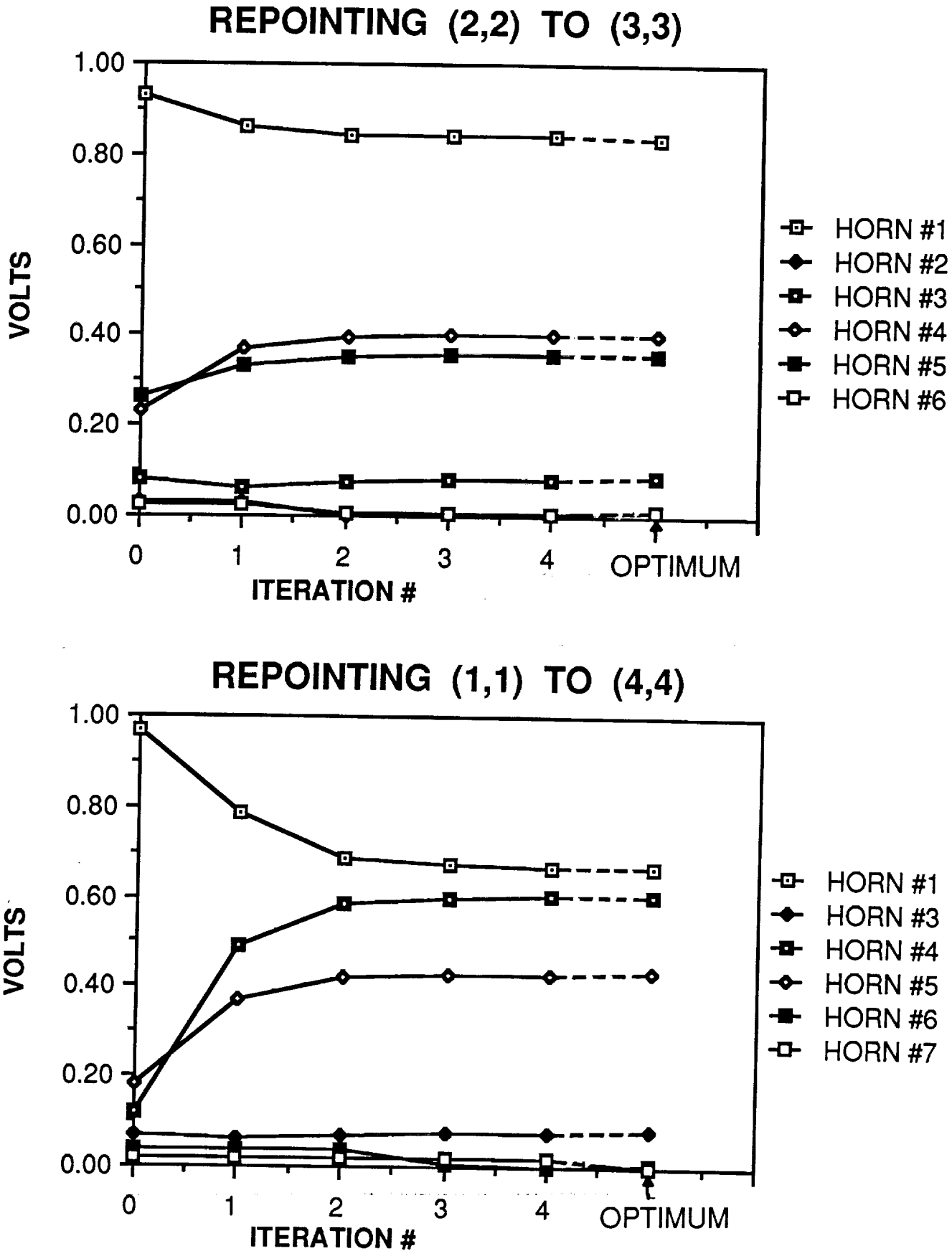

FIG. 5.4-3. SIMULATED ADAPTIVE SYSTEM PERFORMANCE

where "$\Delta P/\Delta V_i$" is the gradient of the i-th feed coefficient "V_i", "ΔV_i" is the incremental voltage used for determining the gradient. This relationship between the new and original coefficients can be obtained in terms of the variation in the output of the BFN. To this end consider the expression relating the total BFN output (P_t) to the excitation coefficient (V_i):

$$P_t = V_i P_i + \sum V_k P_k = V_i P_i + V_R P_R$$

where without any loss of generality, the feed cluster is divided into two subsets: The first subset contains the ith feed, and the second subset contains the rest of the feeds. P_i and P_R are then the element pattern of the ith feed and the composite pattern of the rest of the feeds respectively. A small change in the value of V_i results in:

$$P_t' \approx (V_i+\Delta V_i)P_i + [1-(V_i+\Delta V_i)^2]^{1/2} P_R$$

Assuming $V_i >> \Delta V_i$ and $1-V_i^2 >> \Delta V_i$, one obtains the ensuing approximation

$$P_t' \approx P_t + \Delta V_i (P_i - V_i P_R / V_R)$$

Denoting $\Delta P = P_t' - P_t$ and $V_i' = V_i + \Delta V_i$ yields

$$V_i' \approx V_i + V_R \Delta P / (P_i V_R - V_i P_R)$$

For a well optimized antenna, $P_i V_R - V_i P_R$ is very small, suggesting an expression in the following form

$$V_i' = V_i + Q \cdot \Delta P / \Delta V_i$$

where

$$Q = V_R \Delta V_i / (P_i V_R - V_i P_R) \qquad (A)$$

The exact value of Q is difficult to determine. From a numerical analysis, it has been estimated that the optimum value for Q is unity, which leads to

quickest conversion, minimum tendency to oscillate, and the least deviation in the final gain from the optimized value. Equation (A) relates the new feed coefficient (V_i') to the old one (V_i) by way of the gradient ($\Delta P/\Delta V_i$) of the BFN output.

Table 5.4-1 Simulated Adaptive System Performance

CASE I

Initial Beam Position = (2,2)

New Beam Position = (3,3)

Feedback Factor Q =	0.5	1.0	2.0
Number of Steps to Quit	6	4	6
Final Deviation from Opt. Gain (dB)	.001	.001	.001
No. changes in Sign	3	5	20
Average Dev. in Coeffs. from Optimum (volts)	.005	.006	.015

CASE II

Initial Beam Position = (1,1)

New Beam Position = (4,4)

Feedback Factor Q =	0.5	1.0	2.0
Number of Steps to Quit	8	4	8
Final Deviation from Opt. Gain (dB)	0	0	.003
No. changes in Sign	1	2	20
Average Dev. in Coeffs. from Optimum (volts)	.005	.004	.008

These data were taken using an initial value of 0.05 volts for ΔV, and decreasing this by a factor of two for successive iterations, down to a minimum value of 0.0125 volts. A plot of the convergence of the two cases listed in Table 5.4-1 for Q = 1 is given in Figure 5.4-3.

This proposed adaptive pointing error compensation system would apparently work well for the uplink beam, with the desired ground station transmitting a beacon signal for identification on the satellite. However, for the downlink case, the adaptive feedback loop would require retransmission to the satellite of a sample of the received signal, for determining gradients for the individual feeds.

5.5 Pointing Error Correction Methods Tradeoffs

In assessing the relative merits of the open-loop and closed-loop correction methods, one needs to compare the performance achievable with each method as well as the relative costs. Costs relate primarily to hardware, and so we must analyze the configurations which must be implemented for each scheme. The scenario addressed is that of the multiple scanning/fixed beam environment similar to the requirements set up for the ACTS program, which originally involved 18 fixed beams and 6 independent scanning beams to cover CONUS. These were to achieve inter-beam isolation by means of spatial and polarization separation between beams of the same type, since scanning and fixed beams were to utilize different portions of the frequency spectrum. Accordingly, the total feed array (some 500 feed horns for the FACC approach, or perhaps half that number for the TRW version) would require hardware as shown in Figure 5.5-1 to separate signals on the basis of polarization and/or frequency to form the desired multiple beams. Polarization separation is afforded by orthomode junctions (OMJ's) located at each feed horn; frequency separation requires diplexer filters, potentially at each port of each OMJ, but possibly eliminated at those ports which are not used for fixed beams. Following this basic frequency and polarization separation, beam combining is necessary to form the desired beams, presumably utilizing individual MMIC

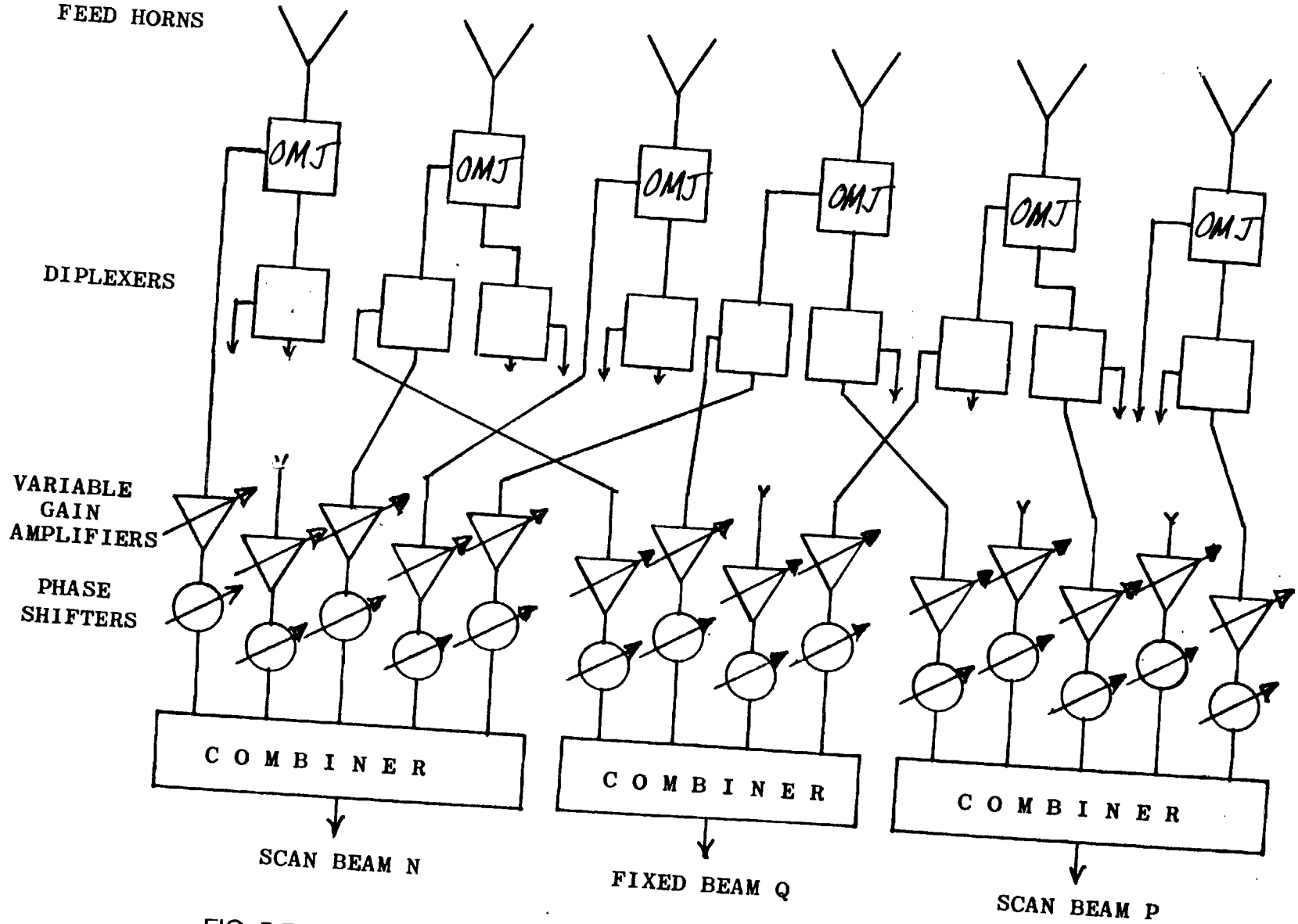

FIG. 5.5-1. ACTS MULTIPLE-BEAM ANTENNA FEED NETWORKS

modules at each combining port, as shown, to allow phase and amplitude control for steering, without compromising noise figure (on receive) or transmission efficiency (on transmit).

The principal purpose of the diplexers in Figure 5.5-1 is to avoid loss of signal in one band to the combining circuits for the other. This loss may be tolerated if sufficient gain is incorporated prior to such loss, by placing low-noise preamplifiers (LNA's) as shown in Figure 5.5-2. These LNA's would require only a modest amount of gain (5 or 6 dB) to establish the noise figure, and could be incorporated with simple 3 dB power dividers as an alternate MMIC configuration. Such usage eliminates the need for diplexers at each antenna OMJ port, while affording optimum noise performance on receive. The transmit case is not so simple, as combining two bands in a common power amplifier could give rise to excessive intermodulation effects, and would thus require further study.

The additional hardware required to implement pointing error correction may be determined from each of these circuits. Aside from extra control circuits and sampling couplers/detectors, added hardware is needed only for the fixed beams, for which a larger number of horns may have to be excited to effect steering. The scanning beams must be steered in any case, and so no additional hardware appears necessary. The following analysis of the fixed beams may be made:

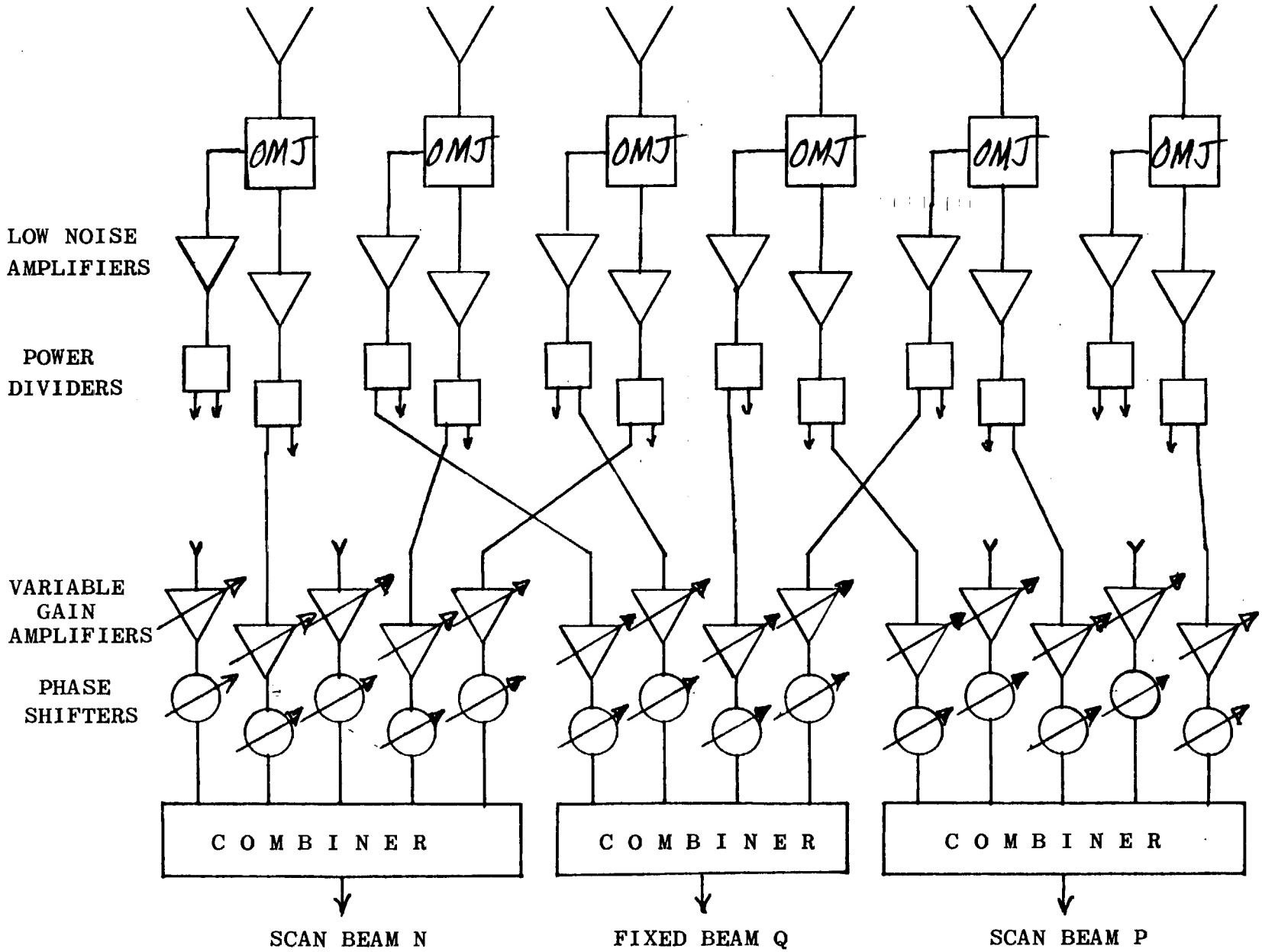

FIG. 5.5-2. ACTS FEED NETWORKS WITH ACTIVE EMBEDDED ELEMENTS (MMIC'S)

	Configuration #1 & #2	Configuration #3
Without Corrections:	(FACC)	(TRW)
No. horns req. per beam	7 - 13	3 - 7
Total No. horns (MMIC's) (for 18 beams)	180	90
With Corrections:		
No. horns req. per beam	13 - 19	7 - 13
Total No. horns (MMIC's)	270	180
Total No. horns for Scanning Beams (6) (MMIC's)	680	340
Increase in No. MMIC's for Corrections	$\frac{90}{860}$ = 10%	$\frac{90}{430}$ = 21%

In addition to the increase in the number of MMIC's required to implement pointing error correction, the hardware to control these MMIC's must be provided, as well as the processors to direct the control process - to determine the actual pointing direction, or the gradients, and thus find a new set of feed coefficients to redirect the beams. Information for use by these processors must be derived from additional hardware in the form of sampling couplers on each feed horn, for both polarizations (for the open-loop system), plus sampling detectors or a switch matrix to a common detector. Interconnection of all these sampled signals would constitute another hardware complexity, as it would probably involve a myriad of coaxial lines. The closed-loop system requires only a signal sample (for each beam), plus a synchronous detector, and thus constitutes a much more hardware efficient system (and thus more cost effective).

A basic circuit for implementing open-loop pointing error correction into one beam (either fixed or scanning) is shown in Figure 5.5-3a, while the corresponding circuit for closed-loop control is shown in Figure 5.5-3b. The number of feeds which have to be combined for forming each beam depends upon the beam location, sidelobe requirements, steering range selected, as well as

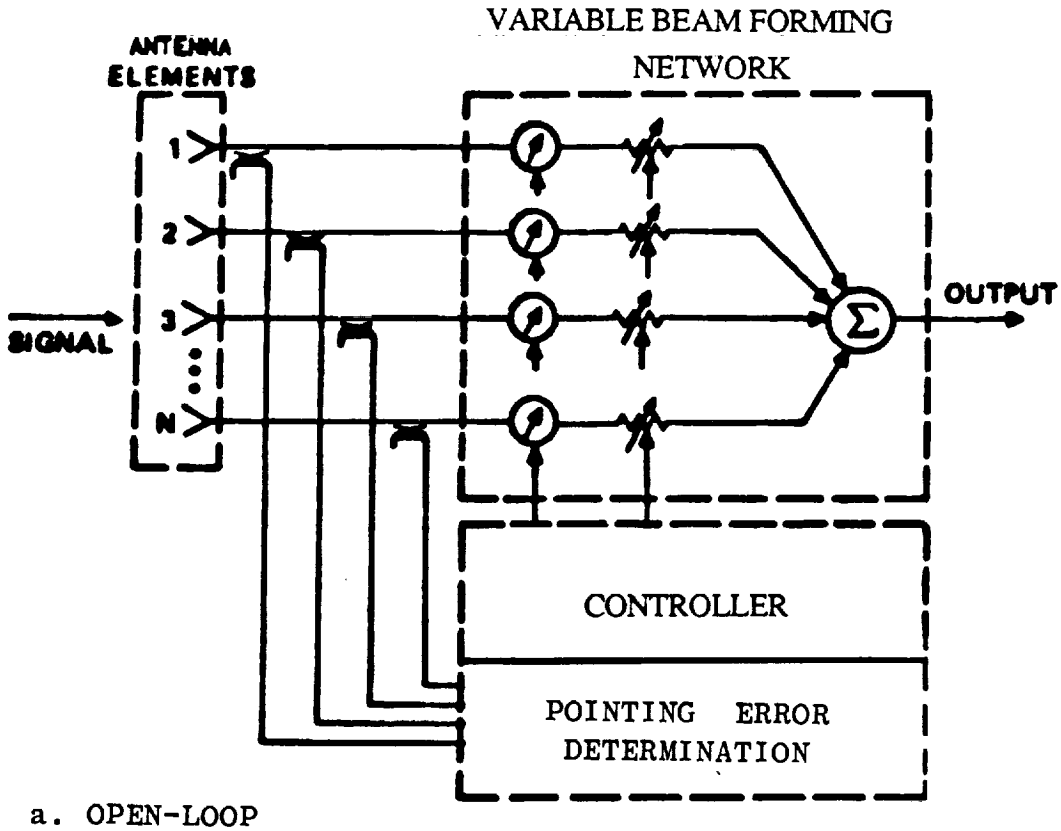

a. OPEN-LOOP

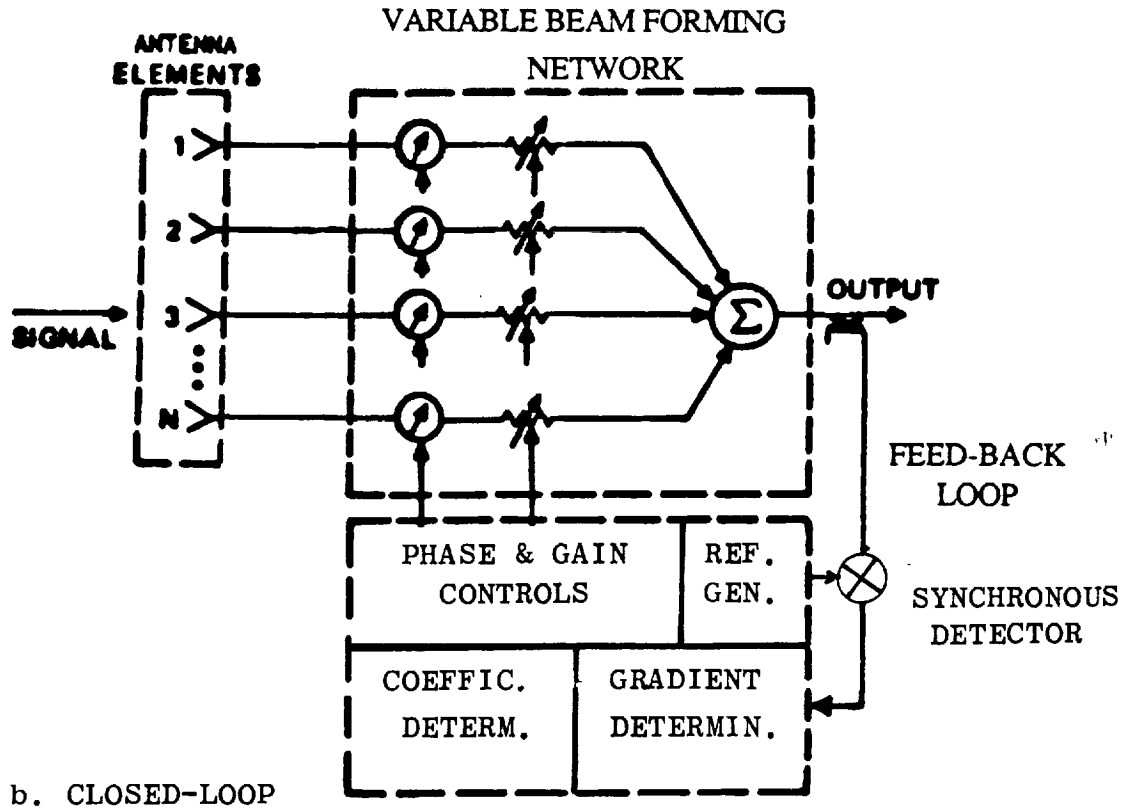

b. CLOSED-LOOP

FIG. 5.5-3. POINTING ERROR CORRECTION SYSTEMS

the basic antenna system design (such as separation of horns), but will generally range between 7 and 19. Another basic system design choice will affect the scan beam BFN configuration: should each elementary feed incorporate a separate MMIC (requiring up to 100 MMIC's per beam), or should a basic set of 13 to 19 MMIC's per beam be switched to the appropriate set of feeds to produce a beam in the desired location (as done in the Ford 30/20 GHz antenna design)?

A summary of the factors affecting the choice between open and closed-loop pointing error compensation is given in Table 5.5-1.

Table 5.5-1 Trade-off Summary

	OPEN-LOOP SYSTEM	CLOSED-LOOP SYSTEM
Hardware Requirements	Sampling coupler & detector on each feed (or RF switching matrix)	Single sampling coupler & synchronous detector
	Phase & gain controls on each element (MMIC) with controller	Phase & gain controls on each element (MMIC) with controller
	Data processor	Adaptive processor
	Additional MMIC modules and associated combiners to implement illuminating larger portions of feed array to allow beam steering	
Correction Limitations	Depends on calibration of phase & gain controls - no indication of errors	Automatically corrects for system errors by detecting corrected output
	Normally implemented for only limited range of corrections (such as one beamwidth), because of excessive hardware requirements	
System Performance	Allows achievement of near maximum gain at any position within range of feed cluster; causes some sidelobe degradation which could reduce isolation between adjacent beams	
	Achieves designated steering in single iteration of feed coefficients	Achieves maximum performance after several iterations of optimization
Cost Effectiveness	Both types are very cost effective when considering alternatives involved - higher power for same coverage, or more complex attitude control system.	
	Somewhat higher costs due to additional hardware	Most cost effective

6.0 EVALUATION OF RESULTS

6.1 General Adaptive Satellite Applications

This section summarizes the efforts made in Section 4. The applicability of the adaptive functions to the communication systems, the potential benefits for the systems, and the hardware requirements for implementation are compared and presented in this section.

6.1.1 Applicability

Table 6.1-1 summarizes the applicability of the five adaptive functions to the three communication systems.

Table 6.1-1 Applicability of Adaptive Functions to Three Systems

SYSTEMS / FUNCTIONS	SCANNING/ FIXED BEAMS	MULTIPLE SHAPED BEAMS	LAND MOBILE SYSTEM
Interference Control	Limited Applicability	Applicable	Limited Applicability
Sidelobe Control	Limited Applicability	Applicable	Limited Applicability
Accurate Beamforming	Applicable	Applicable	Applicable
In-orbit Testing & Adjustment	Applicable	Applicable	Applicable
Propagation Compensation	Limited Applicability	Applicable	Limited Applicability

Limited applicability of interference control, sidelobe control, and propagation compensation to the scanning/fixed beam systems and the land-mobile systems is due to the limited number of horns in a typical beam for these systems. In order to improve the applicability, additional measures are required, which include:

1. Accurate tracking of users to avoid signal loss.
2. Possible increase in the number of feed elements to improve control flexibility.

6.1.2 Potential Benefits

The potential benefits of adaptive functions for the satellite communication systems include satellite capability enhancement, frequency utilization improvement, orbit utilization improvement, reduction in margin

requirements, and reliability enhancement. Table 6.1-2 summarizes the potential benefits of each adaptive function.

Table 6.1-2 Potential Benefits of Adaptive Functions

POTENTIAL BENEFITS / FUNCTIONS	ENHANCE SATELLITE CAPABILITY	IMPROVE FREQUENCY UTILIZATION	IMPROVE ORBIT UTILIZATION	DECREASE MARGIN REQUIREMENTS	INCREASE RELIABILITY
Interference Control	X	X	X	X	
Sidelobe Control	X	X	X		
Accurate Beamforming	X			X	
In-orbit Testing & Adjustment					X
Propagation Compensation				X	

6.1.3 Hardware Requirements

The hardware requirements for the implementation of different adaptive functions are summarized in Table 6.1-3. The table indicates that the required hardware for different adaptive functions are similar. This implies that the same hardwares can be shared by different adaptive functions. A multi-function controller therefore can be realized without excessive cost and weight. Note that the hardware requirements summarized in Table 6.1-3 do not include the hardware for the ground terminals. All the adaptive functions except interference control and in-orbit testing require assistance from ground terminals; therefore, proper ground hardware is required for

those adaptive functions. In order to improve the applicability of interference control, sidelobe control and weather compensation to the land-mobile systems and the scanning/fixed beam systems, additional hardware is required, which includes:

1. Hardware for accurate tracking of users,
2. Hardware for switching the number of feed elements.

Table 6.1-3 Hardware Requirements

	INT. CONTROL (LMS)	INT. CONTROL (HOWELL - APPLEBAUM)	SIDELOBE CONTROL	ACCURATE BEAMFORMING (MUSIC)	IN-ORBIT TESTING	WEATHER COMPENSATION
COUPLERS	X	X		X	X	
PHASE & AMPLITUDE CONTROL	X	X	X	X	X	X
SIGNAL COMBINER	X	X	X	X	X	X
CORRELATOR	X	X		X	X	
MICROPROCESSOR	X	X	X	X	X	X
REFERENCE SIGNAL GENERATOR	X				X	
SWITCH	X	X		X	X	
CONNECTING WAVEGUIDES	X	X	X	X	X	X

6.2 Pointing Error Compensation

6.2.1 Feasibilty of Incorporation of Pointing Error Correction into a Multibeam Antenna System

This feasibility depends critically upon the actual antenna system under consideration, and exactly how the MMIC modules are utilized. If the MMIC modules already incorporate phase and gain adjustments of a more-or-less continuous nature (as needed for precision steering) the feasibility of

incorporating pointing error correction would be enhanced. Incorporation of the adaptive system appears easier on the basis of required hardware (as detailed in the last section), as fewer additional parts are required. The feasibility of adding another set of RF interconnections for the open-loop sampling couplers into the already crowded feed array/feed network environment is not good. However, even this could be accomplished with innovative microstrip (or even fiber optic) techniques. The additions required for the controller and the adaptive processor are minimal, and could certainly be accomodated.

6.2.2 Advantages of Concepts

The open-loop pointing-error correction system has the advantage that it immediately attempts to introduce the optimum correction for any pointing error detected. Furthermore, information as to the size and direction of any pointing error is available for other uses, such as a gauge as to when to initiate spacecraft pointing error corrections which would affect other systems. This information would also be available from the closed-loop system on a derived basis, by noting optimum phase and amplitude settings of individual MMIC's and deriving the associated beam pointing direction, with some loss of accuracy due to component tolerances.

The closed-loop correction system iteratively drives individual feed coefficients toward their optimum values for a desired pointing direction, and automatically corrects for any component inaccuracies (possibly even reflector distortions). The time delay in reaching these near-optimum settings is probably minimal, since only a few iterations are necessary, each of which could probably be accomplished in a few seconds. The possibility of deriving gradient information on individual feeds merely by perturbing gain and phase adjustments at a low modulation rate, allowing use of a sensitive synchronous detector, is attractive.

Both schemes offer the advantage of allowing independent steering of individual beams within the array, to optimize pointing for each user, and allowing the basic antenna to be designed without having to include allowances for pointing errors expected in practice. This results in higher gain achievable for each beam, and better isolation between beams. In fact, this suggests another possible advantage of the adaptive system: the possibility of including isolation maximization in the corrective algorithm. Thus the synchronous detector on the output of one beam could detect the signal leakage from an adjacent beam, and the coefficients for that beam readjusted to minimize such coupling, while maximizing signal from the desired location.

6.2.3 Complexity

Both pointing-error correction systems are extremely simple in their basic concepts, but the open-loop system is a bit more complex in its hardware implementation, because of the large numbers of sampling couplers/detectors required. Control of individual beams through adjustment of feed coefficients is inherent in the basic design of the multibeam antenna system; the concept of steering these beams by varying the feed coefficients is a logical extension of the technique. The process of optimizing these feed coefficients either through a predetermined relationship, or through a gradient search technique, is basically simple and well understood in control system theory.

6.2.4 Availability of Hardware

All hardware items for both the open-loop and closed-loop adaptive pointing error correction schemes are readily available, having been developed on prior NASA contracts or commercially. The basic antenna hardware (reflector, feed horns, OMJ's, diplexers, etc.) were developed on the 30/20 GHz Multibeam Antenna Technology contracts (such as NAS3-22498 by FACC and NASA-22499 by TRW), as well as the current ACTS contract with RCA.

The MMIC transmit and receive modules (including gain and phase adjustments) have also been developed on NASA contracts by TI, Motorola, Rockwell, etc. Sampling couplers and synchronous detectors are well known devices available commercially, while controllers and processors are generally custom designed for individual applications according to well known principles.

6.2.5 Limitations Involved

The principal limitation in both pointing error correction systems is the size of the error to be corrected; it is generally understood that such errors be less than about half a beamwidth, which represents about 0.15^{o} in the ACTS system. Greater errors should probably be corrected by spacecraft re-pointing. While it would be possible to implement larger corrections into the basic systems described (such as by combining outputs from larger groups of feeds for each beam), this would complicate the hardware and interconnection problems, and slow down the adaptive process, since more gradient information would be required.

Another limitation of both correction systems is their speed of response. Normally this factor is non-critical, since changes which have to be corrected occur rather slowly (such as by thermal drift). While the correction hardware and algorithms can be programmed to respond rapidly (perhaps in nanoseconds), the gathering of information to feed these processes may be much slower (such as use of an iterative procedure to sample individual feeds, to allow use of common hardware). Also, the modulation rate for deriving gradient information from each feed must be chosen so as not to interfere with normal system operation (which is why a sub-audio rate was suggested, since it could not be heard on voice channels and would not interfere with video or data transmission, but would place a definite limitation on speed of response).

6.2.6 Penalties Imposed

The only apparent penalties associated with the proposed pointing-error correction systems would be in terms of size, weight, and cost (since any additions to a basic system would affect these items). However, while it is difficult to assess exact values for these increases without attempting to implement an actual system design, such increases appear to be nominal and well worth the advantages outlined above.

7.0 RECOMMENDATIONS FOR FUTURE WORK

7.1 Task I

The study accomplished in Task I shows that the five adaptive concepts are applicable to the three satellite communication systems. Naturally, the extention of Task I would be experimental verification of the feasibilities. We recommend the following three tasks be further explored.

1. Experimental Interference Control Using Reflector Antenna Systems

The theories of adaptive antennas have been available for more than fifteen years. Most works done on adaptive antennas are theoretical and they deal primarily with phased array antennas. Very few papers address the issues of hardware realization of the system, especially with reflector antenna systems. The experiments on an adaptive nulling system with a reflector antenna therefore can provide valuable information for future system applications.

Bench testing of an 8-port 4 GHz adaptive nulling system using the power inversion algorithm has been successfully accomplished at Ford Aerospace. The hardwares in the bench testing can be used with a reflector in the range testing. An alternate algorithm, such as the gradient-search algorithm, can also be implemented in the range testing for performance comparisons. The two algorithms could be compared in the following areas:

- Speed of convergence

- o Jammer cancellation
- o Hardware implementation
- o Wideband performance

2. Experimental Accurate Beamforming Using Reflector Antenna Systems

This task would focus on experimental direction finding using a reflector antenna system. The MUSIC algorithm has been shown to be a viable and versatile direction-finding scheme in recent years. A few papers have already reported experimental phased array systems using this algorithm. However, none of those implements the MUSIC algorithm with a reflector antenna system. The experiments on implementing the MUSIC algorithm with a reflector antenna can provide first-hand information for such an application. The amplitude-comparison direction finding algorithm reported in Task II can also be implemented for comparison. The amplitude-comparison algorithm, though not as versatile as the MUSIC algorithm, is shown to have good accuracy.

3. Experimental In-Orbit Testing

This task does not require a reflector. It focuses primarily on the testing of a beamforming network. The principle of operation and the hardware requirements for this task are clearly described in Section 4.4.

Note that the hardware requirements for the three tasks proposed above are similar. The same hardware therefore can be used directly with slight or no modification for any of the above three tasks.

7.2 Task_II

The most expedient extension of Task II which could be performed next would be to design a pointing-error correction system for a specific spacecraft antenna application, e.g., to be compatible with present designs for the ACTS 30/20 GHz antenna system. This design could be either open-loop

or closed-loop, or one of each could be designed for comparison. These designs could then be modelled either by computer or in actual hardware, to demonstrate the type of performance which could be achieved. Unfortunately, full-scale modelling would require focussing reflector(s), as well as the feed array, feed network, and processor/controller, since the effects of beam steering would not be easily detected from the feed array alone (except by use of a near-field range with computer processing of measured aperture phase and amplitude). The feed array and network from Ford Aerospace's POC-model 20 GHz antenna, developed for NASA on Contract NASA-22498, is available for such a demonstration, and could be used to feed a simple parabolic reflector, since extensive beam scanning would not be required. This model would allow implementation of an 8-element feed array with full phase and amplitude control, which should be sufficient to demonstrate the type of steering contemplated.

No new enabling technologies have been identified for this application since all of the necessary components appear to have been developed, both MMIC and ferrite control units (as alternates), and the control processing is well understood from current technology.

APPENDIX A

PROGRAM TO SIMULATE ADAPTIVE POINTING ERROR COMPENSATION

```
10 DIMENSION V(10),P(10),VP(10),G(10)
20 CALL FPARAM(1,120)
30 10 PRINT,"INITIAL X,Y = ?"          (Initial Beam Position)
40 READ,X,Y
50 IF(X.LT.-5)GOTO 999
60 CALL CALC(X,Y,P,ET)                 (Calculate max. gain at initial
70 PRINT 97,ET,20.*ALOG10(ET)              position)
80 97 FORMAT(12H MAX. GAIN = ,F8.5,3H  =, F8.3,4H  DB)
85 PRINT,"OPTIMIZED FEED COEFFICIENTS:"
90 DO 20 N=1,10
100 20 V(N)=P(N)/ET                    (Calculate feed coefficients for
110 PRINT 98,(V(N),N=1,10)                 max. gain at initial position)
120 98 FORMAT(1H ,10F8.4)
125 PRINT," "
130 30 PRINT,"NEW X,Y = ?"             (Select New Beam Position = Error)
140 READ,X,Y
150 CALL CALC(X,Y,P,ET)                (Calc. max. gain at new position)
160 PRINT 97,ET,20.*ALOG10(ET)
170 PRINT,"OPTIMIZED FEED COEFFICIENTS:"
180 PRINT 98,(P(N)/ET,N=1,10)          (Calc. Coeffs. for max. gain here)
190 ET1=0.
200 DO 40 N=1,10
210 40 ET1=ET1 +V(N)*P(N)              (Calc. Actual Gain at new position
220 PRINT 95,ET1,20.*ALOG10(ET1)           with original coefficients)
222 PRINT," "
225 PRINT,"GRADIENT CORRECTION FACTOR B = ?"
230 DV=0.1                             (Initial ΔV for gradient calc.)
235 READ,B
240 45 ET2=ET1
250 96 FORMAT(20H GRADIENT FACTOR = ? )
260 IF(DV.LT.0.02)GOTO 50
270 DV=0.5*DV                          (Reduce ΔV for 2nd & 3rd iteration)
280 50 DO 75 K=1,10
290 75 VP(K)=V(K)                      (Revised coeffs. for gradient calc.)
300 DO 70 N=1,10
310 VP(N)=VP(N) +DV                    (Revise individual coeff. for grad.)
320 CALL NORM(VP)                      (Re-normalize)
330 GN=0.
340 DO 60 K=1,10
350 60 GN=GN +VP(K)*P(K)               (Calc. gain with revised coeffs.)
360 G(N)=GN-ET2                        (Gradient = gain differential)
370 DO 65 K=1,10
380 65 VP(K)=V(K)                      (Reset coeffs. for next grad. calc.)
390 70 CONTINUE
```

Program Language = Fortran IV

APPENDIX A

SIMULATION PROGRAM FOR ADAPTIVE POINTING ERROR COMPENSATION (Continued)

```
400 PRINT," "
410 PRINT,"GRADIENTS:"                    (Print 100 * Gradients)
420 PRINT 98,(100.*G(N),N=1,10)
430 DO 85 N=1,10                          (Calc. Iterated Feed Coefficients)
440 V(N)=V(N) + Q* G(N)/DV
450 IF(V(N).LT.0.) V(N)=V(N)-1.* G(N)/DV    (Correct if coefficient
460 85 IF(V(N).LT.0.) V(N)=V(N)-1.*G(N)/DV      turns negative)
470 CALL NORM(V)                          (Re-normalize)
480 PRINT,"COEFFICIENTS:"
490 PRINT 98,(V(N),N=1,10)                (Print Iterated Coefficients)
500 ET1=0.
510 DO 90 N=1,10                          (Calc. Gain with Iterated Coeffs.)
520 90 ET1=ET1 +V(N)*P(N)
530 95 FORMAT(7H GAIN = ,F8.5,3H  = ,F8.3,4H  DB)
540 PRINT 95,ET1,20.*ALOG10(ET1)
560 IF(ABS(ET1-ET2).LT.0.0001)STOP        (Stop if gain change minimal)
570 GOTO 45
580 999 STOP;END


590 SUBROUTINE CALC(X,Y,P,ET)             (Subroutine to Calc. Pattern
600 DIMENSION R(10),P(10)                     Roll-off Factors P(N)
610 R(1)=X*X +Y*Y                             & Max. Gains)
620 R(2)=(X+10.)**2 +Y*Y
630 R(3)=(X+5.)**2 +(Y-10.)**2            (Distances from Beam Centers
640 R(4)=(X-5.)**2 +(Y-10.)**2                to Evaluation Point)
650 R(5)=(X-10.)**2 +Y*Y
660 R(6)=(X-5.)**2 +(Y+10.)**2
670 R(7)=(X+5.)**2 +(Y+10.)**2
680 R(8)=(X-15.)**2 +(Y+10.)**2
690 R(9)=(X-15.)**2 +(Y-10.)**2
700 R(10)=(X-20.)**2 +Y*Y
710 ET=0.
720 DO 55 N=1,10
730 DB=-.0597*R(N)**1.25                  (Pattern Roll-off Factors)
740 P(N)=10.**(DB/20.)
750 55 ET=ET+P(N)**2                      (Max. Gain calc.)
760 ET=SQRT(ET)
770 RETURN;END
780 SUBROUTINE NORM(V)                    (Subroutine to Re-normalize
790 DIMENSION V(10)                           Feed Coefficients)
800 S=0.
810 DO 77 N=1,10
820 77 S=S +V(N)*V(N)
830 S=SQRT(S)
840 DO 80 N=1,10
850 80 V(N)=V(N)/S
860 RETURN;END
```

SELECTED REFERENCES - ADAPTIVE ANTENNAS

Spacecraft Applications

1) Mayhan, J. T.; "Nulling Limitations for a multiple beam antenna", IEEE Trans., vol. AP-24, pp. 769-777, 1976.

2) Mayhan, J. T.; "Thinned array configurations for use with satellite-based adaptive antennas", IEEE Trans., vol. AP-28, pp. 846-856, 1980.

3) Rodgers, W. E., and R. T. Compton, Jr., "Adaptive array bandwidth with tapped delay-line processing", IEEE Trans., vol. AES-15, pp. 21-28, 1979.

4) Mayhan, J. T., "Some techniques for evaluating the bandwidth characteristics of adpative nulling systems", IEEE Trans., vol. AP-27, p. 363, May 1979.

5) Mayhan, J. T., A. J. Simmons, and W. C. Cummings, "Wideband adaptive antenna nulling using tapped delay lines", IEEE Trans., vol. AP-29, p. 923, November 1981.

6) Mayhan, J. T., and F.W. Floyd, Jr., "Factors affecting the performance of adaptive antenna systems and some evaluation techniques", Lincoln Laboratory, MIT, Technical Note 1979-14, August 1979.

7) Potts, B. M., J. T. Mayhan, and A. J. Simmons, "Some factors affecting angular resolution in an adaptive antenna", IEEE Conf. on Communication, June 1981.

8) Burrows, M. L., and J. T. Mayhan, "Configuration tradeoffs for satellite nulling arrays", Lincoln Lab, MIT, Technical Note 1978-5, November 1978.

9) Ricardi, L. J., A. J. Simmons, A. R. Dion, L. K. DeSize, and B. M. Potts, "Some characteristics of a communication satellite multiple beam antenna", Lincoln Lab., MIT Technical Note 1975-3, January 1975.

10) Compton, R. J., Jr., "An adaptive array in a spread spectrum communication system", Proc. IEEE, vol. 66, p. 289, March 1978.

11) Mayhan, J. T., "Adaptive antenna design considerations for satellite communication antennas", IEEE Proc., vol. 130, Pts. F and H, no. 1, February 1983.

Books

1) Monzingo, R. A., and T. W. Miller, "Introduction to adaptive arrays", John Wiley & Sons, 1980.

2) Hudson, J. E., "Adaptive array principles", Peter Peregrinus, 1981.

3) "Special issue on adaptive procesing antenna systems", IEEE Trans., vol. AP-34, March 1986.

4) "Special issue on adaptive antennas", IEEE Trans., vol. AP-24, September 1976.

Typical Algorithms

1) Howells, P. W., "Intermediate frequency sidelobe canceller", U.S. Patent 3202990, 24 August 1965.

2) Applebaum, S. P., "Adaptive arrays", Syracuse University Research Corp., Report SPL TR 66-1, August 1966.

3) Brennan, L. E., and I. S. Reed, "Theory of adaptive radar", IEEE Trans., vol. AES-9, no. 2, pp. 237-252, March 1973.

4) Widrow, B., P. E. Mantey, L. J. Griffiths, and B. B. Goode, "Adaptive antenna systems", Proc. IEEE, vol. 55, p. 2143, December 1967.

5) Applebaum, S. P., and D. J. Chapman, "Adaptive arrays with main beam constraints", IEEE Trans., vol. AP-24, no. 5, pp. 650-662, September 1976.

6) Gabriel, W. F., "Adaptive arrays - an introduction", Proc. IEEE, vol. 64, p. 239, February 1976.

7) Compton, R. T., "The power inversion adaptive array: concept and performance", IEEE Trans., vol. AES-15, pp. 803-814, November 1979.

8) Reed, I. S., J. D. Mallet, and L. E. Brennan, "Sample matrix inversion technique", Proceedings of the Adaptive Antenna

9) Widrow, B., and J. M. McCool, "A comparison of adaptive algorithms based on the methods of steepest descent and random search", IEEE Trans., vol. AP-24, no. 5, pp. 615-637, September 1976.

10) Baird, C. A., "Recursive processing for adaptive arrays", Proceedings of the Adaptive Antenna Systems Workship, Vol. I, NRL Report 7803, NAVAL Research Laboratory, Washington DC, pp. 163-182, March 1974.

11) Capon, J., R. J. Greenfield, and R. J. Kolker, "Multidimensional maximum likelihood processing of a large aperture seismic array", Proc. IEEE, vol. 55, no. 2, pp. 192-211, February 1967.

12) Baird, C. A., Jr., "Recursive minimum variance estimation for adaptive sensor arrays", Proceedings of the IEEE International Converence on Cybernetics and Society, Washington, DC, pp. 412-414, October 1972.

13) Acar, L., Compton, R. T., "The performance of an LMS adaptive array with frequency hopped signals", IEEE Trans., Vol. AES-Z1, no. 3, May 1985.

MUSIC Algorithms

1) Schmidt, R. O., "Multiple Emitter Location and Signal Parameter Estimation", IEEE Trans., vol. AP-34, pp. 276-280, March 1986.

2) Schmidt, R. O., and R. E. Franks, "Multiple Source DF Signal Processing = An Experimental System", IEEE Trans., vol. AP-34, pp. 281-290, March 1986.